THE ROLE OF CHEMOTAXIS SYSTEM AND METHYL-ACCEPTING CHEMOTAXIS PROTEINS (MCPs) FOR VIRULENCE OF *PSEUDOMONAS SYRINGAE* PV. *TABACI* 6605

March 2021

STEPHANY ANGELIA TUMEWU

Graduate School of Environmental and Life Science

(Doctor Course)

OKAYAMA UNIVERSITY

The Role of Chemotaxis System and Methyl-accepting Chemotaxis Proteins (MCPs) for virulence of *Pseudomonas syringae* pv. *tabaci* 6605

Pseudomonas syringae pv. *tabaci* 6605 の病原力における走化性システムと受容体タンパク質 MCP の役割

Stephany Angelia Tumewu

Graduate School of Environmental and Life Science
Division of Agricultural and Life Science
Okayama University, Japan
March 2021

Dissertation submitted to Graduate School of Environmental and Life Science of Okayama University in partial fulfillment of the requirements for the degree of Doctor of Philosophy in Agricultural Science.

Written under supervision of Professor Yuki Ichinose and co-supervised by Professor Mikihiro Yamamoto and Professor Kazuhiro Toyoda.

OKAYAMA
UNIVERSITY

CERTIFICATE

This is to certify that Ms. Stephany Angelia Tumewu has worked on the dissertation entitled "The Role of Chemotaxis System and Methyl-accepting Chemotaxis Proteins (MCPs) for virulence of *Pseudomonas syringae* pv. *tabaci* 6605" under my supervision. This dissertation is being submitted to the Graduate School of Environmental and Life Science. Okayama University for the partial fulfillment of the requirement for the degree of Doctor of Philosophy. It is an original record of the work conducted by the candidate and has not been submitted in full or partial to any other university for the award of degree or diploma.

Okayama, Japan

March 25th, 2021

Prof. Dr. Yuki ICHINOSE
Department of Plant Science
Graduate School of Environmental and Life Science
OKAYAMA UNIVERSITY

Summary

Bacterial plant pathogens require various virulence factors to survive and cause disease in compatible host plants. At the early stage of infection, motile bacterial pathogens first need to enter the plant via natural openings or wounds and attach on plant cells. How they can navigate the foliar plant and find such openings might depends on sensing plant-derived chemicals via a system called chemotaxis. Chemotaxis is the movement of an organism toward or away from a chemical stimulus. Motile bacteria can sense changes in the concentration of chemicals in their environments and respond to the changes by altering their motility pattern. *Pseudomonas syringae* pv. *tabaci* 6605 (*Pta*6605) is one of the *Pseudomonas syringae* strain that causes wildfire disease on tobacco plants. To infect host plants, *P. syringae* requires several virulence factors including an Hrp type III secretion system, phytotoxins, quorum-sensing system, flagella- and type IV pili-mediated motilities. However, the involvement of chemotaxis in this pathogen virulence has yet to be determined.

First, I elucidated the chemotaxis gene clusters that responsible for *Pta*6605 chemotaxis and virulence. *Pta*6605 has multiple clusters of chemotaxis genes including *cheA*, a gene for a histidine kinase, *cheY*, a gene for response regulator, *mcp,* a gene for a methyl-accepting chemotaxis protein, and flagellar and pili biogenesis genes. However, only two major chemotaxis gene clusters, cluster I and cluster II, possess *cheA* and *cheY*. Because *cheA* and *cheY* encode the essential components for chemotaxis, deletion mutants of *cheA* or *cheY* were constructed to evaluate their possible role in *Pta*6605 chemotaxis and virulence. Motility tests and a chemotaxis assay to known attractant demonstrated that Δ*cheA2* and Δ*cheY2* were unable to swarm and to perform chemotaxis, whereas Δ*cheA1* and Δ*cheY1* retained chemotaxis ability almost equal to that of the wild-type strain. Although wild-type and Δ*cheY1* of *Pta*6605 caused severe disease symptoms on host tobacco leaves, Δ*cheA2* and Δ*cheY2* did not, and symptom development with Δ*cheA1* depended on the inoculation method. These results indicate that chemotaxis genes located in cluster II are required for optimal chemotaxis and host plant infection by *Pta*6605 and that cluster I may partially contribute to these phenotypes.

Second, I did characterization of a chemoreceptor protein that specifically recognize gamma aminobutyric acid (GABA), a versatile chemical that exists in various niches, mainly as signaling compound bridging in the communication between species in different kingdoms. *Pta*6605 possess more than 50 genes encoding chemoreceptor proteins (methyl-accepting

chemotaxis proteins, MCPs), but no MCP has been characterized yet. In this study I show that a GABA receptor gene, named *mcpG* (A3SK_RS0126685), is also conserved in the highly motile plant-pathogenic bacteria *Pta*6605. I generated a deletion mutant of McpG to further investigate its involvement in GABA chemotaxis using quantitative capillary and qualitative plate assays. The wild-type strain of *Pta*6605 was attracted to GABA, while the Δ*mcpG* was not. However, Δ*mcpG* retained the chemotaxis to the proteinogenic amino acids and succinic semialdehyde, a structural analog of GABA, indicating the specificity of this chemoreceptor. Furthermore, Δ*mcpG* was unable to effectively cause disease on host tobacco plants in three plant inoculation assays, flood inoculation, dip inoculation, and infiltration inoculation. These results revealed that GABA sensing is important for *Pta*6605 host plant infection.

Third, I continued to investigate the importance of several MCPs and the ligands that they perceive. Chemotactic response specifically depends on ligand recognition at the ligand-binding domain (LBD) of each MCP. Usually, the orthologs of GABA chemoreceptors are the receptors for naturally occurring amino acids. They share a common ligand-biding domain (LBD) type, namely dCACHE_1 type, also with their homologs across *Pseudomonas* species, suggesting the involvement of this type of LBD in sensing amino acids. As hypothesized, the deletion mutants of two orthologs of McpG (locus tag: A3SK_RS0106980 and A3SK_RS0112400) showed reduced or lost chemotactic responses to a number of amino acids. In addition, I also identified one additional MCP with dCACHE_1 type LBD, A3SK_RS0114355. A3SK_RS0114355 has less similarity with PctABC, chemoreceptors for GABA and amino acids in *Pseudomonas aeruginosa*. The deletion mutant of A3SK_RS0114355 also showed reduced chemotactic response to amino acids, however, its ligand recognition range seems to be slightly narrower. Therefore, I designate A3SK_RS0112400, A3SK_RS0106980 and A3SK_RS0114355 as *pscA*, *pscB*, and *pscC*, respectively. To assess the role of *pscA*, *pscB*, and *pscC* in virulence on tobacco plant, I conducted inoculation by flood assay and syringe infiltration. Following flood assay inoculation which allow evaluation of chemotaxis in plant infection, it seems that only *pscB* and *pscC* has significant role in *Pta*6605 infection, because the virulence of Δ*pscA* did not differ to that of wild-type strain. However, when bacterial cells were introduced directly into tobacco plants by infiltration method, Δ*pscB* and Δ*pscC* also showed the same less virulent phenotype compared to both wild-type and Δ*pscA*. Both Δ*pscB* and Δ*pscC* increased biofilm formation, indicating the possibility of PscB and PscC-mediated signaling can modulate both chemotaxis-related and virulence-related pathway.

In this dissertation, the evidence for the importance of chemotaxis in bacterial pathogenicity was presented. The characterization of several chemoreceptors and their ligands sheds some lights in virulence-related chemotaxis to host signals and prediction of corresponding ligands based on the LBD type of chemoreceptors. The mounting number of chemoreceptor proteins possessed by bacterial pathogens makes any discovery of their cognate ligand and underlying molecular mechanism a valuable step to further our understanding on the evolution of bacterial chemotaxis repertoire. The knowledge would benefit the development of new disease prevention strategies by specifically interfering with bacterial chemotactic signaling pathways.

Acknowledgments

I would like to express my gratitude to the Ministry of Education, Culture, Sports, Science, and Technology (MEXT) of Japan for granting me scholarship for the completion of my doctor course study. It is such an extremely valuable and unforgettable experience for me to live and study in Japan.

My sincere and deepest gratitude goes to Prof. Yuki Ichinose, Professor of Okayama University, as my supervisor for allowing me to pursue my master and doctor course study under his guidance. His great support, excellent expertise, and encouragement were essential for the successful completion of my study. I will be forever grateful for this.

Special gratitude goes to Prof. Mikihiro Yamamoto, Professor of Okayama University for his helpful ideas and valuable suggestions during throughout my study. My sincere thanks to Prof. Kazuhiro Toyoda and Assoc. Prof. Yoshiteru Noutoshi for every great discussions, guidance, and suggestion during my study. Special thanks and gratitude I express to Dr. Hidenori Matsui, for his technical guidance and expertise in conducting plant infection experiments. It was such an immense help for me.

I would also like to thank Dr. Andi Salamah for recommending me to Prof. Yuki Ichinose as a student to pursue higher education at Okayama University. Also to Dr. Anom Bowolaksono, as my mentor and supervisor since my Bachelor study, with his great encouragement and valuable tips from scholarship application up until now.

In a more personal level, I would like to thank all my colleagues in Genetic Engineering and Plant Pathology Lab for the nice friendship and helps. I hope we all can be successful in the future. Much love for fellow Indonesian friends and other international students in Okayama, it was great to have you all when I was away from home and family.

I would like to thank my big family for their unconditional love and support, for their understanding and cooperation when I was away in Japan. To my always supportive sister and cousin, Caroline and Meidy Ayu, thank you for listening to my problems and cheering me up. To my beloved late mother, Kurniati Kurnain, you encouraged me to pursue my educations and dreams. I dedicate this thesis for you, for all my family, as it is yours more than mine.

List of Publications

Parts of this dissertation have been published as the following journal papers:

1. Tumewu, S. A., Matsui, H., Yamamoto, M., Yoshiteru, N., Toyoda, K., and Ichinose, Y. 2020. Requirement of γ-aminobutyric acid chemotaxis for virulence of *Pseudomonas syringae* pv. *tabaci* 6605. *Microbes and Environments* **35**(4). https://doi.org/10.1264/jsme2.ME20114
2. Tumewu, S. A., Ogawa, Y., Okamoto, T., Taguchi, F., Matsui, H., Yamamoto, M., Yoshiteru, N., Toyoda, K., and Ichinose, Y. 2021. Cluster II *che* genes of *Pseudomonas syringae* pv. *tabaci* 6605, orthologs of cluster I in *Pseudomonas aeruginosa*, are required for chemotaxis and virulence. *Molecular Genetics and Genomics* (Published online on January 2nd, 2021). https://doi.org/10.1007/s00438-020-01745-y

Table of Contents

List of Figures

List of Tables

Chapter 1

General Introduction

1.1. Plant pathology

Plant pathology involves around the application of science to solve disease problems in agriculture, horticulture, and forestry. Research in plant pathology mainly focus on development of methods for disease controls to prevent crop loss, improve productivity, and ensure global food security. Practical application aside, the science of plant pathology also covers fundamental studies concerning the pathogenic organisms that causes disease on plants includes, bacteria, fungi, viruses, parasitic plants, and nematodes. The study of the interaction between plants and pathogens including recognition and response systems, signaling pathways, and innate plant immunity have helped us understand how pathogens cause disease and how plants defend themselves. Plant pathology also includes the study of pathogen identification, disease epidemiology, disease resistance, economic impact, and management of plant diseases.

Disease in plant system occurs when these three components are present at the same time: a susceptible host plant, a virulent pathogen, and a favorable environment. If a susceptible host plant is in interaction with a virulent plant pathogen under favorable environmental conditions, a disease will occur. This concept is represented by the disease triangle (Agrios, 2005). However, various factors can affect these three components that may influence the severity of the disease. For example, genetic diversity, lifecycle of host plant and pathogen, and numerous variables in the environmental conditions itself.

Plant disease cause enormous economic losses, affecting farmers worldwide. It contributes to 10 and even up to 20% yield loss every year in less developed countries. Not only from the economic standpoint, but crop loss also threatens the food availability in this ever-growing world population. Based on the estimation of Food and Agriculture Organization (FAO), about 25% of crop loss are due to pests and diseases. Hence, the world is in a dire need for novel diseases detection and prevention methods. In order to develop more advanced and effective methods, researchers have to gather more in-depth understanding about plant-pathogen interaction. Since this dissertation focus on bacterial pathogen, the next part will focus specifically on plant-microbes interaction.

1.2. Plant-microbes interaction

Plants are static organisms that unable to run away or escape under unfavorable environmental condition. However, plants have evolved a compendium of physical and biochemical defense mechanisms to survive under biotic and abiotic stresses. Naturally, plants and microbes are living in shared niches since ages ago, forming either negative or positive interaction. Positive interaction for example, the interaction of plant roots with microbes living in the soil environment that enhance plants tolerance to stresses and promotes growth. Negative interaction on the other hand, compatible interaction between host plants and pathogenic microorganism which leads to disease development. Both interactions have significant impact on agricultural practices (Newton *et al*., 2010).

Plants produce and release various chemical signals to mediate communication between them and microbes, ensuring nutrient availability and immune system boost for survival (Hücklehoven, 2007). Effective communication can be established into symbiotic, mutualistic and commensalism in which beneficial for either plants or microbes. Plants root exudates include carbon source and nutrients such as sugars, amino acids, and organic acids. These components can repel pathogenic microbes and attract the beneficial microbes (Badri *et al*., 2009). However, in negative interaction, pathogenic microbes, such as bacteria or fungi also secrete various chemicals that can be harmful for plants, leading to disease development (Pritchard and Birch, 2011). While pathogenic bacteria colonize plant apoplastic space and secrete toxins or hydrolytic enzymes, the mutualistic bacteria provide nutrient exchange that benefits both sides. Either way, both mode of interactions requires complicated chemical signaling.

The interaction between plant and pathogenic microbes starts from recognition. Plants possess transmembrane pattern recognition receptors (PRRs) which recognize pathogen-associated molecular patters (PAMPs). Another means of recognition is done by R gene products possessing nuclear binding and leucine rich repeat proteins (LRR) which detect the presence of pathogen effectors and initiate active defense response (Dodds and Rathjen, 2010). The popular representation of the arms race between host and pathogen is the 'zigzag' model (Fig 1.1). First stage of the interaction involves PAMPs recognition by hosts PRRs, leading to PAMP-triggered immunity (PTI) which prevent further colonization of pathogen. In the second stage, pathogens secrete effector molecules to disturb the PTI signaling and function, leading to effector-triggered susceptibility (ETS). Not over yet, hosts possessing R proteins will be able to recognize pathogens effectors thus lead to effector-triggered immunity (ETI) that may induce hypersensitivity response (HR). HR leads to the death of infected and

surrounding cells, preventing further invasion. And finally, once pathogens evolve and produce the new unrecognizable effector proteins, they can once again slip away and stop the ETI, thus establishing infection (Jones and Dangle, 2006).

1.3. *Pseudomonas syringae* as plant pathogens

About 150 of 7100 classified bacteria species are responsible for plant disease (Kannan and Bastas, 2015). Plant pathogenic bacteria can be classified generally into three families, Xantomonadaceae, Pseudomonaceae, and Enterobacteriaceae (Agrios, 2005). The genus *Pseudeomonas* itself belong to gamma-Proteobacteria, which consists of saprophytic, plant growth promoting, and of course the pathogenic species. International community has ranked *Pseudomonas syringae* the first among top 10 plant pathogenic bacteria, because of its significant impact on understanding of microbial pathogenicity and its role on causing economically important plant diseases (Mansfield *et al*., 2012). *P. syringae* is a diverse species complex, consisting of more than 50 pathovars (Höfte and De Vos, 2006). *P. syringae* pathovars can cause multiple disease, such as speck, fleck, spot, blight and canker over wide range of hosts plant (Preston, 2004; Fatmi *et al*., 2008).

P. syringae utilize variety means of mechanism to overcome host resistance and establish infections, for example, using cell wall degrading enzymes, secreting phytotoxins (coronatine, tabtoxin, syringomycin), and injecting Hrp (hypersensitive response and pathogenicity) T3SS (type III secretions system) effectors to damage plant cells (Fig 1.2) (Ichinose *et al*., 2013). However, no matter how they would do it later, first and foremost, bacterial pathogens have to enter the plant. Because unlike fungal pathogens, the epiphytic *P. syringae* requires entry into plant through natural openings such as stomata or wound to colonize intercellular space as a hemi biotroph before causing disease lesions (Hirano and Upper, 2000).

The ability to enter the host plants has been long associated with bacterial motility and chemotaxis, yet not many studies have evaluated the possibility of motility and chemotaxis as one of bacterial virulence determinants. Flagella-related motility is well studied in *P. syringae*. This pathogen requires flagella for liquid swimming motility that the mutation of flagella-related genes severely reduced its fitness in host plants (Ichinose *et al*, 2003; Taguchi *et al*., 2006; Kanda *et al.,* 2011). Flagella-mediated motility is allegedly required for navigating leaf surface during high humidity condition following inoculum dissemination facilitated by water. In low humidity or high viscosity condition like in plant apoplast, *P. syringae* may switch into surface motility, either swimming or swarming. Surface swimming and swarming motility require both flagella and type IV pili (T4P) (Taguchi and Ichinose, 2011). Previously, the involvement of chemotaxis

in *P. syringae* virulence was not clear, even though the closely related *P. syringae* pv. *tomato* DC3000 (*Pto*) preferred to move toward open stoma rather than adjacent closed stoma (Melotto *et al.*, 2006). However, in 2016, Clarke *et al.*, demonstrated that certain chemotaxis gene cluster was required for *Pto* motility and virulence. Moreover, *Pto* mutant that was unable to exhibit taxis toward amino acids also showed reduced virulence (Cerna-Vargas *et al.*, 2019), indicating that chemotaxis plays a significant role on *P. syringae* virulence. Detailed information about bacterial chemotaxis will be described below.

In this dissertation, we will focus specifically on a foliar pathogen, *P. syringae* pv. *tabaci* 6605 (*Pta*), a causal agent of wildfire disease in tobacco plants (Ichinose *et al.*, 2003). *Pta* is capable of producing tabtoxin, a strong toxin which causes yellow lesion on tobacco leaves (Taguchi *et al.*, 2010a). Wildfire of tobacco is a destructive disease that occurs worldwide. In a favorable condition, such as high humidity, wildfire disease can advance rapidly, in the course of just few days. *Pta* cells are disseminated to the leaves by rain splashes or wind, and enters the leaf via stomata, hydathodes, or wounds. Inside of the tobacco leaf, *Pta* multiple rapidly and secrete toxin causing the formation of the chlorotic halo and brown spot surrounding the initial infection zone. If the favorable condition persist, infection will continue to spread intercellularly, leading to the breakdown of leaf tissue parenchyma cells, indicated by large necrotic area. Dead leaf can fall to the ground or carried by the wind and rain to other plants, thus continuing the cycle of infection (Fig. 1.3) (Agrios, 2005).

1.4. Bacterial chemotaxis

It has been discussed above that chemotaxis is one of potential virulence factors of *Pseudomonas syringae*, facilitating bacterial entry through natural openings or wounds. Although not many reports cover the significance of chemotaxis for *P. syringae*, there are ample chemotaxis studies in some model organisms like *E. coli* and *Pseudomonas aeruginosa* (reviewed in Parkinson *et al.*, 2015; Sampedro *et al.*, 2015). Chemotaxis is a directed movement which allows bacteria to sense environmental signals and move toward life-sustaining favorable condition (positive chemotaxis) and away from harmful substances (negative chemotaxis) (Sourjik and Wingreen, 2012). Chemotaxis is based on the movement of motile bacteria upon sensing a chemical gradient in environments and respond to them by altering their motility pattern (Fig 1.4). Chemotaxis signaling pathways controls the rotation of flagella, which affects bacterial cells swimming speed and direction. In general, chemotaxis requires ligand-binding signal transduced by a chemoreceptor to a two-component system, a histidine kinase and a response regulator which controls flagellar rotation (Bi and Lai, 2015).

Turns out, chemotaxis in *Pseudomonas* is an intricate system. Typically, a chemosensory pathway consists of several core genes encoding proteins required for chemotaxis signaling, *cheA*, *cheB*, *che*R, *cheW*, *cheY*, *cheZ*, and *mcp* (Wuichet and Zhulin, 2010), however the arrangement may vary among species. Flagella-mediated and pili-mediated chemotaxis pathways exist in *P. aeruginosa*, with two chemosensory pathways governing the flagellar ones (Darzins, 1994; Kato *et al.*, 1999). The existence of multiple pathways allows the connection of chemotaxis behavior with other phenotypes like biofilm formation (Caiazza *et al.*, 2007). Unlike *E. coli* which possesses only one chemotaxis-related gene cluster, *Pseudomonas aeruginosa*, *Pto*DC3000, and *Rhodobacter sphaeroides* have multiple paralogs of chemotaxis clusters in their genomes (Kato *et al.*, 1999; Porter *et al.*, 2008; Clarke *et al.*, 2016). In *P. aeruginosa*, cluster I (or *che*) pathway is the one that actively regulates its chemotaxis, while cluster II (*che2*) pathway involves in other fine-tuning behavior (Ferrández *et al.*, 2002) and cluster III (Wsp pathway) involves in biofilm formation (Caiazza *et al.*, 2007). In *Pto*DC3000, genes located in cluster II are orthologs of cluster I in *P. aeruginosa* (Clarke *et al.*, 2016).

The canonical flagella-mediated chemotaxis in bacteria is based on the well-studied system in *E. coli* (Sourjik and Wingreen, 2012; Parkinson *et al.*, 2015) (Fig 1.5.A), which consists of four modules: sensor, transducer, actuator, and integral feedback module. Chemotactic signaling begins with binding of ligands on sensor module which is form of chemoreceptor proteins or methyl-accepting chemotaxis proteins (MCPs). MCPs also involve in response adaptation by CheR and CheB on specific sites. Constantly being phosphorylated, CheA shows decreased activity in the presence of molecular signals coming from MCPs. When there is no ligand binding, CheA autophosphorylation activity constantly phosphorylate the response regulator CheY, forming CheY-P. CheY-P can interact directly with a flagellar switch protein FliM (actuator module), causing the flagella to rotate clockwise (CW), producing tumbling movement. However, in the presence of ligand-binding, a decrease in CheA autophosphorylation activity also means less CheY-P. The output is counterclockwise (CCW) flagella rotation, allowing cells to run to one direction for an extended period of time. CheZ phosphatase is required for CheY-P desphosphorylation. The integral feedback module has a role in making sure that bacteria cells can 'memorize' the responses they previously encountered for more effective adaptation. This process requires the methylation of chemoreceptor proteins which occurs at slower rate than the phosphorylation and dephosphorylation. The differences act as memory for bacteria cells when they sense specific chemical gradient. Phosphorylated CheA not only phosphorylate CheY, but also the methylesterase CheB. CheB-P competes with

methyltransferase CheR in removing methyl groups from MCPs methylation sites (Anand and Stock, 2002)

Any compound that induces chemotactic response is called a chemoattractant, whereas any that induces negative chemotaxis is called a repellent. Most identified chemoattractants for *Pseudomonas* are chemicals that can be carbon or nitrogen sources or host-related compounds, such as sugars, amino acids, organic acids, aromatic compounds, chlorinated compounds, plant hormones, and even oxygen and neurotransmitter (Sampedro *et al.*, 2015). Chemotaxis to these compounds depends on the presence of specific MCPs in each species. Adaptation to different environmental conditions leads to diversity in the number of MCPs among bacteria species. Bacteria living in stable, nutrient-rich environment have less MCPs than symbionts or pathogens living in soil or water (Lacal *et al.*, 2010). *Pseudomonas* usually have more than 25 MCP-encoding genes in their genomes (Parales *et al.*, 2004). As many as half of 26 MCPs in *P.* aeruginosa have been identified and characterized (Kato *et al.*, 2008). The interesting point is, plant colonizing strains of *Pseudomonas* tend to have higher number of MCPs compared to the animal pathogenic ones (Matilla and Krell, 2018), suggesting the involvement of various plant-related compounds in plant-microbes interaction. However, not as many that have been characterized because it is relatively difficult to identify their respective ligands.

1.5. Methyl-accepting chemotaxis proteins (MCPs)

Methyl-accepting chemotaxis proteins (MCPs) or chemoreceptor usually have a ligand-binding domain (LBD), transmembrane domains (TM), and a cytoplasmic signaling domain (SD) which interacts with coupling protein CheW and a two-component system CheA. Cytosolic signaling domain of MCPs consist of a histidine kinase, adenyl cyclase MCP and phosphatase (HAMP) region, methylation helices (MH) which is responsible for adaptation process involving methylesterase CheB and methyltransferase CheR, flexible bundle (FB), and a signaling subdomain (SSD) (Ud-Din and Roujeinikova, 2017) (Fig 1.5.B). In *Pseudomonas aeruginosa*, most MCPs are transmembrane proteins with periplasmic LBD and cytosolic signaling domain (Ferrández *et al.*, 2002), with few having cytosolic LBD, like the aerotaxis receptor (Hong *et al.*, 2004).

The specificity of MCPs depends on their ligand binding domains (LBD). Because LBD can be localized at the periplasm or the cytosol, MCPs can recognize broad range of signals from extracellular environmental and intracellular chemical and physical cues. MCPs also can be embedded into the cell membrane or soluble in the cytosol, like McpB of *P. aeruginoasa* (Ferrández *et al.*, 2002). MCPs that sense extracellular signals usually possess transmembrane

domains and periplasmic LBD and are common in bacteria, whereas the cytosolic MCPs are often found in archaea. MCPs can be classified into seven topology groups (class Ia, Ib, II, IIIm, IIIc, IVa, and IVb). Subclass Ia MCPs can be divided further into two clusters according to the size of their LBDs (Ud-Din and Roujeinikova, 2017) (Fig 1.6).

Class I MCP is the common MCPs in bacteria and archaea. This class typically has a periplasmic LBD, TM domains, and a cytosolic SD. The more common subclass Ia harbors two TM domains, while Ib has only one TM domain and lack N-terminal TM domain (Ud-Din and Roujeinikova, 2017). Subclass Ia is further classified by the size of their LBD, cluster I (about 150-200 amino acids) and cluster II (about 220-290 amino acids) (Fig 1.7). Cluster I LBD can have various 3D structures, four-helix bundle (4HB), Per-Arnt-Sim (PAS), calcium channels and chemotaxis receptors (CACHE), and cyclase/histidine kinase associated sensory extracellular (CHASE). Tar (taxis to aspartate and repellent) and Tsr (taxis to serine and repellent) of *E. coli* are the examples of cluster I LBDs (Kim *et al.*, 1999; Mise, 2016). In *Pseudomonas*, cluster II makes up the large portion of their MCPs. LBDs of cluster II MCPs usually have the helical bimodular (HBM) and double CACHE_1 (dCACHE_1) that previously called tandem-PAS or double PDC (PhoQ, DucS, CitA) domain structures. Some examples of cluster II MCPs in *Pseudomonas* are PctABC of *P. aeruginosa* (Taguchi *et al.*, 1997), PsaABC of *Pto*DC3000 (Cerna-Vargas *et al.*, 2019), CtaABC of *P. fluorescens* (Oku *et* al., 2012) that recognize most amino acids and McpG of *Pseudomonas putida* that responsible for chemotaxis to GABA (Reyes-Darias *et al.*, 2015). Interestingly, all the aforementioned MCPs share common dCACHE_1-type LBDs, suggesting the correlation between LBD structures with ligand specificity.

Class II MCPs are less common and only present in bacteria. This class of MCPs have N-terminal cytoplasmic LBD with two TM domains and cytoplasmic SD. Aerotaxis receptor (Aer) of *E. coli* is one of the examples of class II MCPs (Watts *et al.*, 2004; Lacal *et al.*, 2010). Class III MCPs are present mainly in archaea and have 1 up to 8 TM domains. The subclass IIIm MCPs may or may not have LBDs embedded in the cell membrane, while in the subclass IIIc MCPs, LBD is located after the last TM domain before the cytoplasmic HAMP and SD (Lacal *et al.*, 2010). Class IV MCPs are soluble cytoplasmic MCPs and common in archaea. Subclass IVa MCPs possess LBD but not the IVb ones. TlpC of *Rhodobacter sphaeroides* is one of class IV examples in bacteria (Wadhams *et al.*, 2002). How subclass IVb MCPs recognize their ligands without LBDs is not yet elucidated.

P. syringae pv. *tomato* DC3000 possess about 49 genes encoding putative MCPs (Parales *et al.*, 2004). While there are 26 in *P. putida* KT2440 and *P. aeruginosa* PAO1, and only 5 in *E. coli* (Kato *et al.*, 2008). *Pseudomonas syringae* pv. *tabaci* 6605 is also identified to possess more than 50

MCP encoding genes (Table 1.1), and not a single one has been characterized. These MCPs are mostly homologous to those in *Pta*11528, *Pto*DC3000, *P. savastanoi* pv. *phaseolicola* 1448A, and *P. syringae* pv. *syringae* B728a. The striking difference between the number of MCPs possessed by plant pathogens and animal pathogens suggests that plant-pathogenic *Pseudomonas* have the potential to respond to various chemical stimuli but there may be a possibility that plant pathogens evolve more MCPs to allow each of which to be differently regulated by various level of chemoattractant or control other non-chemotaxis-related phenotypes, ensuring survival in harsh environments.

1.6. Association between chemotaxis and virulence

Chemotaxis definitely benefits bacteria by allowing access to growth substrates or favorable conditions for survival but many have guessed the relevance of chemotaxis for microbial virulence and pathogenicity. About half of animal or human pathogens and almost all of important plant pathogens possess chemosensory signaling genes (Matilla and Krell, 2018), with many of them have multiple copies of it. Most of signaling pathways are related directly with chemotaxis of course, but some mediate totally different pathways, such as type IV pili-mediated motility and biofilm formation (Hickman *et al.*, 2005; Wuichet and Zhulin, 2010).

While animal/human pathogens have 17 MCPs-encoding genes on average, the plant pathogens have strikingly 33 genes on average (Matilla and Krell, 2018) demonstrating that chemotaxis-related phenotypes are significantly needed for pathogens to survive the hostile environment within the host and to cause disease. There have been evidences suggesting the association between bacterial chemotaxis and pathogenicity. In animal and human pathogen *P. aeruginosa* encoded four chemotaxis-related gene clusters, the *che* pathway is the one mediating flagellar motility and chemotaxis, *che2* is vaguely suspected to have no connection with chemotaxis, *wsp* pathway controls biofilm formation by altering c-di-GMP levels, and *chp* pathway involves in type IV pili-mediated motility (Ferrández *et al.*, 2002; Whitchurch *et* al., 2004; Hickman *et al.*, 2005; Güvener *et al.*, 2006). However, Garvis *et al.* (2009) elucidate the importance of *cheB2* which is located in *che2* pathway in *P. aeruginosa* virulence in mice. As for *che* pathway, the mutation of *cheYZABW* in this pathway resulted in the reduction of attraction to scratch-wounded epithelial cells (Schwarzer *et al.*, 2016).

Some chemoreceptors and their cognate ligands have also been associated with bacterial virulence. PctABC are the chemoreceptor in *P. aeruginosa* that recognize amino acids and GABA (Taguchi *et al.*, 1997; Rico-Jimenez *et al.*, 2013). The triple mutant of these three chemoreceptor genes reduced bacterial colonization at wound sites, indicating that amino acids sensing is

required for *P. aeruginosa* virulence (Schwarzer *et al.*, 2016). Mlp24 in *Vibrio cholerae*, another human-infecting bacterial pathogen, is homologous to PctA of *P. aeruginosa*. Mlp24 also mediates chemotaxis to certain amino acids and interestingly, amino acids sensing via Mlp24 induces the production of cholerae toxin (Nishiyama *et al.*, 2012). Another example is a nitrate chemoreceptor in *Salmonella enterica* serotype Typhimurium, Tsr. This chemoreceptor mutant was less fit compared to wild type strain in ileum invasion during inflammation (Rivera-Chávez, 2016).

In plant-infecting bacteria, chemotaxis towards plant-derived compounds is believed to facilitate entry into plant through natural opening or wounds (Fig 1.8). Flagella-mediated motility is deemed important for *P. syringae* virulence, because flagella-defective mutants significantly reduced disease symptoms compared to wild type during plant infection assays (Ichinose *et al.*, 2013). However, the role of chemotaxis itself is not clear yet. Some studies gave much needed insight regarding this matter, *Pto*DC3000 has showed attraction to open stomata and not to adjacent closed stomata (Melotto *et al.*, 2006). Furthermore, the mutation of *cheA* located in *che2* pathway resulting in significantly reduced chemotaxis and fitness in tomato (Clarke *et al.*, 2016). Similar phenomenon was observed in *Salmonella enterica* which colonizes lettuce leaves. This pathogen utilizes chemotaxis for internalization through open stomata and the mutation of *cheY* resulted in reduced stomatal penetration (Kroupitski *et al.*, 2009). In the soil-borne pathogen *Ralstonia solanacearum*, the non-chemotactic *cheA* and *cheW* mutant were less virulence following soil soak inoculation assay (Yao and Allen, 2006). Chemotaxis-mediated motility also required by *Dickeya dadantii* for entry into *Arabidopsis thaliana* leaves (Antúnez-Lamas *et al.*, 2009a).

Some chemoreceptors in plant pathogenic bacteria have been characterized and associated with virulence. Recently, PscA of *Pto*DC3000 was identified as chemoreceptor for L-Asp, L-Glu, and D-Asp. The mutation of *pscA* affected *Pto*DC3000 virulence in tomato and saturating D-Asp with wild type strain reduced bacterial virulence (Cerna-Vargas *et al.*, 2019). PscA is the first annotated chemoreceptor among 49 found in *Pto*DC3000. In *R. solanacearum*, McpA and McpM mediate chemotaxis to amino acids and L-malate, respectively. While McpM was involved in tomato roots colonization, McpA seems to have no association with bacterial virulence (Hida *et al.*, 2015). The homologs of *P. aeruginosa* PctABC, CtaABC of *P. fluorescens* are also identified as major amino acids chemoreceptors. *CtaABC* triple mutant was less competitive in tomato root colonization (Oku *et al.*, 2012). In saprophytic *P. putida*, chemotaxis to non-proteinogenic amino acid GABA mediated by McpG was required for optimal plant

colonization (Reyes-Darias *et al.*, 2015). All of these evidences point out to the ability of chemotaxis sensory pathway regulating not only bacterial motility but also bacterial virulence.

P. syringae is adapted to epiphytic and endophytic lifestyle one they gain entry into host plant. In epiphytic bacterial cells, genes for flagellar synthesis and chemotaxis-related were upregulated but were found to be downregulated in apoplastic cells (Yu *et al.*, 2013). This result suggest that motility and chemotaxis are required for early stage of infection, but not so much needed when bacteria cells are inside the plants. However, there are studies that showed contradiction to this. It has been discussed above, chemotaxis pathway mainly controls the flagellar rotation, determining the switch between tumbling and running movement. But apparently, chemotaxis pathway can also modulate gene expression in some bacteria. For example, in *V. cholerae*, the expression of *toxT*, a transcriptional regulator of cholera toxin production, was delayed as the effect of *cheA2*, *cheY3*, and *cheZ* mutation (Lee *et al.*, 2001). Another example is the *wsp* pathway in *P. aeruginosa*. The mutation of a gene called *wspF* in this pathway caused the continuous activation of the response regulator (WspR), leading to increased c-di-GMP level and biofilm formation. Based on a transcriptome assay, it was revealed that mutation of *wspF* caused the expression of *psl* and *pel* operons to be upregulated. Those operons are involved in EPS production and biofilm formation (Hickman *et al.*, 2005).

There are some hints as why some chemosensory pathways are capable of affecting non-chemotactic pathway. One histidine kinase CheA was capable to transphosphorylate more than one CheY proteins (Szurmant and Ordal, 2004), indicating that CheA would be able to control not only chemotaxis but also other pathways. Energy taxis chemoreceptor TlpD in *Helicobacter pylori* can interact directly with CheA2 and enzymes not related with chemotaxis, AcnB (aconitate hydratase) and KatA (catalase). Moreover, about 70 genes expressions were altered in *tlpD* mutant (Behrens *et al.*, 2016). The reasons why would chemotaxis pathway be co-regulated with other functions are still unknown, but for sure it allows better survival chance for bacterial pathogens.

Bacterial pathogens still and will always be one of the threats to agricultural productivity. As world population rises, we could not afford to lose more of crops yields to pathogen in addition to the climate change problems. Research on *Pseudomonas syringae* as one of the model plant pathogens will certainly deepen our understanding on molecular plant-microbes interaction. Inhibition of bacterial chemotaxis is one of the promising sectors for effective disease prevention. However, due to the high number of chemoreceptors in plant pathogens, it is necessary to find out more about virulence-related chemoreceptors and their ligands that some may be specific to host plants, especially in less explored species.

1.7. Objectives

Pseudomonas syringae pv. *tabaci* 6605 (*Pta*6605) is a highly motile plant pathogen. Flagella-based motility is involved in this pathogen virulence. However, the requirement of chemotaxis-based motility is not known yet. Therefore, the general objective of this study is to elucidate how chemotaxis participate in *Pta*6605 pathogenicity on host tobacco plants. First, we aimed to identify and characterize *Pta*6605 chemosensory pathways responsible for chemotaxis-based motility and whether they are crucial for host plant infection. Second, we aimed to identify and functionally characterize pathogenicity-related chemoreceptors proteins and their corresponding ligands in *Pta*6605. As discussed in introduction section above, chemotaxis sensory pathways are intertwined with virulence-related pathways in some pathogenic bacteria. *Pta*6605 has more than fifty chemoreceptors-encoding genes in its genome, but not a single one has been annotated yet. Because of this, we hypothesized that *Pta*6605 would also harbors chemoreceptors which signaling pathway interconnected with cellular function controlling phenotypes indispensable for host plant colonization.

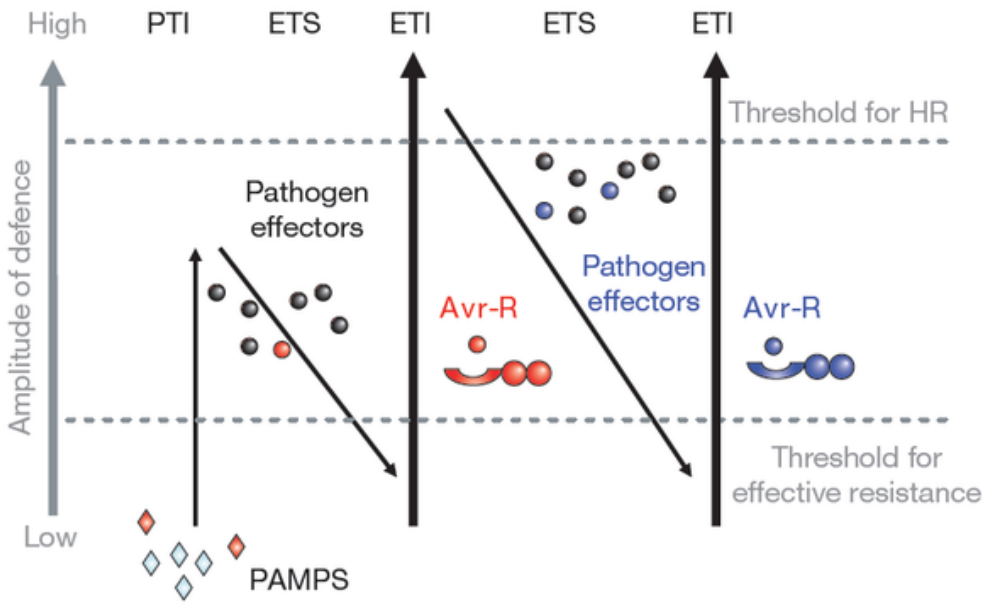

Fig 1.1. The 'zigzag' model of plant-pathogen interaction. PAMPs perceived by plants trigger PTI to stop pathogens invasion. Pathogens fight back using secreted effectors to interfere PTI causing ETS. Plants possessing R-genes would be able to recognize pathogen effectors and trigger ETI. Due to the evolution of pathogen effector genes, pathogen could have new effectors or lose the old ones to avoid recognition and suppress ETI. Figure adapted from Jones and Dangle (2006).

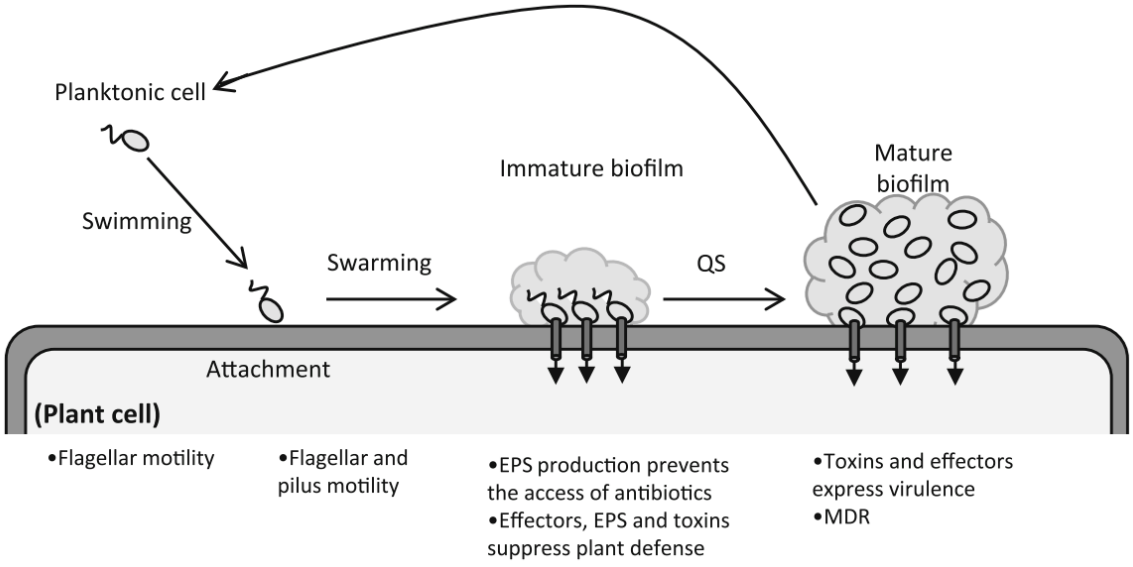

Fig. 1.2. Virulence factors of *Pseudomonas syringae*. Planktonic cells need flagella-based and pili-based motility to enter the plant and attach on plant cells. Sessile cells require biofilm formation, effectors and toxins production to suppress plant defense and cause disease. Figure adapted from Ichinose *et al.* (2013).

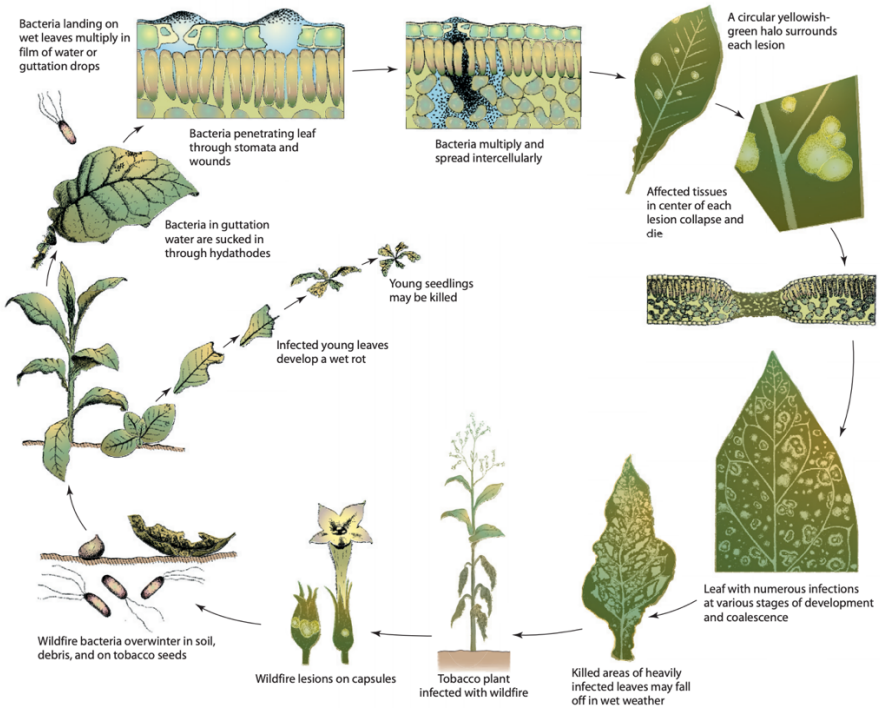

Fig 1.3. Disease cycle of wildfire on tobacco plants caused by *Pseudomonas syringae* pv. *tabaci*. In the field, bacterial inoculum is carried by rain or water splashes. High humidity and warm temperature speed up disease progression. Figure adapted from Agrios (2005).

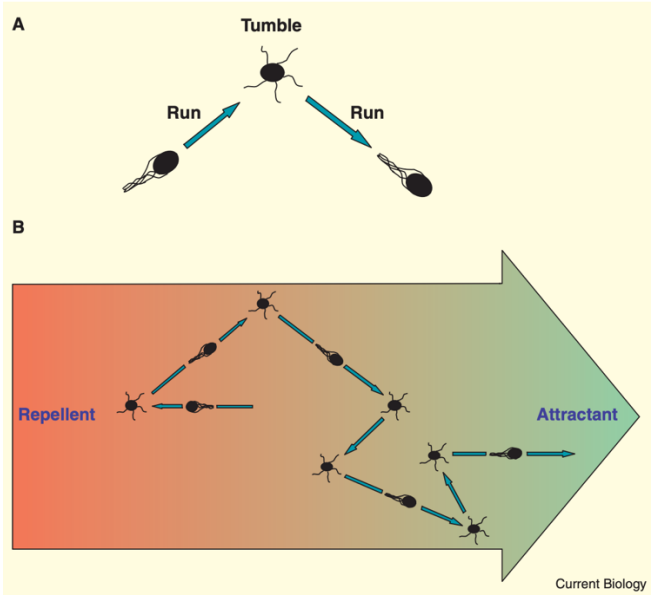

Fig 1.4. Schematic representation of bacterial chemotaxis. (A) Run and tumble movement of motile bacterial cells like *E. coli*. (B) Chemotactic bacteria can sense attractants and swim toward it or moving away from repellents. Figure adapted from Webre *et al.* (2003).

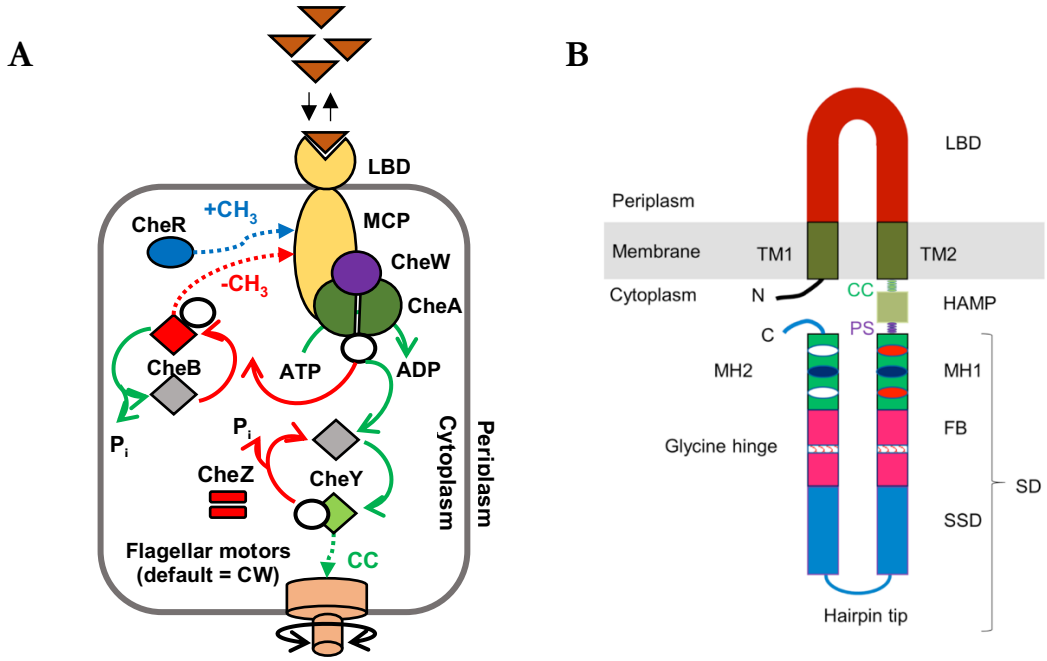

Fig 1.5. Typical signal processing in bacterial chemotaxis system. (A) Signaling network in bacterial chemotaxis system upon ligand binding on cytoplasmic chemoreceptors (MCPs). The chemotactic stimuli are processed further downstream by a histidine kinase CheA and response regulator CheY which controls flagellar rotation. Adaptation of MCPs is mediated by CheB and CheR. (B) Typical topology of MCPs. LBD, ligand binding domain; TM, transmembrane domain/helix; CC control cable; HAMP histidine kinase, adenyl cyclase, methyl-accepting chemotaxi protein and phosphatase region; PS, phase stutter; SD, signaling domain; MH, methylation helix; FB, flexible bundle; SSD, signaling subdomain. Figure adapted from Ud-Din and Roujeinikova (2017).

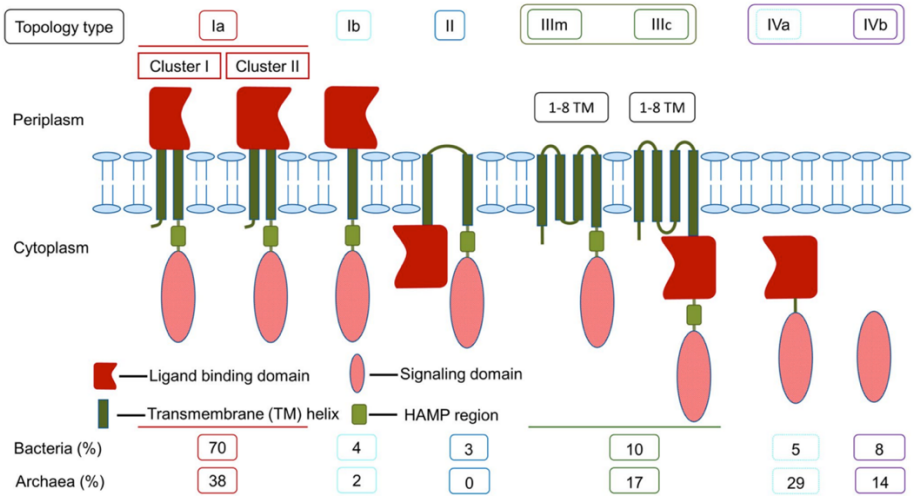

Fig 1.6. MCPs classification based on membrane topology and LBD localization. Class Ia MCPs are common in bacteria and can be further grouped into two subclasses based on the size of their LBDs. Figure adapted from Ud-Din and Roujeinikova (2017).

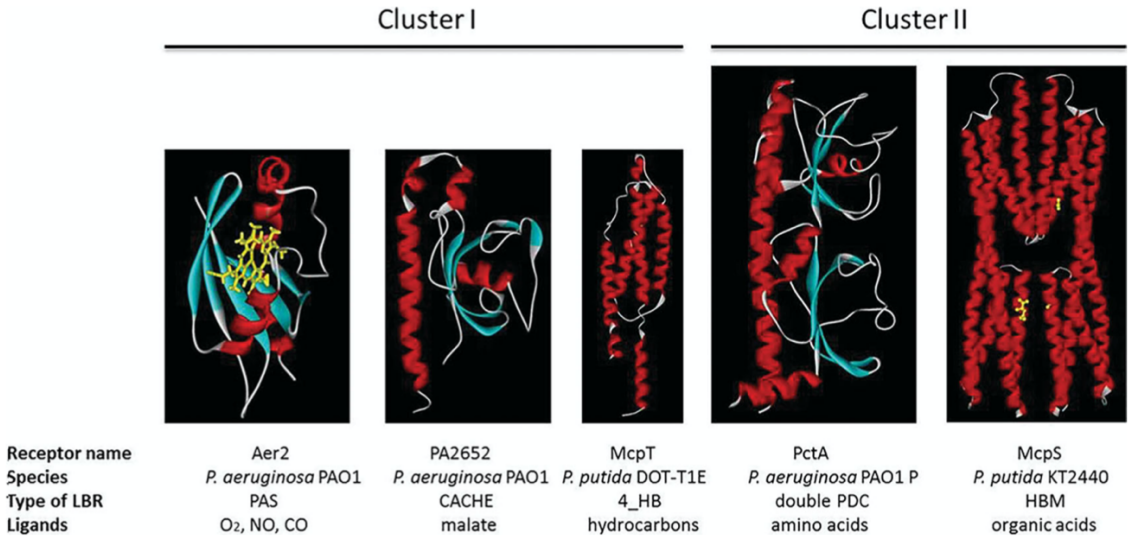

Fig 1.7. Structural diversity of Class Ia MCPs ligand binding domain (LBD). Representative of LBD types of identified chemoreceptors. Depicted in the picture, PAS domain of PA01 Aer2 bound heme (yellow) and HBM domain of KT2440 McpS bound malate and acetate (yellow). Figure adapted from Sampedro *et al.* (2015).

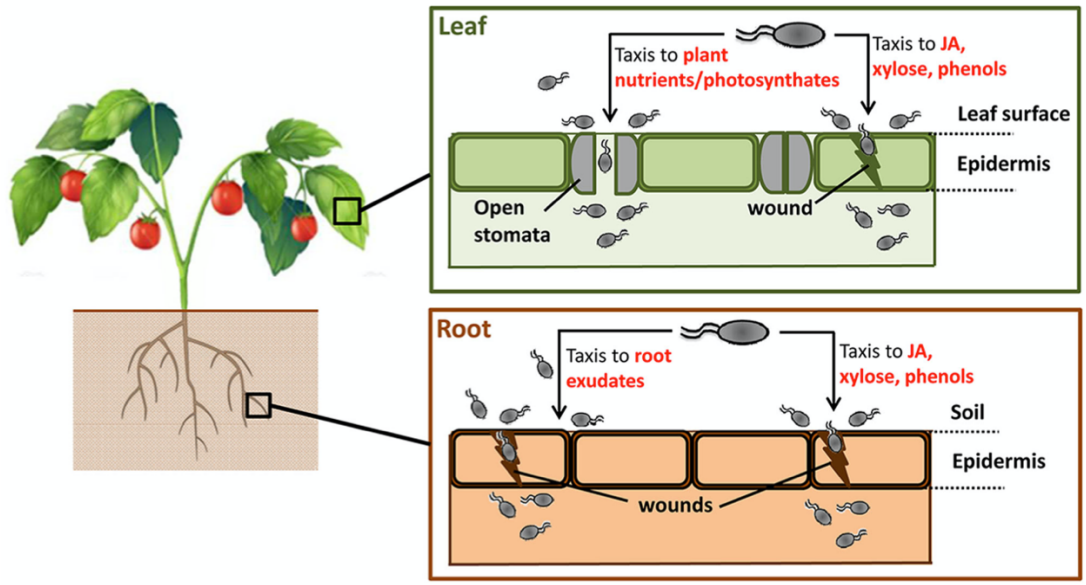

Fig 1.8. Schematic representation of chemotaxis involvement in plant infection by bacterial pathogens. Root and stomata or wounds on leaf can release plant-derived compounds that may trigger bacterial chemotactic response into these openings. Inside the plant, plant pathogen will reproduce and cause disease. Figure adapted from Matilla and Krell (2018).

Table 1.1. Methyl-accepting chemotaxis proteins (MCPs) in *Pta*6605

Locus Tag		LBD Type
A3SK_RS0100395	A3SK_RS0109810	4HB
A3SK_RS0101005	A3SK_RS0112370	
A3SK_RS0103740	A3SK_RS0114255	
A3SK_RS0105765	A3SK_RS0114850	
A3SK_RS0106220	A3SK_RS0116565	
A3SK_RS0106235	A3SK_RS0116645	
A3SK_RS0107170	A3SK_RS0121565	
A3SK_RS0107210	A3SK_RS0123225	
A3SK_RS0108300		
A3SK_RS0105285	A3SK_RS0123180	HBM
A3SK_RS0106985	A3SK_RS0124445	
A3SK_RS0117805	A3SK_RS0124450	
A3SK_RS0120685		
A3SK_RS0106980		dCACHE_1
A3SK_RS0112400		
A3SK_RS0114355		
A3SK_RS0126685		
A3SK_RS0112230		PAS_3-PAS_3-PAS_3-PAS_3
A3SK_RS0118845		PAS_3
A3SK_RS0111330		PAS_3-PAS_3
A3SK_RS0121510		
A3SK_RS0101665		PAS_4-PAS_3
A3SK_RS0105130		PAS_9
A3SK_RS0107145		PAS_9-PAS_3
A3SK_RS0102095		CACHE_2
A3SK_RS0123310		
A3SK_RS0127680		CACHE_3-CACHE_2
A3SK_RS0112260		
A3SK_RS0112125		CHASE_3
A3SK_RS0118485		FIST_N-FIST_C
A3SK_RS0100320		NIT
A3SK_RS0124915		PilJ
A3SK_RS0116555		TarH
A3SK_RS0106950		Unknown
A3SK_RS0109020		
A3SK_RS0112355		
A3SK_RS0114760		
A3SK_RS0120690		
A3SK_RS0109830		No LBD
A3SK_RS0112375		
A3SK_RS0120400		
A3SK_RS0121850		
A3SK_RS0126690		

Chapter 2

Cluster II *che* genes of *Pseudomonas syringae* pv. *tabaci* 6605, orthologs of cluster I in *Pseudomonas aeruginosa,* are required for chemotaxis and virulence

Abstract

Pseudomonas syringae pv. *tabaci* 6605 (*Pta*6605) is a causal agent of wildfire disease in host tobacco plants and is highly motile. *Pta*6605 has multiple clusters of chemotaxis genes including *cheA*, a gene encoding a histidine kinase, *cheY*, a gene encoding a response regulator, *mcp,* a gene for a methyl-accepting chemotaxis protein, as well as flagellar and pili biogenesis genes. However, only two major chemotaxis gene clusters, cluster I and cluster II, possess *cheA* and *cheY*. Deletion mutants of *cheA* or *cheY* were constructed to evaluate their possible role in *Pta*6605 chemotaxis and virulence. Motility tests and a chemotaxis assay to known attractant demonstrated that *cheA2* and *cheY2* mutants were unable to swarm and to perform chemotaxis, whereas *cheA1* and *cheY1* mutants retained chemotaxis ability almost equal to that of the wild-type (WT) strain. Although WT and *cheY1* mutants of *Pta*6605 caused severe disease symptoms on host tobacco leaves, the *cheA2* and *cheY2* mutants did not, and symptom development with *cheA1* depended on the inoculation method. These results indicate that chemotaxis genes located in cluster II are required for optimal chemotaxis and host plant infection by *Pta*6605 and that cluster I may partially contribute to these phenotypes.

Keyword: bacterial virulence, *cheA*, chemotaxis, *cheY*, flagellar motility, *Pseudomonas*

2.1. Introduction

Pseudomonas syringae is a model of foliar plant bacterial pathogens, which comprises about 50 pathovars based on its diverse interaction with their host plants, epiphytic survival, and the nature of the elicited disease symptoms (Xin *et al.*, 2018). *P. syringae* pv. *tabaci* 6605 (*Pta*6605) is one of the *P. syringae* strains that causes wildfire disease on tobacco plants (Ichinose *et al.*, 2003). To infect host plants, *P. syringae* requires several virulence factors including an Hrp type III secretion system, phytotoxins, quorum-sensing, and flagella- and type IV pili-mediated motilities (Ichinose *et al.*, 2003, 2013; Kanda *et al.*, 2011; Taguchi and Ichinose, 2011).

Pathogen entry into plant apoplastic spaces is a first key point for successful invasion and escaping the harsh environment on the leaf surface (Melotto *et al.*, 2006). Unlike fungal pathogens that can directly penetrate the epidermis, foliar bacterial pathogens like *P. syringae* need to enter through natural openings such as stomata, wounds, or hydathodes. The ability of *P. syringae* pv. *tomato* DC3000 (*Pto*DC3000), *Salmonella enterica*, and *Dickeya dadantii* to preferably move toward open stomata and wounding sites has been reported (Antúnez-Lamas *et al.*, 2009b; Kroupitski *et al.*, 2009; Melotto *et al.*, 2006). Nevertheless, how bacteria navigate on the leaf surface and locate natural opening sites is still poorly understood.

Chemotaxis is a way for plant-pathogenic bacteria to sense and respond to chemicals released from plant tissues to the leaf surface, and hence ensures survival and pathogenicity (Yao and Allen, 2006). Chemotaxis itself is the movement of an organism toward or away from a chemical stimulus. Motile bacteria can sense changes in the concentration of chemicals in their environments and respond to the changes by altering their motility pattern (Sourjik and Wingreen, 2012). Genetic analysis of the chemotaxis behavior has been studied extensively in *Escherichia coli*, *S. enterica*, and *Pseudomonas aeruginosa* (Blair, 1995; Bi and Lai, 2015; Kato *et al.*, 1999; Manson, 1992).

Comparative genomics of *Pto*DC3000 revealed that this foliar plant pathogen possesses at least two major chemotaxis-related gene clusters (Buell *et al.*, 2003; Clarke *et al.*, 2016). There are genes encoding two histidine kinases, CheA1 and CheA2, and two response regulators, CheY1 and CheY2. CheA and CheY are essential for a two-component phosphorelay system, enabling the bacteria cells to perform taxis toward chemical stimuli. Binding of a chemotactic signal to a chemoreceptor produces downstream information that modulates the histidine kinase CheA autophosphorylation activity. CheA will be autophosphorylated at specific histidine residues to form CheA-P. A phosphoryl group from CheA-P will be transferred to a specific aspartate residue of CheY to form active CheY-P, which is a response regulator of a two-component regulatory system. CheY-P interacts directly with a flagellar motor switch

protein to control the direction of the flagellar rotation, namely clockwise or counter-clockwise (Wadhams and Armitage 2004).

*Pta*6605 shows high motility and virulence (Taguchi *et al.*, 2010; Taguchi and Ichinose, 2011), making it a suitable model for studying the role of chemotaxis in this species. The bacterial flagellum motor is a molecular machine that generates energy and rotates flagella. The motor complexes are composed of two stator proteins MotA and MotB or MotC and MotD. Genes *motA* and *motB* are tandemly located within a potential operon, whereas *motC* and *motD* are also tandemly located but in a different position from *motAB* on the chromosome. Previous study using Δ*motAB* and Δ*motCD* mutant strains demonstrated that MotCD is required for flagellar motility but not another stator protein MotAB (Kanda *et al.*, 2011). Genes *motCD*, *cheA2*, and *cheY2* are located in the same chemotaxis gene cluster (*che2*), whereas *cheA1* and *cheY1* are located in another chemotaxis gene cluster (*che1*, Fig. 2.1).

Thus, in this study, to investigate how CheA and CheY contribute to *Pta*6605 motility and how chemotaxis affects the virulence of this strain, we generated the *Pta*6605 mutants *cheA1*, *cheA2*, *cheY1*, and *cheY2* from two chemotaxis gene clusters. Based on tests of chemotaxis toward a known attractant, *cheA2* and *cheY2* mutants lack chemotactic ability. Furthermore, the *cheA2* and *cheY2* mutants had reduced or altered surface motility. More importantly, they also had remarkably reduced virulence on host tobacco plants, which suggests that chemotaxis is indeed required for effective host plant colonization and that the chemotaxis required for virulence in *Pta*6605 is *che2* pathway–dependent. The nomenclature for chemotaxis genes is confusing: chemotaxis gene cluster I in *P. syringae* is an ortholog of chemotaxis gene cluster II in *P. aeruginosa*, whereas chemotaxis gene cluster II in *P. syringae* is an ortholog of chemotaxis gene cluster I in *P. aeruginosa* (Fig. 2.1, Clarke *et al.*, 2016; Ferrández *et al.*, 2002). To avoid confusion, we designated the former genes as a group II chemotaxis gene cluster and the latter genes as a group III chemotaxis gene cluster, as described below in the Results section.

2.2. Materials and methods

2.2.1. CheA and CheY phylogenetic analysis

We obtained the CheA and CheY amino acid sequences from previous reports that characterized chemotaxis genes functions from the Pseudomonas Genome Database and GeneBank. Bacteria strains included in the phylogenetic tree were *P. syringae* pv. *tabaci* 6605 (*Pta*6605), *P. syingae* pv. *phaseolicola* 1448a (*Pph*1448A) (Joardar *et al.*, 2005), *P. syringae* pv. *tomato* (*Pto*DC3000) (Buell *et al.*, 2003), *P. fluorescens* F113 (Redondo-Nieto *et al.*, 2011), *Ralstonia solanacearum* GMI1000 (Salanoubat *et al.*, 2002), *P. aeruginosa* PAO1 (Stover *et al.*, 2000), *Vibrio*

cholera O395 (Feng *et al.*, 2008), *S. enterica* serovar Typhimurium LT2 (McClelland *et al.*, 2001), and *E. coli* K12 (Blattner *et al.*, 1997). Amino acid sequences of CheA and CheY were aligned with ClustalW, and neighbor-joining trees were constructed based on the alignment using MEGA7 software.

2.2.2. Bacterial strains and growth condition

The bacterial strains used in this study are listed in Table 2.1. *Pta*6605 strains were maintained in King's B (KB) medium supplemented with 50 μg/ml nalidixic acid (Nal) at 27ºC (King *et al.* 1954; Taguchi *et al.*, 2003). *E. coli* strains were grown in Luria Bertani (LB) medium supplemented with appropriate antibiotics at 37ºC.

2.2.3. Host plant and inoculation procedure

Tobacco plants used in this study (*Nicotiana tabacum* L. var. Xanthi NC) were grown at 28ºC with an 18-h photoperiod. Plant infection assays were carried out by several methods. We modified a flood inoculation system for tobacco seedlings based on the system that was described in Ishiga *et al.* (2011). Tobacco seeds were sterilized and sown on Murashige-Skoog (MS) 0.8% agar plates containing 1% sucrose and vitamin stock solution (thiamin hydrochloride 3 mg/L, nicotinic acid 5 mg/L, pyridoxine hydrochloride 0.5 mg/L), and grown at 28ºC under 16 h light-8 h dark conditions for 2 wk. Tobacco seedlings were transplanted to MS 0.8% agar plates containing 0.1% sucrose and vitamin stock solution as described above and grown for 2 d under the same conditions.

Bacteria were grown overnight at 27ºC in LB medium with 10 mM $MgCl_2$. The bacterial inoculum was adjusted to OD_{600} = 0.004 (8×10^6 colony forming unit, (CFU)/ml) with sterilized 10 mM $MgSO_4$ containing 0.025% (v/v) Silwet L-77 (OSI Specialties, Danbury, CT). Sterilized 10 mM $MgSO_4$ was used as a mock inoculation. The bacterial suspension (approximately 30 ml) was poured onto the plate of tobacco seedlings. After about 10 sec incubation, the bacterial suspension was decanted, and the plate was air-dried on a clean bench for 15 min. The plants were incubated under 16 h light-8 h dark conditions at 22ºC and disease symptoms were observed for 3 d post-inoculation (dpi). To determine the bacterial population at 3 h post-inoculation (hpi) and 3 dpi, leaf disks were punched out using a disposable biopsy hole punch and then ground with a mortar and pestle. The homogenates were serially diluted in sterile distilled water and then spread on KB plates containing Nal. The plates were dried and incubated at 27ºC for 2 d, after which the bacterial population was measured by counting the number of colonies, CFU.

We also employed the classical dip inoculation method described by Taguchi and Ichinose (2011) with some modifications. A single colony of bacteria was grown in 3 mL LB with $MgCl_2$. After 8 h incubation at 27ºC, bacteria were re-inoculated into 10 mL KB medium without antibiotic and further incubated at 27ºC for 12–16 h. The bacteria suspension was then washed with 10 mM $MgSO_4$ and adjusted to OD_{600} of 0.1 (approximate density of bacteria was 2×10^8 CFU/mL). Silwet L-77 was added at 0.04% (v/v) to the bacterial suspension prior to the dip inoculation experiment. Detached leaves of 8-wk-old tobacco plants were dipped into the bacterial suspension for 2 min and placed in a tray covered with plastic wrap. Cut petioles were wrapped and supplied water with cotton. Pictures were taken 5 and 10 dpi. In one experiment, three leaves from independent plants were used for each bacterial strain.

The infiltration experiment was done by injecting bacterial cells with a needleless syringe at density 2×10^5 CFU/mL into attached leaves of whole plants or detached tobacco leaves (three leaves for each bacterial strain). The inoculated detached leaves and plants were incubated in a growth chamber at 22ºC with a long-day photoperiod (16 h light-8 h dark). Disease development was observed, and photographs were taken at 14 dpi.

2.2.4. Construction of *che* deletion mutant strains

To generate deletion mutant strains, genetic regions containing *cheA1* (A3SK_RS0109815), *cheY1* (A3SK_RS0109825), *cheA2* (A3SK_RS0105665), and *cheY2* (A3SK_RS0105655) in *Pta*6605 were amplified and subcloned into a pGEM®-T Easy Vector (Promega, Madison, WI, USA) by the respective primer pairs listed in Table 2.2. The next sets of primer pairs then were used to delete each open reading frame (ORF) by inverse PCR. This procedure resulted in the internal deletion of 2080 bp, 340 bp, 2270 bp, and 360 bp of *cheA1*, *cheY1*, *cheA2*, and *cheY2*, respectively (Fig. 2.1). PCR products were treated by *Dpn*I and digested by *Bam*HI, then self-ligated using 2 × Ligation mix (Nippon Gene, Tokyo, Japan). Each deletion mutant DNA fragment was excised and inserted into the mobilizable cloning vector pK18*mobsacB* via *Eco*RI site (Schäfer *et al.*, 1994). The resulting plasmids were transformed into *E. coli* strain S17-1 and integrated into the wild-type (WT) strain of *Pta*6605 by conjugation and homologous recombination according to the previously described method (Shimizu *et al.*, 2003; Ichinose *et al.*, 2020). The sequence of each recombinant DNA was confirmed by DNA sequencing using a Big Dye Terminator Cycle Sequencing Kit and ABI PRISM 3100 sequencer (Thermo Fisher Scientific, Waltham, MA, USA).

2.2.5. Construction of complemented strains

To generate complemented strains of *cheA1*, *cheA2,* and *cheY2*, full lengths of each gene fragment with their predicted promoter regions were amplified using the primers listed in Table 2, and then cloned into expression vector pDSK519 (Keen *et al.*, 1988) at *Bam*HI (*cheA2*), *Not*I (*cheY2*), and *Eco*RI (*cheA1*) sites. Recombinant plasmids were transformed into *E. coli* S17-1 and introduced into Δ*cheA2*, Δ*cheY2*, and Δ*cheA1* by conjugation.

2.2.6. Chemotaxis assay

Chemotaxis was assayed by a microtiter plate multi-capillaries method (Reyes-Darias *et al.*, 2016) with minor modification. Bacteria were grown in 3 mL LB with 10 mM $MgCl_2$ overnight and inoculated into 3 mL fresh minimal medium supplemented with 10 mM of mannitol and fructose (MMMF, 50 mM potassium phosphate, 7.6 mM $(NH_4)_2SO_4$, 1.7 mM $MgCl_2$, 1.7 mM NaCl, and 10 mM mannitol and fructose) for further 5 h incubation. Then cells were washed twice with 10 mM HEPES buffer by 1700 × g centrifugation for 10 minutes at 25ºC. The cell density was adjusted to OD_{600} of 0.05 with 10 mM HEPES as chemotaxis buffer.

To prepare the capillary for the chemotaxis assay, one end of a 5 μL capillary (Drummond Scientific Company, Broomall, PA, USA) was sealed with a flame. The heated capillary was dipped into 1% yeast extract or 10 mM HEPES buffer to fill it as negative control. A rubber collar was fitted onto the capillary to support it during the assay. Each well of the round-bottom Falcon® microtiter plate (Corning, Corning, NY, USA) was filled with 230 μL bacterial suspension and the prepared capillary was dipped into the bacterial suspension. After incubation for 30 minutes at 27ºC, the capillary was washed with sterile distilled water, and the contents of the capillary (5 μL) was squirted into 45 μL 0.9% NaCl. Following serial dilution, 10 μL of bacterial suspension was plated onto a KB plate containing 50 μg/ml Nal. The plate was incubated at 27ºC for 2 d, and the number of colonies that appeared was counted to determine the strength of chemotaxis.

2.2.7. Motility assay

Bacterial surface swarming and swimming motility tests were conducted as described previously (Taguchi and Ichinose, 2011). Briefly, bacteria cultured overnight in 3 mL LB with 10 mM $MgCl_2$ were washed and resuspended in 10 mM $MgSO_4$ to an OD_{600} of 0.1. Three μL of bacterial suspension was spotted on the center of SWM plates (0.45% agar, 0.5% peptone, and 0.3% yeast extract; Difco, Detroit, MI, USA) for the swarming assay and 0.25% agar

MMMF plates for the swimming assay. The swarming plate was incubated at 27ºC and photographed at 48 h after inoculation, while the swimming plate was incubated at 23ºC and was photographed at 72 h after inoculation.

2.2.8. Statistical analyses

The results of chemotaxis assays and measurements of bacterial growth are expressed as means with standard error. One-way/two-way ANOVA followed by Tukey's or Dunnett's highly significant difference tests were performed using GraphPad Prism ver. 8 (GraphPad Software Inc., San Diego, CA, USA). $P < 0.05$ was considered statistically significant.

2.3. Results

2.3.1. Identification of chemotaxis gene clusters in *P. syringae* pv. *tabaci* 6605

In a draft genome sequence of *Pta*6605, we found two chemotaxis gene clusters that include the genes encoding CheA and CheY proteins (Fig. 2.1). A phylogenetic tree of CheA was constructed (Fig. 2.2). The CheA2 of *P. syringae* belongs to the same clade as those of *P. aeruginosa* (CheA1), *P. fluorescens* (CheA1), and *V. cholerae* (CheA2) which are known to be functional (Ferrández *et al.*, 2002; Gosink *et al.*, 2002; Manoharan *et al.*, 2015; Muriel *et al.*, 2015) (group III). It is known that there are plural *cheA* genes in the genome of the above species. Meanwhile, CheA1 of *P. syringae* is similar to other members of the CheA proteins such as *P. aeruginosa* (CheA2), *P. fluorescens* (CheA2 and CheA3), and *V. cholerae* (CheA3), and all members of group II belong to the same clade. We also observed that functional CheA proteins from *E. coli*, *R. solanacearum*, and *S. enterica* (Olsen *et al.*, 2013; Parkinson, 1978; Yao and Allen, 2006) constructed a single clade, and each species has only single gene for *cheA* (group I). The remaining CheA, CheA1 of *V. choletrae*, showed low homology with other CheA proteins and comprised another independent clade (group IV).

Phylogenetic analysis of CheY amino acid sequences also showed four clades (Fig. 2.3). Interestingly, each CheY protein of the clade in Fig. 2.3 is a partner protein of CheA of the corresponding group (Fig. 2.2). For example, CheA1 of *Pto*DC3000 and *Pta*6605 and CheA2 of *P. aeruginosa* belong to group II (Fig. 2.2), and CheY1 of *Pto*DC3000, *Pta*6605, and CheY2 of *P. aeruginosa* also belong to group II (Fig. 2.3). Furthermore, CheA2 of *Pto*DC3000 and *Pta*6605 and CheA1 of *P. aeruginosa* belong to group III, and CheY2 of *Pto*DC3000 and *Pta*6605 and CheY1 of *P. aeruginosa* also belong to group III (Clarke *et al.*, 2016; Ferrández *et al.*, 2002). In the

same way, CheA and CheY proteins of *S. enterica*, *E. coli*, and *R. solanacearum* belong to group I (Fig. 2.2 and 2.3, Kuo and Koshland, 1987; Stecher *et al.*, 2004), and the remaining CheA1, CheY1, and CheY2 of *V. cholerae* belong to group IV. In this paper, we used the names 'group II chemotaxis gene cluster' and 'group III chemotaxis gene cluster' to avoid confusion (Fig. 2.1, 2.2 and 2.3).

2.3.2. Surface motility of *cheA* and *cheY* deletion mutants

To investigate how CheA and CheY contribute to *Pta*6605 motility, we first conducted surface swarming assays. In liquid medium, both Δ*cheA2* and Δ*cheY2* mutants were still able to swim, but only in a 'running' mode. On the other hand, both Δ*cheA1* and Δ*cheY1* mutants were able to 'run' and 'tumble' just like WT (data not shown). In semi-solid media, however, some surface motilities were compromised. Surface swarming assays showed that Δ*cheA1* and Δ*cheY1* have swarming abilities similar to the WT strain, whereas the swarming ability of both Δ*cheA2* and Δ*cheY2* was lost (Fig. 2.4.A). Complementation by introducing full length *cheA2* and *cheY2* to each respective mutant strain restored surface swarming motilities. The swimming motility of Δ*cheA2* and Δ*cheY2* was also lost, whereas that of Δ*cheA1* and Δ*cheY1* was reduced to some extent (Fig. 2.4.B). Furthermore, complementation of *cheY2* in the Δ*cheY2* mutant restored some swimming motility, while the complementation of strain *cheA2* did not restore the phenotype (Fig. 2.4.B).

2.3.3. Chemotaxis ability

Quantitative chemotaxis assays were conducted to investigate how the deletion of *cheA* and *cheY* genes on both clusters affect chemotaxis of *Pta*6605 to 1% yeast extract as a known attractant. Quantified results clearly showed that the chemotaxis of Δ*cheA1* and Δ*cheY1* was slightly reduced from the WT strain, whereas Δ*cheA2* and Δ*cheY2* had remarkably reduced chemotaxis, and both complemented strains restored the phenotype (Fig. 2.5). These indicated that the group III chemotaxis gene cluster (cluster II) is indispensable for *Pta*6605 chemotaxis, whereas mutation in the group II chemotaxis gene cluster (cluster I) has almost no effect.

2.3.4. Virulence of mutants on host tobacco leaves

The ability of the WT and *che* mutant strains to cause disease on host tobacco plants was investigated by a flood assay optimized for tobacco seedlings (Fig. 2.6), dip inoculation, and infiltration (Fig. 2.7). In the flood assay inoculation, Δ*cheA1*, Δ*cheA2*, and Δ*cheY2* were less

virulent than the WT strain, whereas Δ*cheY1* was virulent, and complemented strains, Δ*cheA2*-C and Δ*cheY2*-C, restored the virulence although it was still weaker than that of the WT strain (Fig. 2.6.A). We also investigated bacterial propagation in the seedling leaves (Fig. 2.6.B) and found that both Δ*cheA2* and Δ*cheY2* mutants and Δ*cheA1* grew less than the WT strain at both time points, although the differences are not significant at 3 hpi, while Δ*cheY1* propagated to the same level as the WT strain. Both complemented strains, Δ*cheA2*-C and Δ*cheY2*-C, retained the same ability to propagate on host tobacco seedlings as the WT strain.

Dip inoculation with detached leaves showed that WT and Δ*cheY1* caused similar severe disease symptoms, and Δ*cheA1* also caused disease symptoms, although the severity of symptoms of Δ*cheA1* was weaker than those of WT and Δ*cheY1* (Fig. 2.7.A). Furthermore, Δ*cheA2* did not cause any symptoms, and Δ*cheY2* caused very mild chlorosis and necrotic lesions. However, we observed that Δ*cheA1* was less virulent in the flood inoculation method (Fig. 2.6). We confirmed the reproducibility these results with different lines of Δ*cheA1* mutant strains and got the same results (Fig. 2.8).

Differences in virulence of WT and mutant strains were also investigated by the infiltration inoculation method with attached leaves of whole plants. Although we speculated that mutation of the *che* genes would not have any effect when the bacteria were directly injected into the leaf's apoplastic spaces by infiltration, Δ*cheA1*, Δ*cheA2*, and Δ*cheY2* caused just few localized lesions, while WT and Δ*cheY1* caused the same level of disease symptoms in the inoculated leaves of whole plants (Fig. 2.7.B). The complemented strains, Δ*cheA2*-C and Δ*cheY2*-C, showed partially restored virulence. Because Δ*cheA1* showed different phenotypes between dip and infiltration inoculation (Fig. 2.7), we also performed infiltration inoculation using detached leaves and attached leaves of whole plants. As shown in Fig. 2.8.C, all Δ*cheA1* strains did not cause any disease symptoms when we used whole plants, but developed disease symptoms like the WT strain on detached leaves.

To investigate the viability, all mutant strains were grown in liquid rich KB and MMMF media (Fig. 2.9). In rich KB medium, no mutant strain showed delayed logarithmic growth compared to WT. Instead, Δ*cheY1*, Δ*cheA2* and Δ*cheY2* mutants grew faster. However, in a minimal media that mimics the apoplastic space of plants, only Δ*cheA1* and Δ*cheY2* grew less than WT at most time points.

2.3.5. In *trans* complementation of *cheA1* does not restore Δ*cheA1* phenotypes

Δ*cheA1* had reduced swimming motility and lost virulence on host tobacco plants. To elucidate the reason behind the loss of phenotypes, we introduced the *cheA1* gene into the mutant strain. However, the complementation did not help the mutant strain to recover its swimming motility and virulence (Fig. 2.10).

2.3.6. Phenotypic assay of *cheY1*/*cheA1* overexpression on Δ*cheY2*/Δ*cheA2*

We also conducted experiments on overexpressing *cheY1* in Δ*cheY2* as well as *cheA1* in Δ*cheA2* to determine whether overexpression of *cheY1*/*cheA1* can replace *cheY2*/*cheA2* functions. Our results showed that overexpressing both *che1* genes did not complement the Δ*cheY2* and Δ*cheA2* ability to swim and swarm on soft agar, and further the ability to infect tobacco seedlings (Fig. 2.11 and 2.12).

2.4. Discussions

Plant pathogenic bacteria employ various virulence factors for effective plant infection. Among the virulence factors including the well-characterized type III secretion system, motility of flagella and type IV pili, and phytotoxin production, chemotaxis is considered important for bacteria to navigate through the plant phylloplane toward signal cues coming from stomata or wounds (Ichinose *et al.*, 2013; Matilla and Krell, 2018). The versatility of chemotaxis in phytopathogenic bacteria can be understood from the large number of chemotaxis receptor genes compared to animal pathogenic bacteria: for example, *P. syringae* possesses about 50 genes for chemoreceptors, MCP, whereas *P. aeruginosa* possesses only 24–26 *mcp* genes (Matilla and Krell 2018). Furthermore, it is known that Pseudomonad bacteria possess plural chemotaxis gene clusters (Clarke *et al.*, 2016; Ferrández *et al.*, 2002; Muriel *et al.*, 2015). In the beneficial strains like *P. fluorescens* F113, more than one chemotaxis system is necessary for rhizosphere colonization (Muriel *et al.*, 2015). Such versatility makes the chemotaxis system difficult to characterize. In this study, we attempted to characterize the function of chemotaxis systems in a highly motile bacterium, *Pta*6605.

2.4.1. *Pta*6605 possesses two major chemotaxis systems

P. syringae shares high genomic DNA homology among its pathovars. The whole genome sequence of *Pto*DC3000 was previously determined (Buell *et al.,* 2003), and it possesses *che1* (group II chemotaxis gene cluster) and *che2* (group III chemotaxis gene cluster) containing *cheA* and *cheY* for a two-component system and three minor chemotaxis gene clusters without *cheA* and *cheY* (Clarke et al. 2016). Because *cheA* and *cheY* are indispensable genes for chemotaxis, we speculated that there are two major chemotaxis gene clusters.

The existence of multiple *che* clusters in the *P. syringae* genome indicates the complexity of the chemotaxis configuration. Like *Pto*DC3000, *Pta*6605 has group II and group III chemotaxis gene clusters containing *cheA* and *cheY,* demonstrating the importance of these two major chemotaxis gene clusters (Fig. 2.1). We compared *Pta*6605 CheA and CheY amino acid sequences with those of other Gram-negative bacteria and generated phylogenetic trees (Fig. 2.2 and 2.3). The effects of mutation in each *cheA* or *cheY* gene obtained from the previous reports and this study was incorporated into the phylogenetic trees as symbols. Interestingly, the *cheA* and *cheY* gene mutations that resulted in the remarkable reduction or loss of motility were concentrated in two respective clades, groups I and III; furthermore, mutation of *cheA* and *cheY* genes in the other clades, groups II and IV, only weakly reduced motility or had no effect.

The group I bacteria such as *R. solanacearum*, *E. coli*, and *S. enterica* have only one *cheA* and *cheY*, while *Pseudomonas* and *Vibrio* species have plural sets of chemotaxis genes (groups II, III, and IV). Among them, *cheA* and *cheY* genes in group III seem to be essential and major, and those of group II and IV seem to be redundant. Therefore, the group III chemotaxis gene cluster in *Pta*6605 is the major chemotaxis gene cluster controlling the flagellar-based chemotaxis and motility. However, Δ*cheA1* showed less virulence than the WT strain in all inoculation methods (Fig. 2.6 and 2.8), indicating that CheA1 plays some role in plant–pathogenic bacteria interactions.

2.4.2. Group III chemotaxis gene cluster controls flagellar-based motility and chemotaxis of *Pta*6605

Swarming is a movement of coordinated multicellular flagellated bacteria across a solid surface (Kearns, 2010). Unlike swarming, swimming motility is a movement of individual cells in a liquid environment and is associated with flagella rotation and chemotaxis (Wadhams and Armitage, 2004). Previous studies reported that Δ*fliC* and Δ*motCD* mutants lost surface

swarming and swimming motilities in a semisolid agar medium (Kanda *et al.,* 2011; Shimizu *et al.,* 2003; Taguchi *et al*., 2006), and the Δ*pilA* mutant lost surface swarming motility and had reduced swimming motility, although Δ*pilA* retained the swimming ability in a liquid medium (Taguchi and Ichinose, 2011). These results demonstrated that surface motility is dependent on bacterial flagella and pili, and are consistent with our finding that Δ*cheA2* and Δ*cheY2* had lost surface swarming motility (Fig. 2.4.A) and had remarkably reduced chemotaxis to 1% yeast extract (Fig. 2.5).

Furthermore, the swimming ability of Δ*cheA2* and Δ*cheY2* was completely abolished on MMMF semisolid media (Fig. 2.4.B), therefore implying that the group III chemotaxis gene cluster is the canonical chemotaxis pathway responsible for flagellar-mediated motility and chemotaxis. In *P. aeruginosa*, the PAO1 mutation of genes located in the group III chemotaxis gene cluster also resulted in the loss of chemotactic motility (Ferrández *et al*., 2002; Güvener *et al*., 2006).

However, the function of the group II chemotaxis gene cluster is still unclear. Although these genes were not necessary for surface swarming motility and chemotaxis in *Pta*6605, the *cheA1* mutant had reduced swimming motility and was less virulent in the flood inoculation method (Fig. 2.6.A & 2.8.A) and infiltration of attached leaves (Fig. 2.8.C). The partially similar results were obtained by Clarke *et al.,* (2016), using a *cheA* mutant of *Pto*DC3000, in which *cheA1* retained swimming and swarming motilities but reduced virulence on its host tomato plant. Unexpectedly, the complemented strain of *cheA1* mutant that we generated did not restore the swimming motility and virulence (Fig. 2.10). This might be due to polar effects that occurred during mutagenesis, and the complemented strain might have a defect in the gene expression of the group II chemotaxis gene cluster because this region is known to be important for chemotaxis and signal transduction. For example, *mcpB*, which localizes downstream of *cheA2* in PAO1 is possibly essential for signal transduction (Güvener *et al.,* 2006), and mutation of *cheB2* reduced chemotaxis (Ferrández *et al.,* 2002).

2.4.3. Group III chemotaxis gene cluster may modulate not only chemotaxis functions but also other virulence factors

Virulence assays were done to further investigate how necessary motility and chemotaxis are for *Pta*6605 to cause disease in host plants. The flood assay inoculation (Fig. 2.6) which mimics the condition in nature provided the idea that *cheA2* and *cheY2* mutants that are impaired in motility and chemotaxis are unable to enter and colonize the apoplastic space and thus fail to cause disease. These data are also consistent with those reported by Clarke *et al.*

(2016). Clarke *et al.* found that *cheA2* mutants of *Pto*DC3000 and another strain *Pto*1108 propagated less in host plants, indicating that the motility and chemotaxis dominated by group III chemotaxis gene cluster are primarily important during the early stage of infection. However, following dip inoculation, *cheA1* and *cheY1* may not be needed for *Pta*6605 virulence (Fig. 2.7.A). This might be because a detached leaf does not have the optimal defense against infection that seedlings have.

We also inoculated tobacco leaves of whole plants by infiltration (Fig. 2.7.B). Contrary to the previous beliefs that motility and chemotaxis are not important once bacteria enter a favorable infection site (Clarke *et al.*, 2016; Yu *et al.*, 2013), Δ*cheA2*, Δ*cheY2*, and even Δ*cheA1* had decreased ability to cause disease in infiltration inoculation (Fig. 2.7.B). These results indicate that beside chemotactic motility, *cheA2* and *cheY2* may regulate another signal transduction pathway. Recently, Cerna-Vargas *et al.*, (2019) also reported that the amino acid chemoreceptor, PscA of *Pto*DC3000 mediates not only chemotaxis but also controls the level of cyclic di-GMP, biofilm formation, and swarming motility through perception of the abundant plant amino acids. The chemotactic signaling pathway may affect not only directional motility but also the expression of various virulence-related genes. Furthermore, the virulence of Δ*cheA1* differed depending on the inoculation method: a moderate level of disease symptoms was developed by the dip inoculation method (Fig. 2.7.A), whereas no symptoms appeared with flood and infiltration inoculation methods (Fig. 2.6 and Fig. 2.7.B).

Because the dip inoculation method uses detached leaves, whereas flood and infiltration inoculation methods use whole plants, we performed infiltration experiments using detached leaves and leaves of whole plants (Fig. 2.8). The Δ*cheA1* caused WT level disease symptoms in detached leaves, whereas it did not cause any symptoms in whole plants, suggesting that a weakened defense system in detached leaves allowed the successful Δ*cheA1* invasion. We also cannot rule out the possibility of Δ*cheA1* bacterial viability inside the attached leaves because of its slower growth in minimal media (Fig. 2.9). However, a complemented strain of the *cheA1* mutant did not recover virulence by infiltration and flood assay inoculation method (Fig. 2.7.B and 2.10.B), as discussed above. Further, these results indicate that *cheA1* also necessary for *Pta*6605 to cause disease on host tobacco plants.

Overexpression of *cheY1* in the Δ*cheY2* and *cheA1* in the Δ*cheA2* did not change the phenotypes (Fig. 2.11 and 2.12), unlike overexpression of *cheB2* in the Δ*cheB* mutant of PAO1, which was able to partially complement the phenotype (Ferrández *et al.*, 2002). Possessing multiple chemotaxis cluster indicating the complexity of *Pta*6605 chemotaxis system. There have been discussions about the relation between the localization of chemotaxis protein and

their functions in *Rhodobacter sphaeroides* and *E. coli* (Sourjik and Armitage, 2010). Deletion of a chemotaxis gene cannot be complemented by expressing its homologs from different chemotaxis gene clusters because one of them is localized in cell pole while the another is cytoplasmic. This result suggests that the roles of CheY1/CheA1 and CheY2/CheA2 in the *Pta*6605 chemotaxis signaling pathway and their localization are not identical, thus CheY1/CheA1 is not able to substitute the loss of CheY2/CheA2.

Some reports have described how chemotaxis systems are correlated with other functions beside chemotaxis, such as cholera toxin production in *V. cholera* (Bandyopadhaya and Chaudhuri, 2009; Lee *et al.*, 2001). As discussed above, the ability of CheA2 to phosphorylate other CheYs opens the possibility that *Pta*6605 CheA2 may regulate many bacterial functions other than chemotaxis (Porter and Armitage, 2002; Szurmant and Ordal, 2004). Several characterizations of relevant virulence factors and gene expression analysis in *Pta*6605 are needed to support this idea. Nevertheless, considering all the inoculation results, we propose that the group III chemotaxis gene cluster in *Pta*6605 might function as a major part of the complex virulence regulators, and is thus required for fully functional chemotaxis and optimal host infection.

Table 2.1. Bacterial strains and plasmids used in this study

Bacterial strain, plasmid	Relevant characteristics	Reference or source
Escherichia coli		
DH5α	*F– λ– ϕ80dLacZ ΔM15 Δ (lacZYA-argF)U169 recA1 endA1 hsd*R17(*rK – mK +) supE44 thi-1 gyrA relA1*	Nippon Gene, Tokyo, Japan
S17-1	*thi pro hsd*R *hsd*R *hsdM+ recA(chr::RP4-2-Tc::Mu-Km::Tn7)*	Schäfer *et al.* 1994
Pseudomonas syringae pv. *tabaci*		
Isolate 6605	Wild-type isolated from tobacco, Nal^r	Shimizu *et al.* 2003
6605-Δ*cheA1*	Isolate 6605 Δ*cheA1,* Nal^r	This study
6605-Δ*cheY1*	Isolate 6605 Δ*cheY1*, Nal^r	This study
6605-Δ*cheA2*	Isolate 6605 Δ*cheA2*, Nal^r	This study
6605-Δ*cheY2*	Isolate 6605 Δ*cheY2*, Nal^r	This study
6605-Δ*cheA2-C*	pD-*cheA2* containing Δ*cheA2*, Nal^r Km^r	This study
6605-Δ*cheY2-C*	pD-*cheY2* containing Δ*cheY2*, Nal^r Km^r	This study
6605- Δ*cheA1-C*	pD-*cheA1* containing Δ*cheA1*, Nal^r Km^r	This study
6605- Δ*cheY2-C(Y1)*	pD-*cheY1* containing Δ*cheY2*, Nal^r Km^r	This study
6605- Δ*cheA2-C(A1)*	pD-*cheA1* containing Δ*cheA2*, Nal^r Km^r	This study
Plasmid		
pGEM-TEasy	Cloning vector, Amp^r	Promega, Madison, WI, USA
pG-*cheA1*	*cheA1* fragment-containing pGEM-TEasy, Amp^r	This study
pG-*cheY1*	*cheY1* fragment-containing pGEM-TEasy, Amp^r	This study
pG-*cheA2*	*cheA2* fragment-containing pGEM-TEasy, Amp^r	This study
pG-*cheY2*	*cheY2* fragment-containing pGEM-TEasy, Amp^r	This study
pG-*pro-cheA2*	*cheA2* and its predicted promoter fragment-containing pGEM-TEasy, Amp^r	This study
pG-*pro-cheY2*	*cheY2* and its predicted promoter fragment-containing pGEM-TEasy, Amp^r	This study
pG-*pro-cheA1*	*cheA1* and its predicted promoter fragment-containing pGEM-TEasy, Amp^r	This study
pG-*pro-cheY1*	*cheY1* and its predicted promoter fragment-containing pGEM-TEasy, Amp^r	This study
pK18*mob*Sac*B*	Small mobilizable vector, Km^r, sucrose sensitive (*sacB*)	Schäfer *et al.* 1994
pK18- Δ*cheA1*	*cheA1* deleted DNA-containing pK18*mobsacB*, Km^r	This study
pK18- Δ*cheY1*	*cheY1* deleted DNA-containing pK18*mobsacB*, Km^r	This study
pK18- Δ*cheA2*	*cheA2* deleted DNA-containing pK18*mobsacB*, Km^r	This study
pK18- Δ*cheY2*	*cheY2* deleted DNA-containing pK18*mobsacB*, Km^r	This study
pDSK519	Broad host range cloning vector, Km^r	Keen *et al.* 1988
pD-*cheA2*	pDSK519 possessing expressible *cheA2*, Km^r	This study
pD-*cheY2*	pDSK519 possessing expressible *cheY2*, Km^r	This study
pD-*cheA1*	pDSK519 possessing expressible *cheA1*, Km^r	This study
pD-*cheY1*	pDSK519 possessing expressible *cheY1*, Km^r	This study

Nal^r, nalidixic acid resistant; Amp^r, ampicillin resistant; Km^r, kanamycin resistant.

Table 2.2. Primer sequences used in this study

Primer Name	Sequence (5'--3')	Description
*cheA1*_1	ATGGCTAAGAGTGTATTGGTGGTCG	Amplification of *cheA-1* and surrounding region
*cheA1*_2	GTCTCGTCCTTGGAACCGTG	
*cheA1*_3	CGCggatccTGTTGCCCACTTCTCGCTGA	Deletion of *cheA-1* ORF
*cheA1*_4	CGCggatccCTGCTGTGCCTGATCGAGAT	
*cheA2*_1	ACGCTGTGCAGCTGATCCAT	Amplification of *cheA-2* and surrounding region
*cheA2*_2	TGGCAACTGGGTAAGTACCCGT	
*cheA2*_3	CGCggatccCACGGCGTATCTGAACCCGG	Deletion of *cheA-2* ORF
*cheA2*_4	CGCggatccTCATCGGCGCCGAAGCTCAT	
*cheY1*_1	ACCAACCTGCTGGCCCTTAA	Amplification of *cheY-1* and surrounding region
*cheY1*_2	GCGGTCGAGCACGTCTTCAA	
*cheY1*_3	CGCggatccCCAAGCTGATCCTGCCCTGA	Deletion of *cheY-1* ORF
*cheY1*_4	CGCggatccCCACCAATACACTCTTAGCCAT	
*cheY2*_1	GCCGAACTCCAGTTGAGTCT	Amplification of *cheY-2* and surrounding region
*cheY2*_2	CTGGCCATGAGCACCAGTTT	
*cheY2*_3	CGCggatccTCAATAGCTGATGCATGCCG	Deletion of *cheY-2* ORF
*cheY2*_4	CGCggatccTCATGTTCTTGTCCAATTCGACC	
*che2pro*_R	GG*ggtacc*GTTCTTGTCCAATTCGACCTCC	Amplification of *che2* predicted promoter (paired with *cheY2-C*_F) for complementation
*cheA2-C*_F	GG*ggtacc*ATGAGCTTCGGCGCCGAT	Amplification of *cheA2* ORF for complementation
*cheA2-C*_R	ggatccTCAGATACGCCGTGCGGC	
*cheY2-C*_F	ggatccCTGAACCTCAAGGAAATCGG	Amplification of *cheY2* and its predicted promoter region for complementation
*cheY2-C*_R	ggatccCGGCATGCATCAGCTATTGA	
*che1pro*_F	GGCCCGCCAGCCGAGAGG	Amplification of *che1* predicted promoter (paired with *cheA1/Y1pro* for complementation
cheA1pro	TAATACTCACGGGTTCGATCCTTGAACAGT	Amplification of *che1* predicted promoter for seamless attachment to *cheA1* ORF
cheY1pro	TCTTAGCCATGGGTTCGATCCTTGAACAGT	Amplification of *che1* predicted promoter for seamless attachment to *cheY1* ORF
cheA1-C_F	GATCGAACCCGTGAGTATTAATCTCGATCAGGCAC	Amplification of *cheA1* ORF for complementation
cheA1-C_R	TCAGCGAGAAGTGGGCAACA	
cheY1-C_F	GATCGAACCCATGGCTAAGAGTGTATTGGT	Amplification of *cheY1* ORF for complementation
cheY1-C_R	TCAGGGCAGGATCAGCTTGG	

Lowercase letters indicate artificial nucleotide sequence for *Bam*HI in Δ*cheA-1*, Δ*cheA-2*, Δ*cheY-1*, and Δ*cheY-2*, *cheA2-C* and *cheY2-C*. Lowercase italic letters indicate artificial nucleotide sequence for *Kpn*I in *che2* promoter and *cheA2-C*.

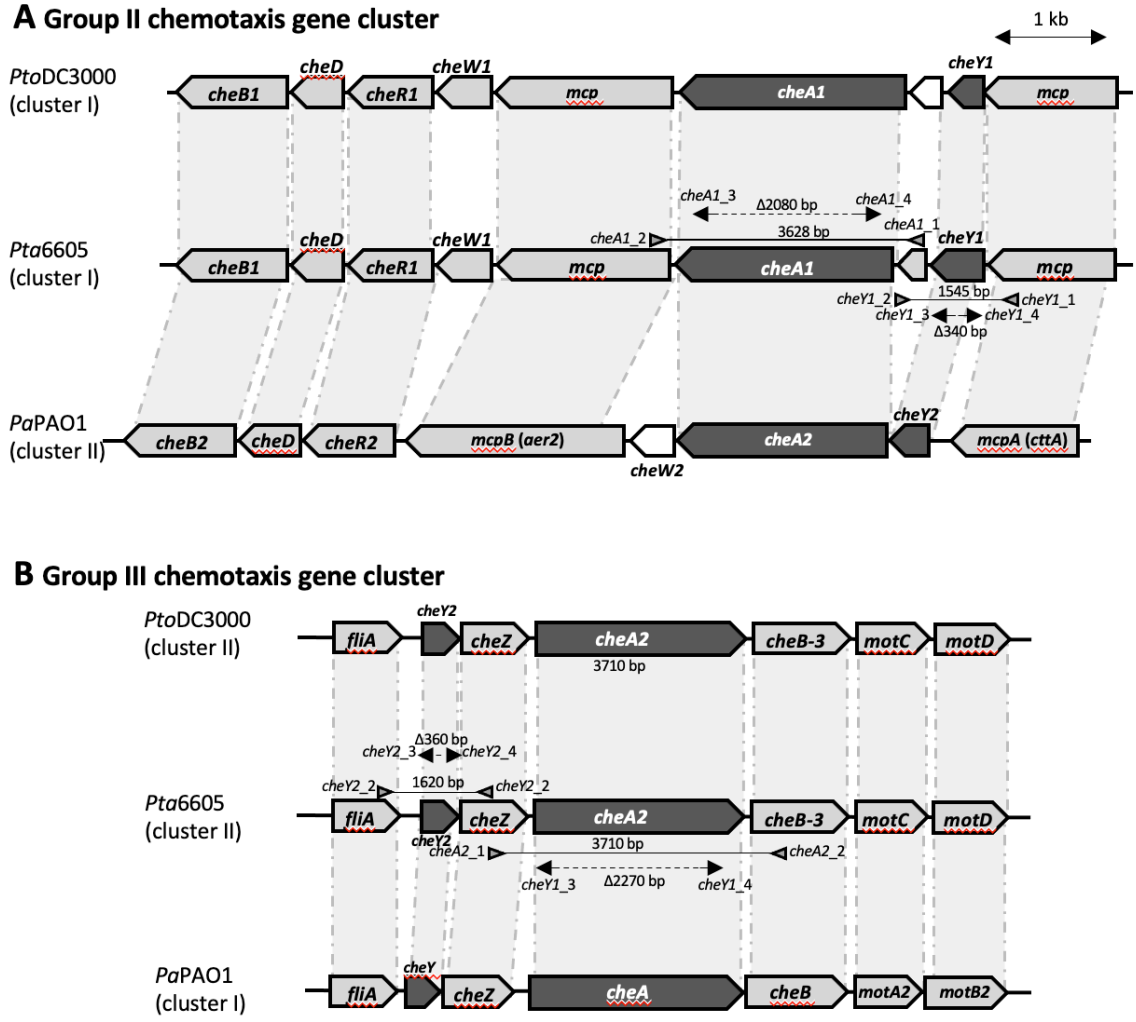

Fig. 2.1. Chemotaxis gene clusters in *P. syringae* pv. *tomato* (*Pto*) DC3000, pv. *tabaci* (*Pta*) 6605 and *P. aeruginosa* (*Pa*) PAO1. Schematic organization of group II chemotaxis gene clusters including cluster I in *Pto*DC3000 and *Pta*6605, and cluster II in *Pa*PAO1 (**A**) and group III chemotaxis gene cluster including cluster II in in *Pto*DC3000 and *Pta*6605, and cluster I in *Pa*PAO1 (**B**). The constructions of the Δ*cheA1*, Δ*cheY1*, Δ*cheA2*, and Δ*cheY2* mutants are also illustrated in *Pta* 6605. Light grey arrowheads indicate the positions of the PCR primers used to clone each *cheA* and *cheY* gene. Each gene name is shown in or above the pentagons. Inverse PCR was carried out to generate ORR-deleted DNA in each gene using primers indicated by dark grey arrowheads. Each ortholog is connected with shadow background.

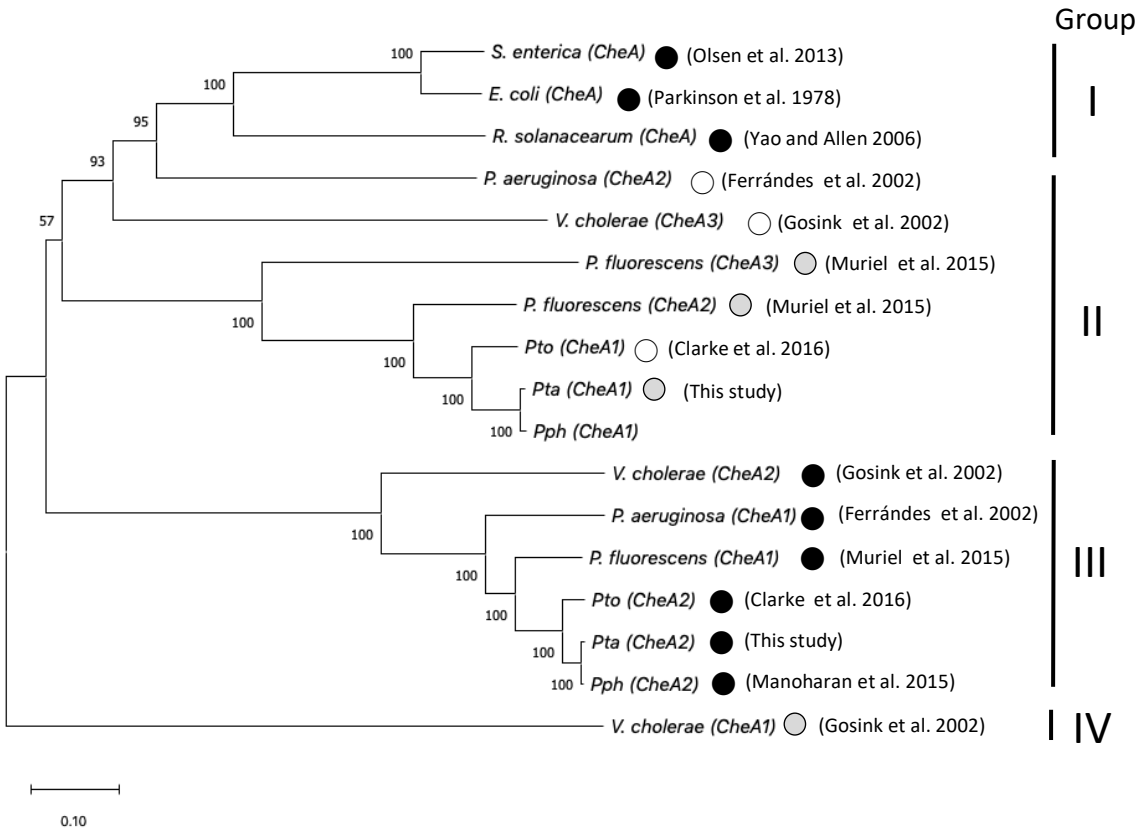

Fig. 2.2. Phylogenetic tree comparing CheA protein sequences. A neighbor-joining tree based on aligned CheA protein sequences of *Pta*6605, *Pto*DC3000, *Pph*1448A, *R. solanacearum* GMI1000, *P. aeruginosa* PAO1, *E. coli* K-12, *P. fluorescens* F113, *V. cholerae* O395, and *Salmonella enterica* serovar *typhimurium* LT2. Numbers at nodes represent bootstrap support based on 1000 replicates. Evolutionary distances were determined using the Poisson correction method and are in units of the number of amino acid substitutions per site. The tree was generated using MEGA7 software. Circle marks indicate that mutation of *cheA* resulted in lost (black), reduced (grey), or unaffected (white) chemotaxis-related phenotypes. Each reference is also shown on the right.

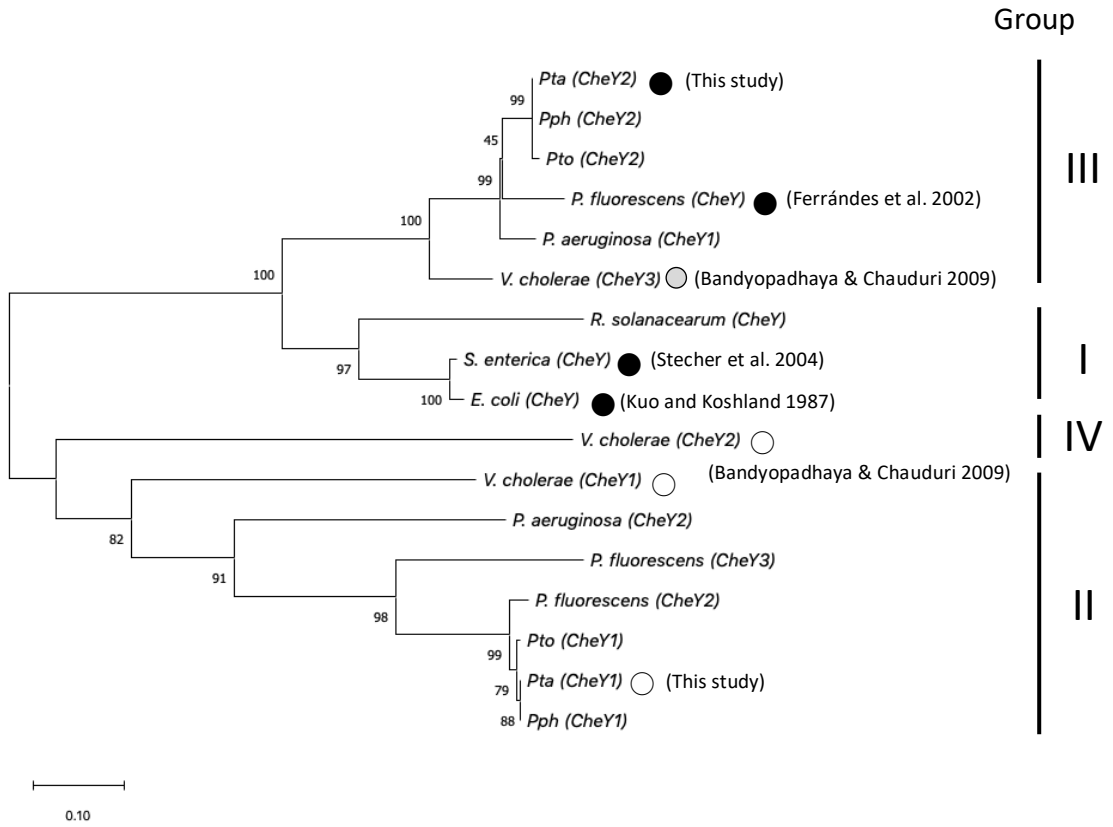

Fig. 2.3. Phylogenetic tree comparing CheY protein sequences. Neighbor-Joining tree based on aligned CheY protein sequences in *Pta*6605, *Pto*DC3000, *Pspph*1448A, *R. solanacearum* GMI1000, *P. aeruginosa* PAO1, *E. coli* K-12, *P. fluorescens* F113, *V. cholerae* O395, and *S. enterica* serovar *typhimurium* LT2. Number at nodes represent bootstrap support based on 1000 replicates. Evolutionary distances were determined using the Poisson correction method and are in the units of the number of amino acid substitutions per site. The tree was generated using MEGA7 software. A circle mark indicates that mutation of *cheY* resulting in lost (black), reduced (grey), or did not affect (white) chemotaxis related phenotype. Each reference is also shown on the right.

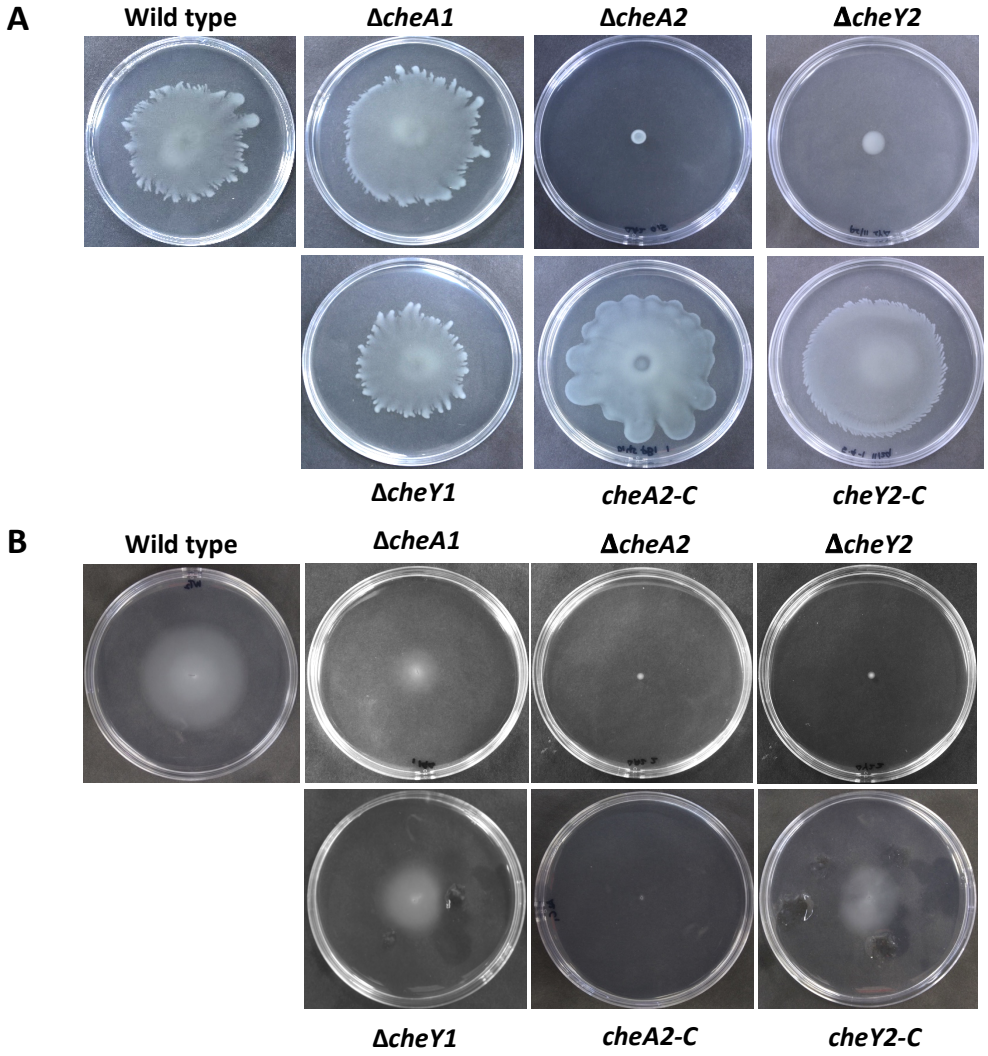

Fig. 2.4. Surface motility phenotypes of wild type and each mutant. (A) Surface swarming assay on SWM plates with 0.45% agar at 27 ºC and **(B)** swimming assay on MMMF plates with 0.25% agar at 27 ºC. Three µl of each bacterial suspension (2×10^8 CFU/ml) was spotted on the center of the plate and incubated for 48 h (swarming) and 72h (swimming). The photographs show representative results obtained from three independent experiments (each with 2 technical replicates).

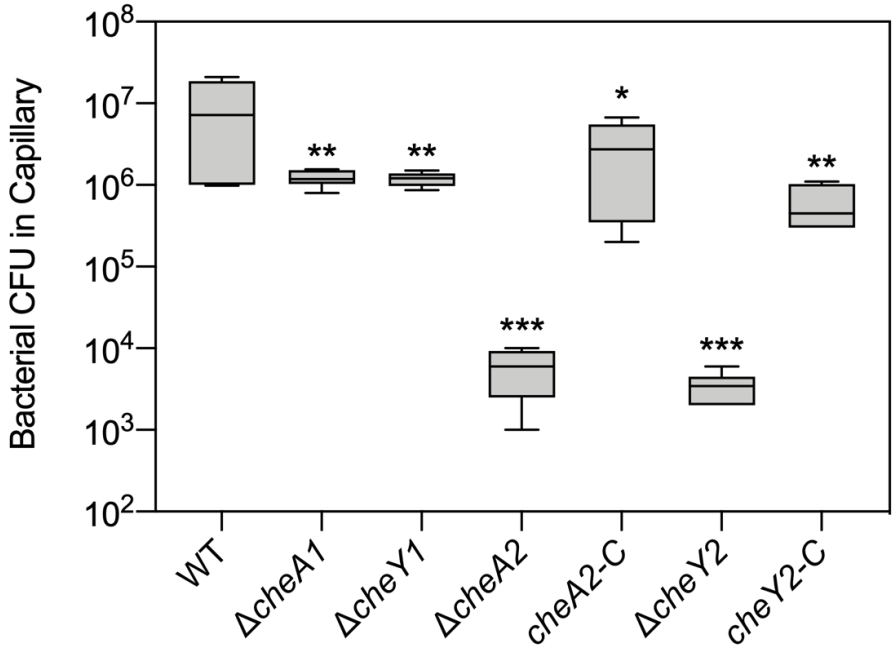

Fig. 2.5. Quantitative capillary chemotaxis assay of wild type and each mutant to 1% yeast extract. The number of bacteria attracted into the capillary was measured in each strain. The experiment was repeated two times with two different colony of each mutant, and similar results were obtained. Asterisks indicate statistically significant differences between WT and mutant strains (*$P < 0.05$; **$P < 0.01$; ***$P < 0.001$; by Dunnett's multiple comparisons test). Error bars represent standard errors from two independent experiments (each with three technical replicates).

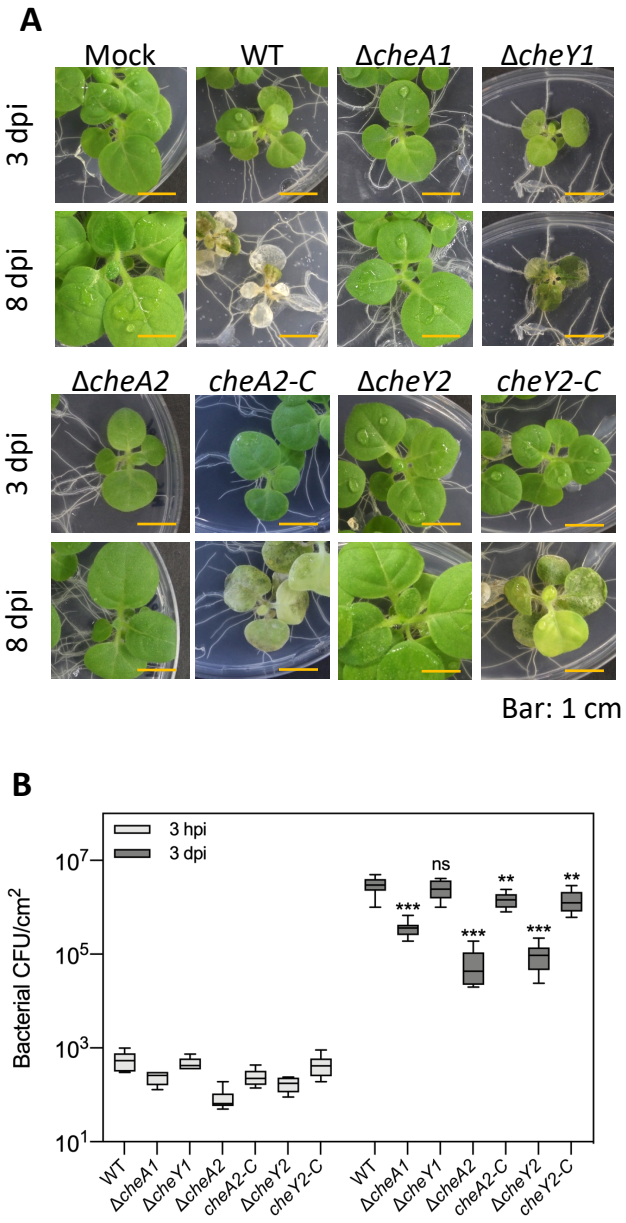

Fig. 2.6. Inoculation of host tobacco leaves by flood assay method. (**A**) Tobacco seedlings were inoculated by flooding with 8 × 10^6 CFU/ml bacterial suspension of each strain and incubated at 22 ºC. Photographs taken 3 and 8 dpi show representative results from three independent experiments. (**B**) Bacterial populations were counted at 3 hpi and 3 dpi. The bars represent standard error from two independent experiments. Bacterial CFUs for each strain in one experiment were pooled from 3 (3 hpi) or 4 (3 dpi) individuals. Asterisks indicate statistically significant differences between WT and mutants (ns: not significant; $^{**}P < 0.01$; $^{***}P < 0.001$ by Dunnett's multiple comparisons test).

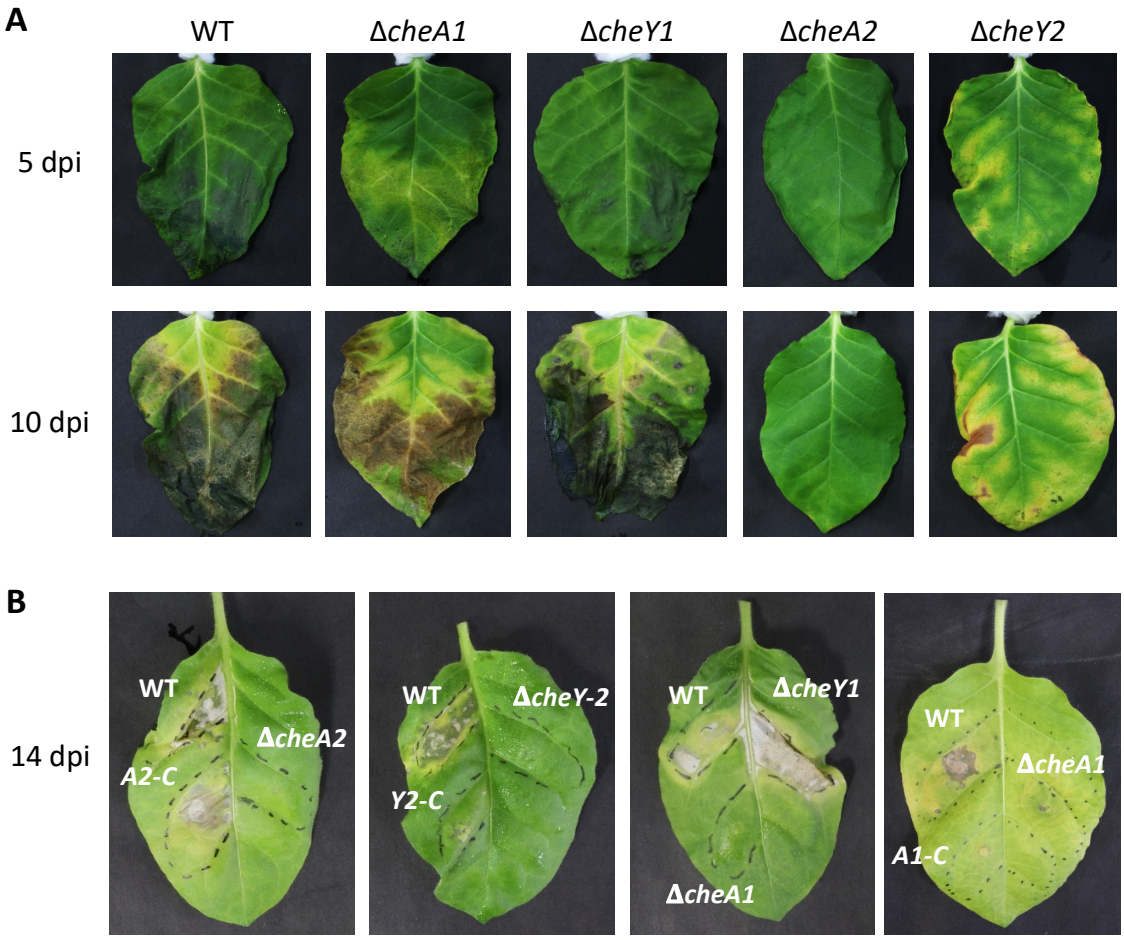

Fig. 2.7. Dip and infiltration inoculation test on host tobacco leaves by the wild type and each mutant. (A) Detached tobacco leaves were inoculated by dipping into 2×10^8 CFU/ml bacterial suspension of each strain and incubated at 22°C. Photographs taken 5 and 10 days after inoculation show representative results from three independent experiments. **(B)** Attached tobacco leaves of whole plants were infiltrated by 2×10^5 CFU/ml of each strain incubated at 22°C. Photograph taken 14 dpi show representative results from two independent experiments. In one experiment, three leaves from independent plants were used for each bacterial strain.

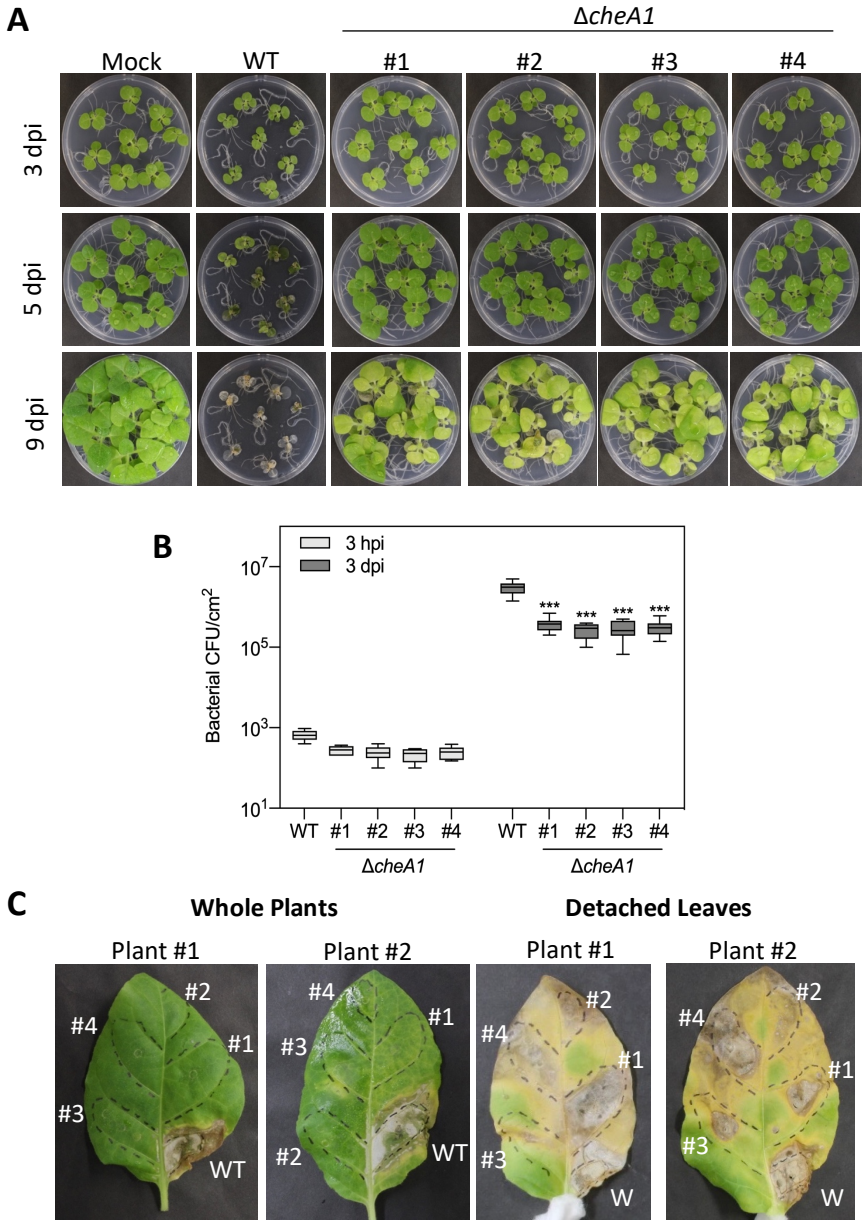

Fig. 2.8. Flood assay and infiltration inoculation test on host tobacco plants (whole plants and detached leaves) of the wild type and Δ*cheA1*. (A) Tobacco seedlings were inoculated by flooding with 8 × 10^6 CFU/ml bacterial suspension of each strain and incubated at 22 ºC. Photographs taken 3, 5 and 9 dpi show representative results from two independent experiments. **(B)** Bacterial populations were counted at 3 hpi and 3 dpi. The bars represent standard error from two independent experiments. Bacterial CFUs for each strain in one experiment were pooled from 3 (3 hpi) or 4 (3 dpi) individuals. Asterisks indicate statistically significant differences between WT and mutants (***P < 0.001 by Dunnett's multiple comparisons test). **(C)** Tobacco leaves were infiltrated by 2×10^5 CFU/ml of each strain and incubated at 22ºC. Photographs taken 14 dpi show representative results from two independent experiments. In one experiment, two leaves from two independent plants were used.

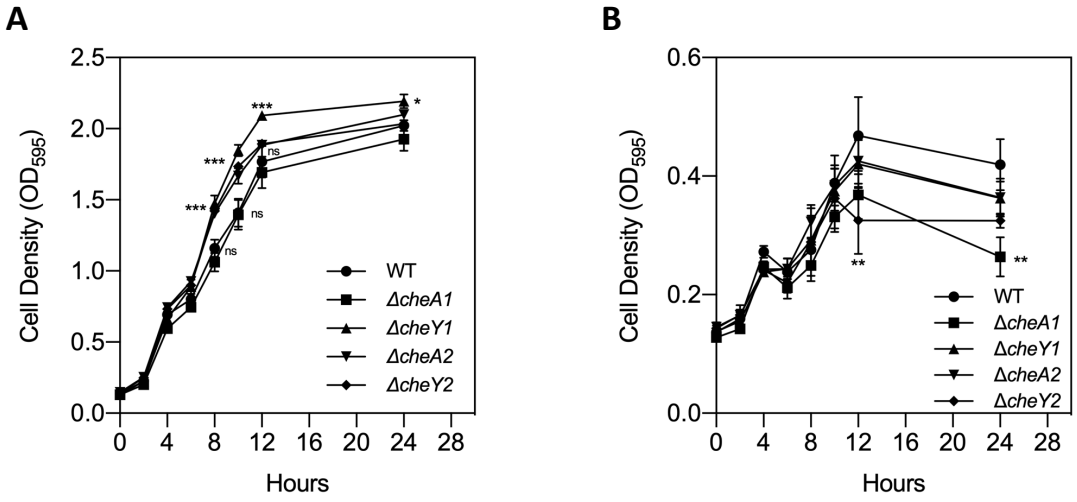

Fig. 2.9. Growth curves of *P. syringae* pv. *tabaci* 6605 wild type and its *che* mutant strains in (A) King's B medium and (B) MMMF medium. Bacterial growth was measured at OD_{595}. Asterisks indicate statistically significant differences between WT and mutants (ns: not significant; $*P < 0.05$; $**P < 0.01$; $***P < 0.001$ by Dunnett's multiple comparisons test). Data are means of two independent experiments conducted in triplicate.

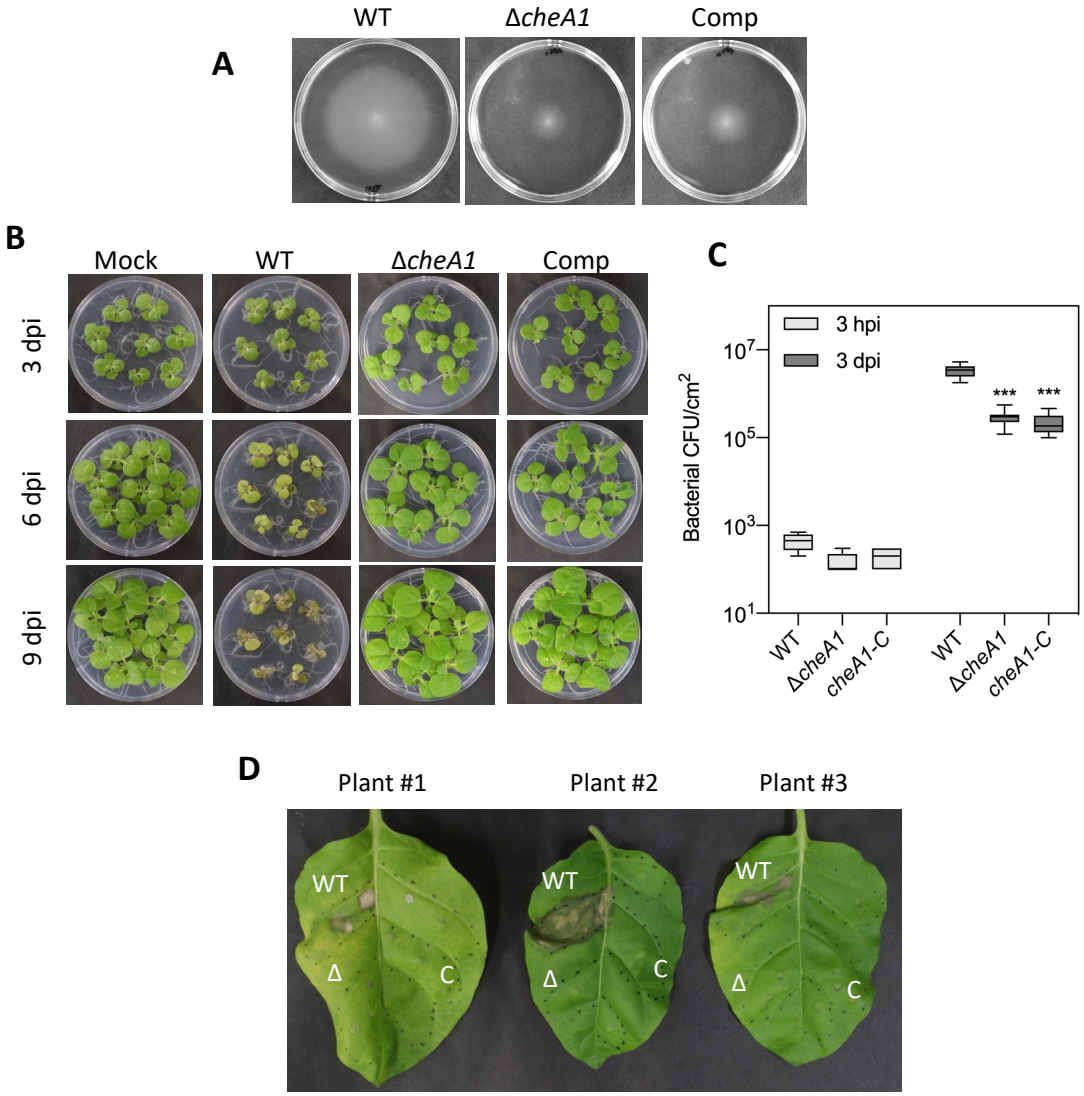

Fig. 2.10. Swimming motility and virulence of Δ*cheA1* and its complementary strain. (A) Swimming motility on MMMF plates with 0.25% agar at 27 ºC. Three µl of each bacterial suspension (2×10^8 CFU/ml) was spotted on the center of the plate and incubated for 72h. The photographs show representative results obtained from two independent experiments (each with 3 technical replicates). **(B)** Flood assay inoculation. Tobacco seedlings were inoculated by flooding with 8×10^6 CFU/ml bacterial suspension of each strain and incubated at 22 ºC. Photographs taken 3, 6 and 9 dpi show representative results from two independent experiments. **(C)** Bacterial populations were counted at 3 hpi and 3 dpi. The bars represent standard error from two independent experiments. Bacterial CFUs for each strain in one experiment were pooled from 3 (3 hpi) or 4 (3 dpi) individuals. Asterisks indicate statistically significant differences between WT and other tested strains (***$P < 0.001$ by Dunnett's multiple comparisons test). **(D)** Tobacco leaves were infiltrated by 2×10^5 CFU/ml of each strain and incubated at 22ºC. Photographs taken 10 dpi show representative results from two independent experiments. In one experiment, three leaves from three independent plants were used.

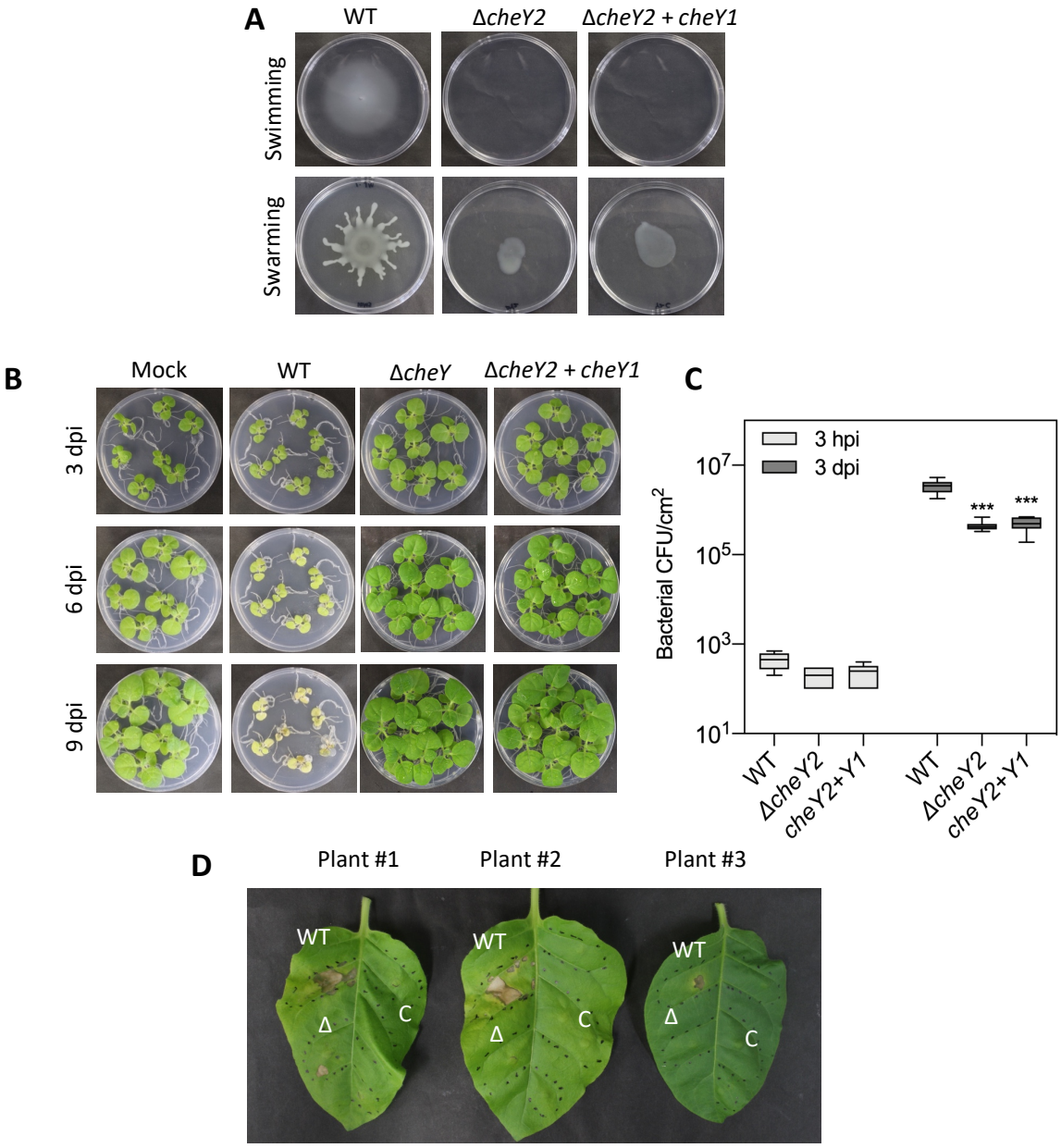

Fig. 2.11. Effect of *cheY1* overexpression in *cheY2* mutant. (A) Swimming (MMMF plates with 0.25% agar) and swarming motilities (SWM plates with 0.45% agar) at 27 °C. Three µl of each bacterial suspension (2×10^8 CFU/ml) was spotted on the center of the plate and incubated for 72h (swim) and 48h (swarm). The photographs show representative results obtained from two independent experiments (each with 3 technical replicates). **(B)** Flood assay inoculation. Tobacco seedlings were inoculated by flooding with 8×10^6 CFU/ml bacterial suspension of each strain and incubated at 22 °C. Photographs taken 3, 6 and 9 dpi show representative results from two independent experiments. **(C)** Bacterial populations were counted at 3 hpi and 3 dpi. The bars represent standard error from two independent experiments. Bacterial CFUs for each strain in one experiment were pooled from 3 (3 hpi) or 4 (3 dpi) individuals. Asterisks indicate statistically significant differences between WT and other tested strains (***$P < 0.001$ by Dunnett's multiple comparisons test). **(D)** Tobacco leaves were infiltrated by 2×10^5 CFU/ml of each strain and incubated at 22°C. Photographs taken 10 dpi show representative results from two independent experiments. In one experiment, three leaves from three independent plants were used.

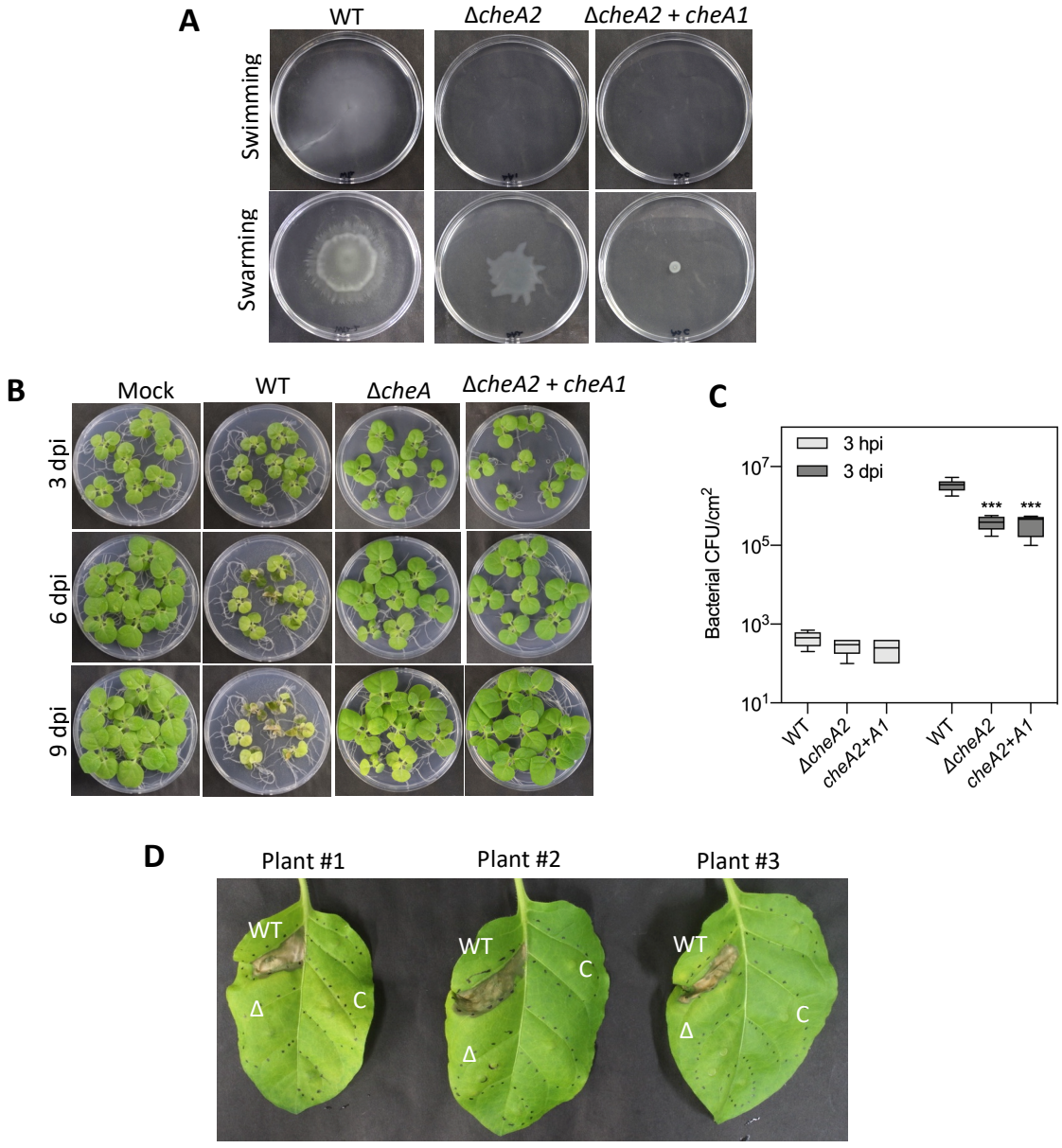

Fig. 2.12. Effect of *cheA1* overexpression in *cheA2* mutant. (A) Swimming (MMMF plates with 0.25% agar) and swarming motilities (SWM plates with 0.45% agar) at 27 ºC. Three µl of each bacterial suspension (2×10^8 CFU/ml) was spotted on the center of the plate and incubated for 72h (swim) and 48h (swarm). The photographs show representative results obtained from two independent experiments (each with 3 technical replicates). **(B)** Flood assay inoculation. Tobacco seedlings were inoculated by flooding with 8×10^6 CFU/ml bacterial suspension of each strain and incubated at 22 ºC. Photographs taken 3, 6 and 9 dpi show representative results from two independent experiments. **(C)** Bacterial populations were counted at 3 hpi and 3 dpi. The bars represent standard error from two independent experiments. Bacterial CFUs for each strain in one experiment were pooled from 3 (3 hpi) or 4 (3 dpi) individuals. Asterisks indicate statistically significant differences between WT and other tested strains (***$P < 0.001$ by Dunnett's multiple comparisons test). **(D)** Tobacco leaves were infiltrated by 2×10^5 CFU/ml of each strain and incubated at 22ºC. Photographs taken 10 dpi show representative results from two independent experiments. In one experiment, three leaves from three independent plants were used.

Chapter 3

Requirement of γ-aminobutyric acid chemotaxis for virulence of *Pseudomonas syringae* pv. *tabaci* 6605

Abstract

γ-Aminobutyric acid (GABA) is a widely distributed non-proteinogenic amino acid. GABA accumulates in plants under biotic and abiotic stresses. More recent studies suggested that GABA might also function as an intracellular signaling molecule in plants as well as a signal mediating interaction between plants and phytopathogenic bacteria. Yet the molecular mechanism of GABA response to bacterial pathogens is largely unknown. In this study we show that a GABA receptor, named McpG, is also conserved in the highly motile plant-pathogenic bacteria *Pseudomonas syringae* pv. *tabaci* 6605 (*Pta*6605). We generated a deletion mutant of McpG to further investigate its involvement in GABA chemotaxis using quantitative capillary and qualitative plate assays. The wild-type strain of *Pta*6605 was attracted to GABA, while the Δ*mcpG* mutant abolished chemotaxis to 10 mM GABA. However, Δ*mcpG* retained the chemotaxis to the proteinogenic amino acids and succinic semialdehyde, structural analog of GABA. Furthermore, Δ*mcpG* was unable to effectively cause disease on host tobacco plants in three plant inoculation assays, flood inoculation, dip inoculation, and infiltration inoculation. These results revealed that GABA sensing of *Pta*6605 is important for interaction of *Pta*6605 with its host tobacco plant.

Keyword: bacterial virulence, chemotaxis, GABA, plant-microbe interaction, *Pseudomonas*

3.1. Introduction

Phytopathogenic bacteria encounter harsh environmental conditions as soon as they arrive at the surface of their host, which can decrease the chance of their survival. Thus, phytopathogenic bacteria need to develop a system that enables them to sense environmental stimuli and respond accordingly. Most phytopathogenic bacteria detect and use signals coming from a host plant for their advantage by moving toward nutrient sources or away from potential danger. Such sophisticated behaviors are known as chemotaxis (Adler, 1966; Sourjik and Wingreen, 2012).

The chemoreceptors are methyl-accepting chemotaxis proteins (MCPs) located outside the cell membrane and in cytosol. When MCP perceived environmental compounds, MCPs transduce the signals to their cytoplasmic signaling domain (SD). Bacteria possess 5 to 60 *mcp* genes encoding MCPs (Alexandre *et al.*, 2004). Methylation helices, parts of SD, are important for adaptation with help from methyltransferase CheR and methylesterase CheB. Then SD relays the signals to coupling protein CheW and down to two component systems, CheA and CheY. Phosphorylated CheY affects the direction of flagellar motor rotation (clockwise/tumble or counter-clockwise/swim) (Bi and Lai, 2015; Haung *et al.*, 2019).

Some MCPs in plant-associated bacteria have been successfully characterized. In *Pseudomonas fluorescens* Pf0-1, a plant-protective bacterium, MCPs for amino acid and organic acids were identified (Oku *et al.*, 2012, 2014). Furthermore, McpS, McpQ, and McpG of *Pseudomonas putida* KT2440 are the chemoreceptors for tricarboxylic cycle intermediates (Lacal *et al.*, 2010), citrate (Martin-Mora *et al.*, 2016b), and γ-aminobutyric acid (GABA) (Reyes-Darias *et al.*, 2015), respectively. Identification of bacterial chemoreceptors has expanded to bacterial species with different lifestyles.

Pathogenic bacteria are known to employ chemotaxis to enhance pathogenicity and virulence (Matilla and Krell, 2018). In *Pseudomonas aeruginosa*, an animal pathogen and a major model pathogen in the study of chemotaxis, several chemoreceptors were identified for proteinogenic amino acids (Kato *et al.*, 2008), GABA (Rico-Jiménez *et al.*, 2013), and α-ketoglutarate (Martin-Mora *et al.*, 2016a). Furthermore, specific chemoreceptors for malate, amino acid, and boric acid, which are thought to be important for mediating chemotaxis in plant infection, were identified in the tomato bacterial wilt pathogen, *Ralstonia pseudosolanacearum* (Hida *et al.*, 2015, 2017).

As previously reported, *Pseudomonas syringae* can move toward wounds or natural openings in host plants and evoke disease, indicating chemotactic behavior toward molecules coming from those openings (Melotto *et al.*, 2006). The requirement to be adaptable for survival

might force pathogens to evolve multiple chemoreceptor proteins, MCPs. In *Escherichia coli* strain K-12, which possesses only five chemoreceptors, the specificity of ligand recognition within the ligand-binding domain (LBD) has been extensively characterized (Bi and Lai, 2015). Very recently, PscA of *P. syringae* pv. *tomato* DC3000 (*Pto*DC3000) was identified as chemoreceptor for L-Asp, L-Glu, and D-Asp, and the virulence of *pscA* mutant was reduced (Cerna-Vargas *et al.*, 2019). However, most of the chemoreceptor functions are still in the dark due to the difficulty of functionally analyzing up to 50 MCPs.

PctC and McpG, chemoreceptors for GABA, were recently reported in *P. aeruginosa* PAO1 (Rico-Jiménez *et al.*, 2013) and saprophytic *P. putida* KT2440 (Reyes-Darias *et al.*, 2015), respectively, supporting the universal importance of GABA as a signaling molecule. Furthermore, PscC of kiwifruit pathogen *P. syringae* pv. *actinidiae* NZ-V13 (*Psa*NZ-V13) reported to be a potential MCP for GABA, because GABA bound LBD of PscC by isothermal titration calorimetry (McKellar *et al.*, 2015). However, chemotaxis assay and virulence test of *Psa* were not carried out. Thus, the chemoreceptor of GABA in plant-pathogenic bacteria have not been well characterized. Seeing that GABA controls multiple aspects of microbe-plant interactions, identification of GABA chemoreceptors in plant-pathogenic bacteria hopefully would be useful to understand its physiological relevance in plant-pathogen interactions.

Plants synthesize various chemical compounds to cope with stresses. One of the chemicals produced is GABA, a non-proteinogenic amino acid widely distributed in prokaryotic and eukaryotic organisms (Fig. 3.1.A, Dhakal *et al.*, 2012; Seifikalhor *et al.*, 2019). GABA is produced inside plant cells and regulates plant growth (Tarkowski *et al.*, 2020). GABA is also a plant defense modulator that plays an important role during environmental stresses (Tarkowski *et al.*, 2020). In plant GABA is synthesized via GABA shunt where glutamate decarboxylase (GAD) converts glutamate into GABA (Michaeli and Fromm, 2015). GABA accumulates especially in plant apoplast when plants experience biotic (i.e. pathogen invasion) (Rico and Preston, 2008) or abiotic stresses (i.e. mechanical damage) (Mei *et al.*, 2016). Furthermore, GABA levels is reported to affect stomatal closure (Mekonnen *et al.*, 2016).

In *Agrobacterium tumefaciens*, GABA mediates quorum sensing by stimulating inactivation of quorum-sensing molecules (Chevrot *et al.*, 2006). Furthermore, in *A. tumefaciens*, reduction of the GABA concentration by introduction of *gabT*, a gene encoding GABA transaminase, enhances the transfer efficiency of Ti plasmids to tomato plants (Nonaka *et al.*, 2017), and elevated GABA levels in transgenic tobacco plants reduced sensitivity to *A. tumefaciens* infection (Chevrot *et al.*, 2006). On the other hand, accumulation of GABA in *P. protegens* seems to enhance its colonization ability (Takeuchi, 2018). GABA has been found to

reduce the ability of *Pto*DC3000 to infect host plants (Park *et al.*, 2010; Chatnaparat *et al.*, 2015; McCraw *et al.*, 2016). Another study demonstrated that *Phaseolus vulgaris* accumulates extracellular GABA during the incompatible interactions with *P. syringae* pv. *phaseolicola* (O'Leary *et al.*, 2016). It seems that GABA functions vary specifically among species, yet GABA in common serves to mediate inter-kingdom communication in both cases.

In this study, the highly chemotactic *Pseudomonas syringae* pv. *tabaci* 6605 (*Pta*6605), which possesses about 50 MCPs, exhibited strong chemotaxis towards GABA and was found to possess a GABA chemoreceptor. As previously discussed, chemotaxis is indispensable for *Pta*6605 virulence (Tumewu *et al.*, 2021). Therefore, we wondered whether sensing GABA can modulate *Pta*6605 interactions with its host plant. Using a deletion mutant of the predicted GABA receptors, different virulence assay methods were conducted to investigate the importance of GABA chemotaxis for *Pta*6605.

3.2. Materials and methods

3.2.1. Bacterial strains and plasmids

Bacterial strains and plasmids are listed in Table 3.1. *Pta*6605 strains were grown in King's B (KB) medium supplemented with 50 μg/ml nalidixic acid (Nal) at 27°C (King *et al.*, 1954; Taguchi *et al.*, 2006). *E. coli* strains were grown in Luria Bertani (LB) medium supplemented with appropriate antibiotics (50 μg/ml) at 37°C.

3.2.2. Construction of predicted GABA receptor mutants in *Pta*6605

Three deletion mutants were generated for the locus tags, A3SK_RS0126685, A3SK_RS0106980, and A3SK_RS0112400 in *Pta*6605. Because they are not yet annotated, hereafter we use tentative names for each locus tag, RS26685, RS06980, and RS12400, respectively. Several primer pairs (listed in Table 3.2) were used to amplify the corresponding regions with surrounding sequences from *Pta*6605 genomic DNA. Resulting PCR products were inserted into a pGEM T-Easy Vector (Promega, Madison, WI, USA), and inverse PCR was performed with appropriate primer pairs to delete each open reading frame of *mcp* (Fig 3.1.B). Following *Xba*I digestion and self-ligation, mutated DNA fragments were subcloned into pK18*mob*SacB via a *Not*I site (Schäfer *et al.*, 1994) and transformed to *E. coli* S17-1 for conjugation and subsequent homologous recombination with *Pta*6605 wild-type (WT) as previously reported (Ichinose *et al.*, 2020). To confirm, colony PCR of the conjugants was

carried out using respective primer pairs. The deletion mutants are designated as ΔRS26685 (Δ*mcpG*), ΔRS06980, and ΔRS12400.

3.2.3. Complementation of *Pta*6605 Δ*mcpG*

To investigate the ability of *mcpG* to restore the phenotype of Δ*mcpG*, complementation strains were constructed by introducing the full length of *mcpG* gene along with its native promoter in the expression vector pDSK519 (Keen *et al*., 1988) at *Not*I sites. Constructed plasmid was transformed into *E. coli* S17-1 and introduced into Δ*mcpG* by conjugation. Conjugants were selected with Nal- and kanamycin-containing KB plates.

3.2.4. Chemotaxis assays

Quantitative chemotaxis assays were performed by a microtiter plate multi-capillaries method (Reyes-Darias *et al*., 2016) with minor modification. Bacteria were cultured overnight in 3 ml LB with 10 mM $MgCl_2$, washed, and resuspended in 3 ml minimal medium (MM: 50 mM potassium phosphate, 7.6 mM $(NH_4)_2SO_4$, 1.7 mM $MgCl_2$, 1.7 mM NaCl). Then, 150 μl of bacterial suspension was inoculated into 3 ml fresh MM supplemented with 10 mM of mannitol and fructose (MMMF) for 5 h further incubation. Bacterial cells were washed twice and resuspended with 10 mM HEPES (pH 7.4) to OD_{600} of 0.05.

Capillary preparation was as follows: one end of a 5 μl capillary (Drummond Scientific Company, Broomall, PA, USA) was sealed by heating with a flame. The capillary body was dipped into a potential chemoattractant solution or 10 mM HEPES buffer as a control. A rubber collar was used to support the capillary during the assay. Two hundred μl of bacterial suspension was pipetted into three wells of a round-bottom Falcon® microtiter plate (Corning, Corning, NY, USA). The chemical-filled capillary was dipped into the wells and further incubated for 30 minutes at 27ºC. After rinsing with sterile distilled water, 5 μl of capillary contents was squirted into 45 μl of 0.9% NaCl. A series of 10-fold dilution was performed, and 10 μl of diluted bacterial suspension was plated onto a KB plate with 50 μg/ml nalidixic acid. After 2 d incubation at 27ºC, the number of colonies was counted.

A qualitative chemotaxis assay was performed by observing the ability of WT and mutant strains to swim on MM plate supplemented with 1 mM of GABA (Wako Pure Chemicals, Osaka, Japan) and 0.25% Bacto agar (Difco, Detroit, MI, USA). Briefly, overnight bacterial cultures in LB with 10 mM $MgCl_2$ were washed and resuspended in liquid MM to OD_{600} of 0.1. Three μl of bacterial suspension was dropped carefully on the center of a freshly made chemotaxis swimming plate. Photographs were taken after incubation at 23ºC for 3 d.

3.2.5. Surface motility assay

Surface motility assays measured swimming and swarming abilities on semi-solid agar plates. Bacteria cultured overnight in 3 ml LB with 10 mM $MgCl_2$ were washed and resuspended in 10 mM $MgSO_4$ to an OD_{600} of 0.1. Three μl of bacterial suspension was spotted on the center of the plate. Swimming plates (MMMF with 0.25% agar) were incubated at 23ºC, while swarming plates (0.5% peptone and 0.3% yeast extract, and 0.45% agar) were incubated at 27ºC. Photographs were taken at 2 d for swarming assay and 3 d for swimming assay after inoculation.

3.2.6. Bacterial growth *in vitro*

Bacteria were cultured overnight in 3 ml KB with 50 μg/ml Nal, washed with KB or MMMF, and resuspended in the same fresh medium to a starting OD_{595} of 0.1. Each bacterial suspension was pipetted into a flat-bottomed 96-well microtiter plate and incubated at 27ºC with shaking. Bacterial cell density (OD_{595}) was measured using an iMark™ Microplate Absorbance Reader (Bio-Rad Laboratories, Inc., Hercules, CA, USA) every 2 h to generate growth curves.

3.2.7. Virulence assays and *in planta* bacterial populations

To thoroughly assess the involvement of McpG in *Pta*6605 virulence, three plant inoculation assays, flood inoculation, dip inoculation, and infiltration, were done. A flood inoculation method (Ishiga *et al.*, 2011) was modified for tobacco seedlings. Sterilized tobacco seeds (*Nicotiana tabacum* L. var. Xanthi NC) were sown on Murashige-Skoog (MS) 0.8% agar plates containing 1% sucrose and vitamin stock solution (thiamin hydrochloride 3 mg/l, nicotinic acid 5 mg/l, pyridoxine hydrochloride 0.5 mg/l). Sown plates were incubated at 28ºC under 16 h light-8 h dark conditions. After 2-wks, 8 seedlings were transplanted to one MS 0.8% agar plate containing 0.1% sucrose and vitamin stock solution and further incubated for 2 d. To prepare the inoculum, bacteria cultured overnight in LB medium with 10 mM $MgCl_2$ were washed and adjusted to OD_{600} = 0.004 (8×10^6 colony forming units (CFU)/ml) with 10 mM $MgSO_4$ (approx. 30 ml) and 0.025% (v/v) Silwet L-77 (OSI Specialties, Danbury, CT). The inoculum was flooded onto the seedlings and swirled to spread it evenly. After decanting the bacterial suspension, the plate was air-dried on a clean bench for 15 min. Seedlings on the plates were incubated under 16 h light-8 h dark conditions at 22ºC. To count the bacterial populations, leaf disks were punched out using a disposable biopsy hole punch and then grounded with a mortar and pestle. Leaf disks were collected 3 h post inoculation (hpi), and the homogenates

were mixed with 1 ml sterile water, then 100 µl was spread on KB with Nal plates. For 3 d post inoculation (dpi), after 10-fold serial dilutions, 10 µl was dropped on KB with Nal plates. After incubation at 27ºC for 2 d, the bacterial population was measured.

The dip inoculation method was also done using detached tobacco leaves (Taguchi and Ichinose, 2011). Inoculum preparation was basically the same as for the flood inoculation method, except the inoculum density was adjusted to OD_{600} of 0.1 (approx. density of bacteria was 2×10^8 CFU/ml) with 0.04% (v/v) Silwet L-77 for this method. In this method, detached leaves of 8-wks-old tobacco plants were dipped into the bacterial suspension for 2 min and placed in a tray covered with plastic wrap. Cut petioles were wrapped with water-soaked cotton. The tray was incubated under 16 h light-8 h dark conditions at 22ºC for 10 days. The same inoculum preparation was also done for the infiltration method. Eight-wks-old tobacco leaves (attached leaves) were infiltrated by bacterial cells at a density of 2×10^5 CFU/ml using a needleless syringe. Inoculated tobacco plants were incubated in a domed tray at 22ºC with a long-day photoperiod (16 h light-8 h dark) for 14 d.

3.2.8. Data analysis

Bacterial population counts of chemotaxis assays and virulence assay are expressed as means with standard error. One-way/two-way ANOVA followed by Dunnett's or Tukey's highly significant difference tests were performed using GraphPad Prism ver. 8 (GraphPad Software Inc., San Diego, CA, USA). $P < 0.05$ was considered statistically significant.

3.3. Results

3.3.1. *Pta*6605 was predicted to have three GABA receptor homologs

An MCP typically has LBD, transmembrane domains (TMD), and cytoplasmic *h*istidine kinase, *a*denyl cyclase, *m*ethyl-accepting chemotaxis proteins and *p*hosphatase (HAMP) domain and SD (Ud-Din and Roujeinikova, 2017). A BLAST search with LBD of McpG (PP1371), a GABA receptor in *P. putida* KT2440 (Reyes-Darias *et al.*, 2015) revealed three GABA chemoreceptor homologs in *Pta*6605 with 64.9% (RS26685), 59.9% (RS06980), and 59.4% (RS12400) amino acid sequence identities.

Amino acid sequences of LBDs of GABA chemoreceptors in *P. aeruginosa* PAO1 (PctC and its paralogs PctA and PctB) (Taguchi *et al.*, 1997) and *P. putida* KT2440 (McpG) (Reyes-Darias *et al.*, 2015), amino acid receptors in *P. fluorescens* Pf0-1 (CtaA, CtaB, and CtaC) (Oku *et al.*, 2012), amino acid receptors in *Psa*NZ-V13 (PscA and PscB) (McKellar *et al.*, 2015), potential

GABA receptor in *Psa*NZ-V13 (PscC) (McKellar *et al.*, 2015), amino acid receptors in *Pto*DC3000 (PscA and its paralogs PscB and PscC) (Cerna-Vargas *et al.*, 2019), and three suspected GABA receptor homologs in *Pta*6605 were aligned (Fig. 3.2) to generate phylogenetic tree (Fig. 3.3). RS12400 was clustered together with PscA of *Pto*DC3000 and *Psa*NZ-V13, and RS06980 of *Pta*6605 was clustered together with PscB of *Pto*DC3000 and *Psa*NZ-V13. However, RS26685 of *Pta*6605 was apparently clustered separately from LBD of other MCPs, suggesting that any of the three MCPs in *Pta*6605 has the probability of being chemoreceptors for GABA in *Pta*6605.

MCPs can be classified into seven topology types (Ia, Ib, II, IIIm, IIIc, IVa, and IVb) based on the number of TMD, the presence or absence of LBD and its localization (Ud-Din and Roujeinikova, 2017). Three GABA receptor homologs in *Pta*6605 belong to type Ia MCP. Type Ia MCPs consist of an N-terminal TMD followed by a periplasmic LBD, a second TMD, HAMP, and a C-terminal cytoplasmic SD (Fig. 3.1.C). We confirmed that all MCPs for GABA and amino acids listed in Fig. 1B belong to type Ia.

3.3.2. Identification of McpG as a GABA chemoreceptor in *Pta*6605

Quantitative capillary assays were conducted to investigate how the mutation of each predicted GABA receptor affects *Pta*6605 chemotaxis to GABA. Quantified results showed significant reduction of ΔRS26685 chemotaxis to 10 mM GABA, while ΔRS06980 and ΔRS12400 retained chemotaxis to GABA comparable to the WT (Fig. 3.4.A). ΔRS26685 did not lose its general chemotaxis ability because ΔRS26685 was attracted to 1% yeast extract as WT, ΔRS06980, and ΔRS12400 (Fig. 3.4.B). These results indicated that RS26685 encodes chemoreceptor for GABA in *Pta*6605, and we designated it as McpG.

3.3.3. Δ*mcpG* swims and swarms on soft agar at wild type level

Surface motilities of WT and Δ*mcpG* (ΔRS26685) were examined using low-agar-concentration plates. Δ*mcpG* exhibited the same swimming and swarming abilities as WT (Fig. 3.4.C). The results indicate that the inability of Δ*mcpG* to respond to GABA was not due to lack of motility.

3.3.4. Δ*mcpG* chemotaxis to GABA with different concentration and complementation test

We further investigated the chemotaxis of both WT and Δ*mcpG* to different concentrations of GABA. While WT responded to GABA in dose-dependent manner, Δ*mcpG* showed significant reduction at all concentrations (Fig. 3.5.A). Complementation by introducing full-length *mcpG* with its native promoter into Δ*mcpG* restored the chemotaxis to GABA (Fig. 3.5.B). We also qualitatively investigated Δ*mcpG* chemotaxis using 0.25% agar minimal media (MM) supplemented with 1 mM GABA. The Δ*mcpG* was unable to expand its growth from its inoculation point at 2 dpi and even 3 dpi, while its complemented and WT strains expanded at similar levels (Fig. 3.5.C).

3.3.5. McpG is the specific chemoreceptor for GABA

We tested the chemotaxis ability of WT and Δ*mcpG* to 20 proteinogenic amino acids, butyric acid, and succinic semialdehyde (SSA) that share similar structure with GABA. Quantitative chemotaxis assay results demonstrated that *Pta*6605 was attracted to most proteinogenic amino acids except tyrosine. *Pta*6605 was also attracted to SSA but not to butyric acid (Fig. 3.6). Furthermore, there was no significant difference on chemotactic ability between WT and Δ*mcpG* to all amino acids and SSA. These results indicate that McpG of *Pta*6605 is a specific chemoreceptor for GABA.

3.3.6. Growth characteristics of Δ*mcpG*

Growth characteristics of WT and Δ*mcpG* were evaluated to determine if mutation affects their growth and to confirm that the lack of chemotaxis in Δ*mcpG* was not due to a growth defect. Growth experiments were done in KB (nutrient rich) and MMMF liquid medium (Fig. 3.7.A), and in MM supplemented with GABA as a sole source of carbon and nitrogen (Fig. 3.7.B). The growth of Δ*mcpG* in KB and MMMF liquid medium was not significantly different from that of the WT. In MM supplemented with GABA, although Δ*mcpG* seemed to have slower growth compared to WT, the difference was not statistically significant at all time points, indicating that the phenotypic difference between them was not due to a growth defect.

3.3.7. Δ*mcpG* had reduced virulence on host tobacco plant

Plant inoculation assays were done to elucidate how McpG-mediated chemotaxis affects the *Pta*6605 virulence in host tobacco plants. First, virulence was tested by a flood inoculation

assay method. The photographs in Fig. 3.8.A clearly show that Δ*mcpG*-inoculated seedling still survived at 7 dpi, although the seedling was smaller than that of the mock treatment. On the other hand, the complemented strain restored full virulence. We also counted the bacterial populations inside the leaves. The number of bacteria recovered from Δ*mcpG*-inoculated leaves was significantly lower at both 3 hpi and 3 dpi (Fig. 3.8.B), indicating that the GABA sensing is required for early stage of virulence in *Pta*6605.

A second virulence test was done by a dip-inoculation method with cut leaves. The Δ*mcpG* caused mild disease symptoms than the WT strain (Fig. 3.9.A), indicating that the McpG is required for development of disease symptoms also in a dip inoculation method. The virulence of WT and Δ*mcpG* was also investigated by directly infiltrating bacterial cells into 5-wk-old tobacco leaves. Area of the Δ*mcpG*-infiltrated leaf showed disease symptom progression, although not as robust as WT (Fig. 3.9.B). However, the complemented strain caused more extensive symptoms than Δ*mcpG*.

3.4. Discussions

RS26685 (McpG) was identified as a GABA chemoreceptor in *Pta*6605 based on the results of quantitative chemotaxis assay (Fig. 3.4 and Fig. 3.5) and the qualitative swimming plate assay (Fig. 3.5.C). Normal chemotaxis to 1% yeast extract (Fig. 3.4.B), surface motility (Fig. 3.4.C), and growth speed (Fig. 3.7) proved that its lost ability to sense GABA was not due to impaired motility or a growth defect. Therefore, the reduction of virulence of Δ*mcpG* mutant is principally due to loss of GABA chemotaxis. PscC is a potential GABA receptor of *Psa*NZ-V13, but PscC is not yet confirmed with quantitative chemotaxis assay, and its requirement in infection process is not examined yet (McKellar *et al.*, 2015). This paper is the first report showing that GABA chemotaxis is required for infection by phytopathogens. Identification of a GABA chemoreceptor in plant pathogen *Pta*6605 widened the relevance of GABA chemotaxis not only for attraction to neurotransmitters by animal pathogen *P. aeruginosa* PAO1 and root colonization in non-pathogenic *P. putida* KT2440 (Reyes-Darias *et al.*, 2015).

Some GABA chemoreceptors are known to recognizes multiple amino acids. For example, PctC of *P. aeriginosa* recognizes GABA, L-Pro, and L-His (Rico-Jimenez *et al.*, 2013), and PscC of *Psa* binds GABA, L-Pro and L-Ile (McKellar *et al.*, 2015). While McpG of *P. putida* is a specific GABA receptor (Reyes-Darias *et al.*, 2015). McpG of *Pta*6605 also specifically mediates chemotaxis to GABA just like McpG of *P. putida* KT2440, because the Δ*mcpG* mutant of *Pta*6605 strain still attracted to 19 amino acids and SSA (Fig. 3.6). The presence of specific GABA receptor suggests the importance of GABA chemotaxis for *Pta*6605 infection.

The plant-pathogenic bacterium *Pta*6605 apparently possesses three paralogs of McpG, RS26685, RS06980, and RS12400, among about 50 MCPs. They might serve a similar function to PctA, PctB, and PctC of PAO1, PsaA, PsaB, and PsaC of *Psa*NZ-V13, and CtaA, CtaB, and CtaC of *P. fluorescens* Pf0-1 (Kato *et al.*, 2008; Rico-Jimenez *et al.*, 2013; McKellar *et al.*, 2015; Oku *et al.*, 2012), further suggesting that *Pta*6605 responds environmental signals like GABA and amino acids.

As for the other two paralogs, both phylogenetic trees constructed from LBDs (Fig. 3.3) and SDs (Fig. 3.10) suggested that RS06980 and RS12400 might be the MCP involved in amino acid sensing, given the close similarity to the amino acid chemoreceptors, McpA in *P. putida* KT2440 (Corral-Lugo *et al.*, 2016), Psc paralogs in *Psa*NZ-V13 and *Pto*DC3000 (McKellar *et al.*, 2015; Cerna-Vargas *et al.*, 2019), and Cta paralogs in *P. fluorescens* Pf0-1 (Oku *et al.*, 2012). However, the phylogenetic tree based on the sequence similarity of LBD suggests that the ability to sense GABA is not really reflected in the general sequence similarities of LBDs, thus proving that characterization of responsible chemoreceptors should not depend on only sequences clustering from one or two strains of bacteria (Fig. 3.3). More experiments are needed to clarify the function of both chemoreceptor proteins.

Bacteria often exhibit chemotaxis to molecules that they can utilize as growth substrates. Most of the chemical compounds that bacteria are attracted to are carbon or nitrogen sources, such as amino acids, sugars, organic acids, hydrocarbons, and oxygen (Sampedro *et al.*, 2015). Previous studies regarding a fungal pathogen in tomato, *Cladosporium fulvum* (Solomon and Oliver, 2002), animal pathogen *P. aeruginosa* (Rico-Jiménez *et al.*, 2013), and saprophytic plant root-colonizing bacterium *P. putida* (Reyes-Darias *et al.*, 2015) further support the idea that GABA has physiological relevance in host-microbe interactions.

Plant-related compounds are known to regulate virulence factors in addition to attractants of chemotaxis (Leonard *et al.*, 2017). GABA is produced in plants infected by bacterial pathogens (Deeken *et al.*, 2006) and secreted to the apoplast and outer environment (Mei *et al.*, 2016). *Pta*6605 GABA-sensing mutant, Δ*mcpG*, was shown to be significantly less virulent in host tobacco by the flood inoculation method (Fig. 3.8) and dip inoculation using detached leaves (Fig. 3.9.A). These results revealed the necessity of GABA chemotaxis in the early stage of infection when the bacterial cells arrive on the leaf surface.

Furthermore, Δ*mcpG* was also somehow less virulent than WT when infiltrated using a needleless syringe (Fig. 3.9.B). This could suggest the involvement of GABA not only in early, but also in late infection stages, since the virulence of Δ*mcpG* that entered plant apoplastic spaces by infiltration independent of chemotaxis was also reduced. GABA perception by *Pta*6605 via

McpG might be required not only for chemotaxis but also expression of virulence genes. Similarly, the *pscA* mutant of *Pto*DC3000 also impaired not only chemotaxis to L-Asp, L-Glu, and D-Asp but also some regulation of pathogenicity-related traits such as biofilm formation, swarming motility and the amount of c-di-GMP (Cerna-Varga *et al.*, 2019). Therefore, some MPCs including McpG of *Pta*6605 and PscA in *Pto*DC3000 act as both chemoreceptor and regulator of pathogenicity.

Since GABA is widely distributed, the physiological relevance of GABA as a signaling compound is likely to be high. Accumulation of intracellular and extracellular GABA in plants is induced by biotic and abiotic stresses, such as nutrient depletion, mechanical wounding, pathogen infection, and lack of oxygen (Allan *et al.*, 2008; Reyes-Darias *et al.*, 2015; Mei *et al.*, 2016; Seifikalhor *et al.*, 2019). In addition, the expression level of type III secretion system (T3SS) genes in plant pathogenic bacteria is higher *in planta*, indicating that the presence of plant-derived signals is likely to be required for the expression of T3SS genes and full virulence (Rahme *et al.*, 1992; Tang *et al.*, 2006). Considering this, it is plausible for a plant pathogen like *Pta*6605 to have a specific chemoreceptor for GABA for fitness in host plants infection. The restored ability of GABA sensing and virulence in the complemented strain on tobacco plants further demonstrated the significance of McpG for *Pta*6605. In line with current findings, previously studied plant pathogenic bacteria have shown chemotaxis ability to various plant-related compounds (Matilla and Krell, 2018). Adding to the current theory, GABA indeed plays a significant role in plant-microbe communication, either symbiotic or parasitic.

Table 3.1 Bacterial strains and plasmids used in this study

Bacterial strain, plasmid	Relevant characteristics	Reference or source
Escherichia coli		
DH5α	*F⁻λ⁻ ϕ80dLacZ ΔM15 Δ(lacZYA-argF)U169 recA1 endA1 hsdR17(rK⁻ mK⁺) supE44 thi-1 gyrA relA1*	Nippon Gene, Tokyo, Japan
S17-1	*thi pro hsdR hsdR hsdM⁺ recA(chr::RP4-2-Tc::Mu-Km::Tn7)*	Schäfer *et al.* 1994
Pseudomonas syringae pv. *tabaci*		
Isolate 6605	Wild-type isolated from tobacco, Nal^r	Ichinose *et al.* 2020
6605-ΔRS26685	Isolate 6605 ΔPS26685 (Δ*mcpG*), Nal^r	This study
6605-ΔRS06980	Isolate 6605 ΔRS06980, Nal^r	This study
6605-ΔRS12400	Isolate 6605 ΔRS12400, Nal^r	This study
6605-Δ*mcpG*-C	pD-*mcpG* containing Δ*mcpG*, Nal^r Km^r	This study
Plasmid		
pGEM-T Easy	Cloning vector, Amp^r	Promega, Madison, WI, USA
pG-RS26685	RS26685 fragment-containing pGEM-TEasy, Amp^r	This study
pG-RS06980	RS06980 fragment-containing pGEM-TEasy, Amp^r	This study
pG-RS12400	RS12400 fragment-containing pGEM-TEasy, Amp^r	This study
pK18*mob*Sac*B*	Small mobilizable vector, Km^r, sucrose sensitive (s*acB*)	Schäfer *et al.* 1994
pK18-ΔRS26685	RS26685 deleted DNA-containing pK18*mobsacB*, Km^r	This study
pK18-ΔRS06980	RS06980 deleted DNA-containing pK18*mobsacB*, Km^r	This study
pK18-ΔRS12400	RS12400 deleted DNA-containing pK18*mobsacB*, Km^r	This study
pDSK519	Broad host range cloning vector, Km^r	Keen *et al.* 1988
pD-*mcpG*	pDSK519 possessing expressible *mcpG*, Km^r	This study

Nal^r, nalidixic acid resistant; Amp^r, ampicillin resistant; Km^r, kanamycin resistant.

Table 3.2 Primer sequences used in this study

Primer Name	Sequence (5'--3')	Description
RS26685_1	GAGCCCGAAATAACCGAAGA	Amplification of RS26685 and surrounding region
RS26685_2	CTGGCAATAAACGCGCTGAT	
RS26685_3	GCtctagaTGCCGATAAGGGCCTTTAGA	Deletion of RS26685 ORF
RS26685_4	GCtctagaCAAGCCGCTGCCAGAGAA	
RS06980_1	GTTGCGGCCTTGAAGCTCT	Amplification of RS06980 and surrounding region
RS06980_2	CCCACGGATGCAGAATAGAC	
RS06980_3	GCtctagaAGACAATATTTTGCCGCACC	Deletion of RS06980 ORF
RS06980_4	GCtctagaCATCCAGTAACAGAGGTCGG	
RS12400_1	GACGATCTTTGGCAGCGGT	Amplification of RS12400 and surrounding region
RS12400_2	GGAACTGTTTGCTGAGATCC	
RS12400_3	GCtctagaATAGCGGTTACTTCCACGGC	Deletion of RS12400 ORF
RS12400_4	GCtctagaGATGTACAGGTCCCGATGGG	

Lowercase letters indicate artificial nucleotide sequence for *Xba*I in RS26685_3, RS26685_4, RS06980_3, RS06980_4, RS12400_3, and RS12400_4.

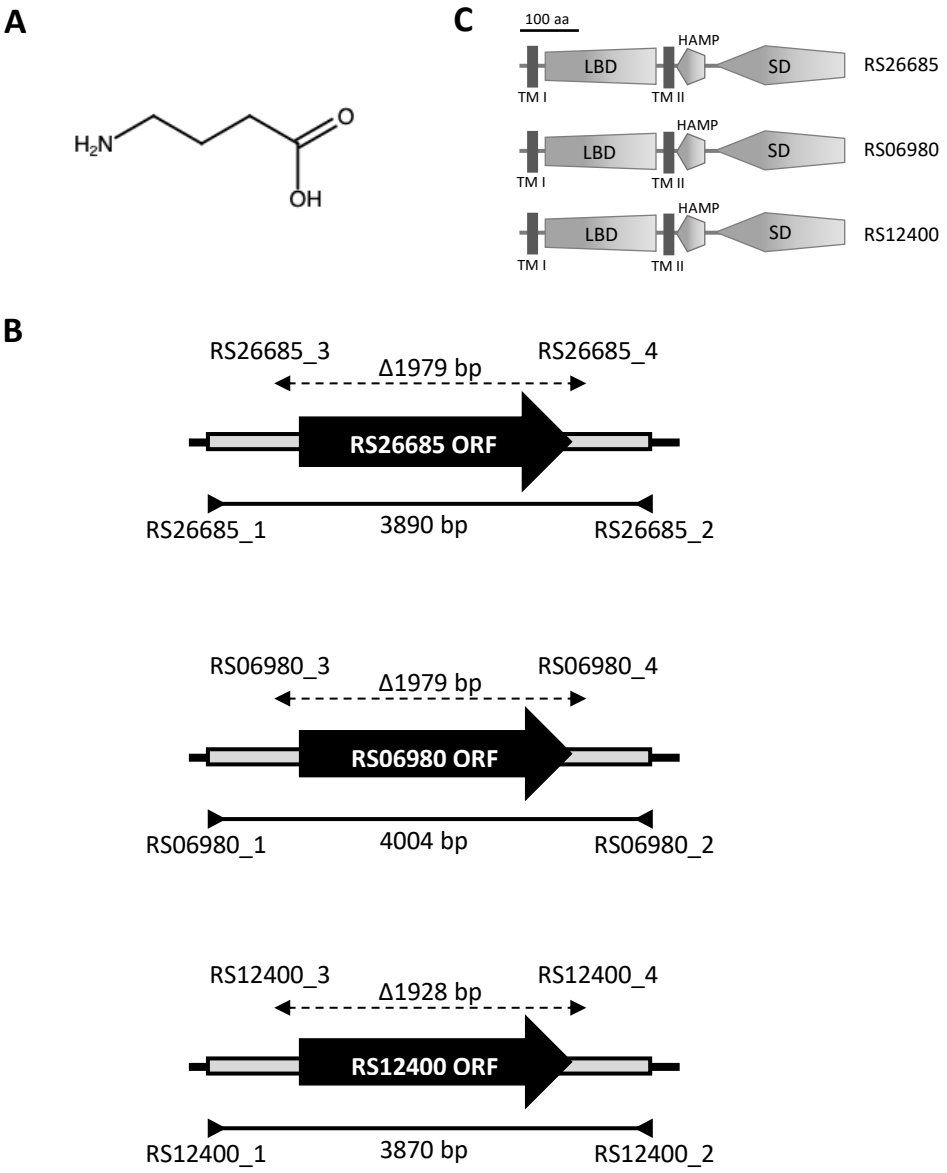

Fig. 3.1. GABA chemoreceptor homologs in *Pta*6605. (A) GABA structure. (B) Schematic structure of three MCP proteins of *Pta*6605. Transmembrane domains (TMI and TMII), ligand-binding domains (LBD), *h*istidine kinase, *a*denyl cyclase, *m*ethyl-accepting chemotaxis proteins and *p*hosphatase (HAMP) domains, signaling domains (SD), and scale of 100 amino acids are indicated. (C) Construction of the RS26685, RS06980, and RS12400 mutants. Light gray-shaded arrowheads indicate the position of the PCR primers that amplify each ORF with upstream and downstream regions. Black arrowheads indicate the position of the PCR primers that amplify the upstream and downstream regions prior to ORF deletion.

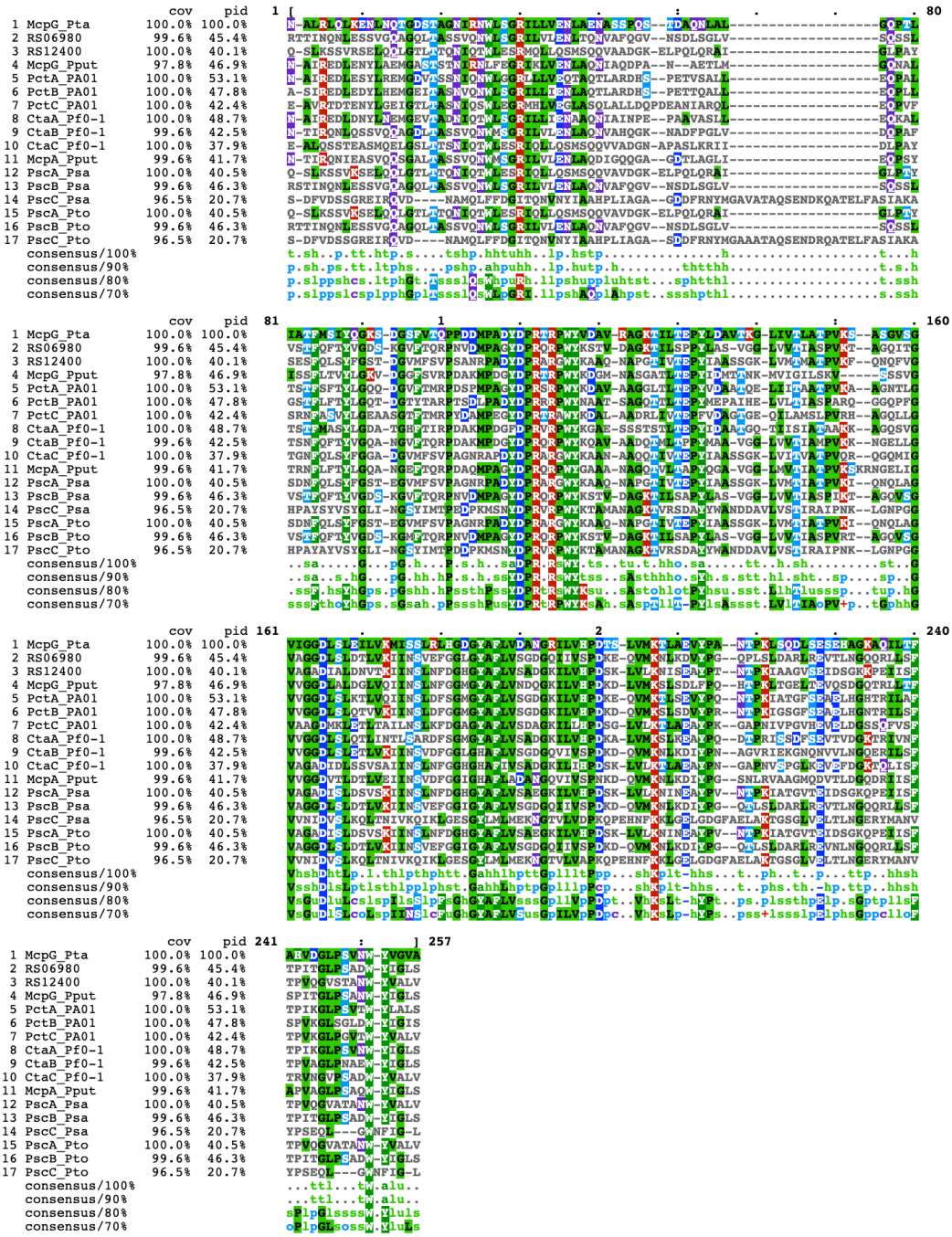

Fig. 3.2. Aligned amino acid sequences of *Pseudomonas* strains GABA chemoreceptor homologs. Colored backgrounds indicate identical sequence to McpG of *Pta*6605. Cov and pid values indicate percent coverage and percent identity, respectively. Multiple sequence alignment was generated using T-Coffee (tcoffee.crg.cat) (Notredame *et al.* 2000).

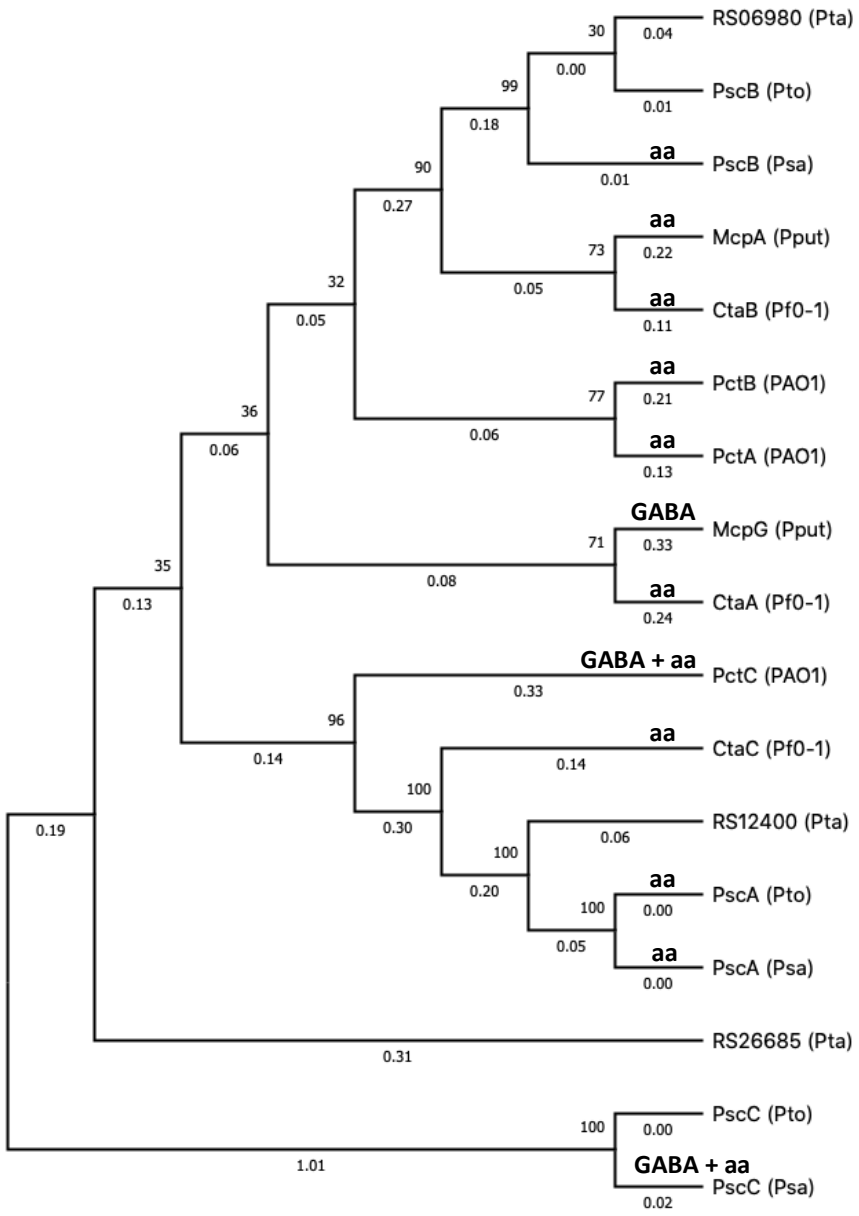

Fig. 3.3. Maximum likelihood tree based on ligand binding domains (LBDs) of the amino acid (aa) receptors and their homologs in *Pseudomonas* species. Phylogenetic tree of amino acid sequences of LBD of McpG and McpA, a GABA and amino acid receptor of *P. putida* KT2440; PctC, a GABA receptor and PctA and PctB, amino acid receptors of *P. aeruginosa* PAO1; CtaABC, amino acid receptors of *P. fluorescens* Pf0-1; PscABC, potential receptors for amino acids and GABA of *Psa*NZ-V13 and amino acid receptor and its paralogs of *Pto*DC3000; RS26685, RS12400 and RS06980, predicted GABA and amino acid receptors of *Pta*6605. Corresponding ligands are indicated by bold letters (**aa** and **GABA**). Branch length and bootstrap values are indicated on the tree. The tree was generated using MEGA version X software.

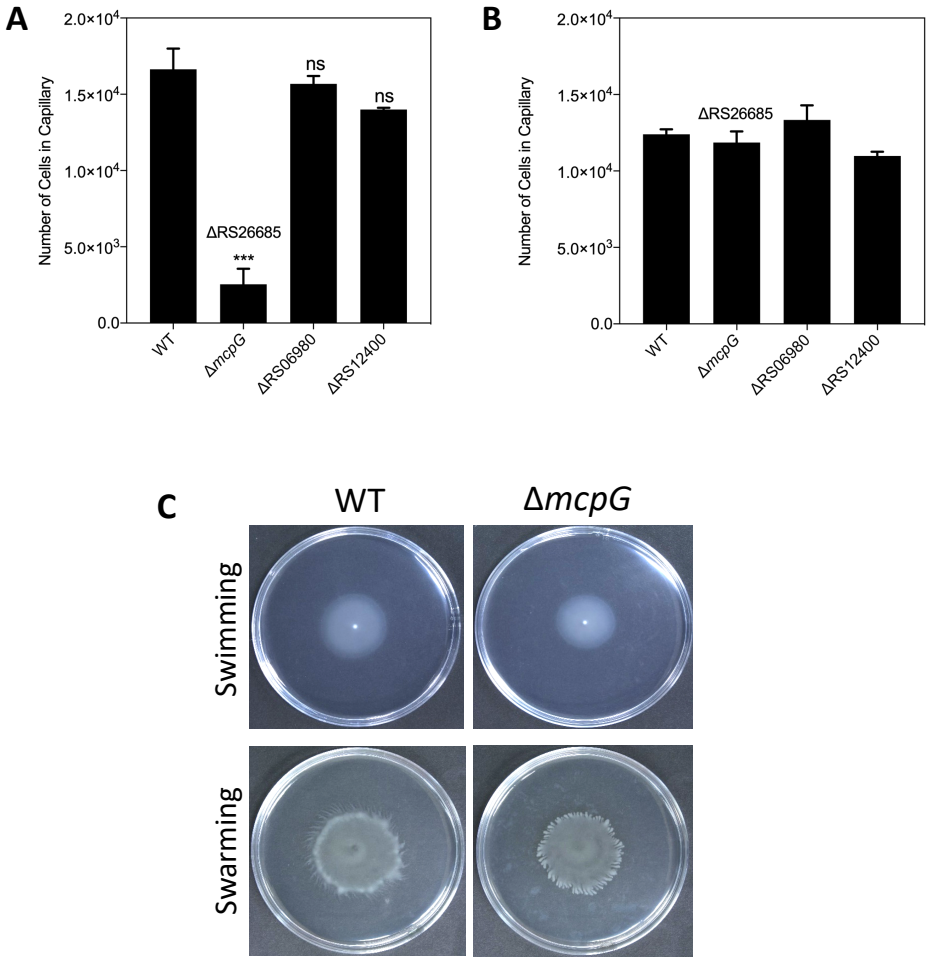

Fig. 3.4. Screening for GABA receptor. Chemotaxis to 10 mM GABA (A) and 1% yeast extract (B). Asterisks indicate a statistically significant difference compared to WT strain (ns: not significant; *** $P < 0.001$ by one-way ANOVA followed by Dunnett's multiple comparisons test). Error bars represent standard errors from 2 independent experiments conducted in triplicates. (C) Surface motility assay of WT and Δ*mcpG*. Swarming assay on SWM plates with 0.45% agar at 27ºC for 2 d and swimming assay on MMMF plates with 0.25% agar at 23ºC for 3 d. The photographs show representative results obtained from three independent experiments with two replicates.

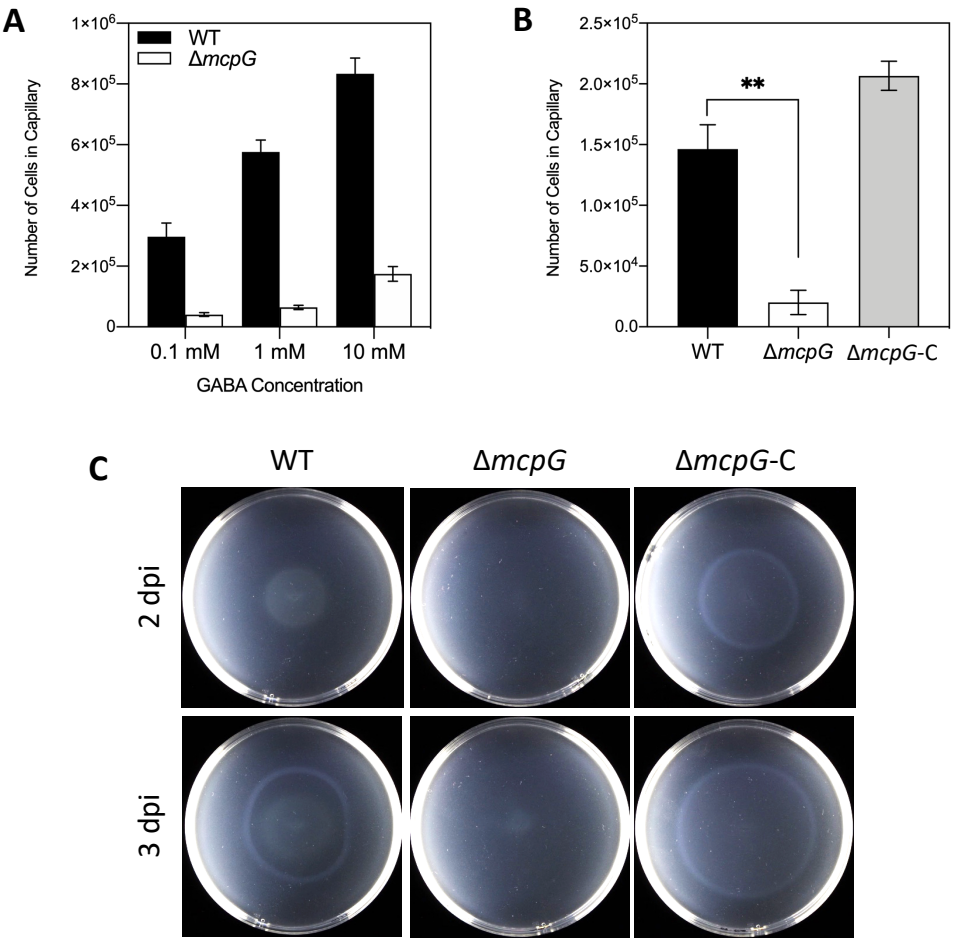

Fig. 3.5. Chemotaxis assays. (A) Quantitative chemotaxis assay of WT and Δ*mcpG* toward different GABA concentrations. (B) Chemotaxis of Δ*mcpG* and its complementation strain (Δ*mcpG*-C) to 10 mM GABA. Asterisks indicate statistically significant difference compared to WT strain (** $P < 0.01$ by one-way ANOVA followed by Dunnett's Multiple Comparisons Test). Error bars represent standard errors from 2 independent experiments conducted in triplicates. (C) Qualitative chemotaxis plate assay on 0.25% agar minimal media supplemented with 1 mM of GABA at 2 dpi and 3 dpi at 23ºC. The photographs show representative results from three independent experiments with 2 plates each.

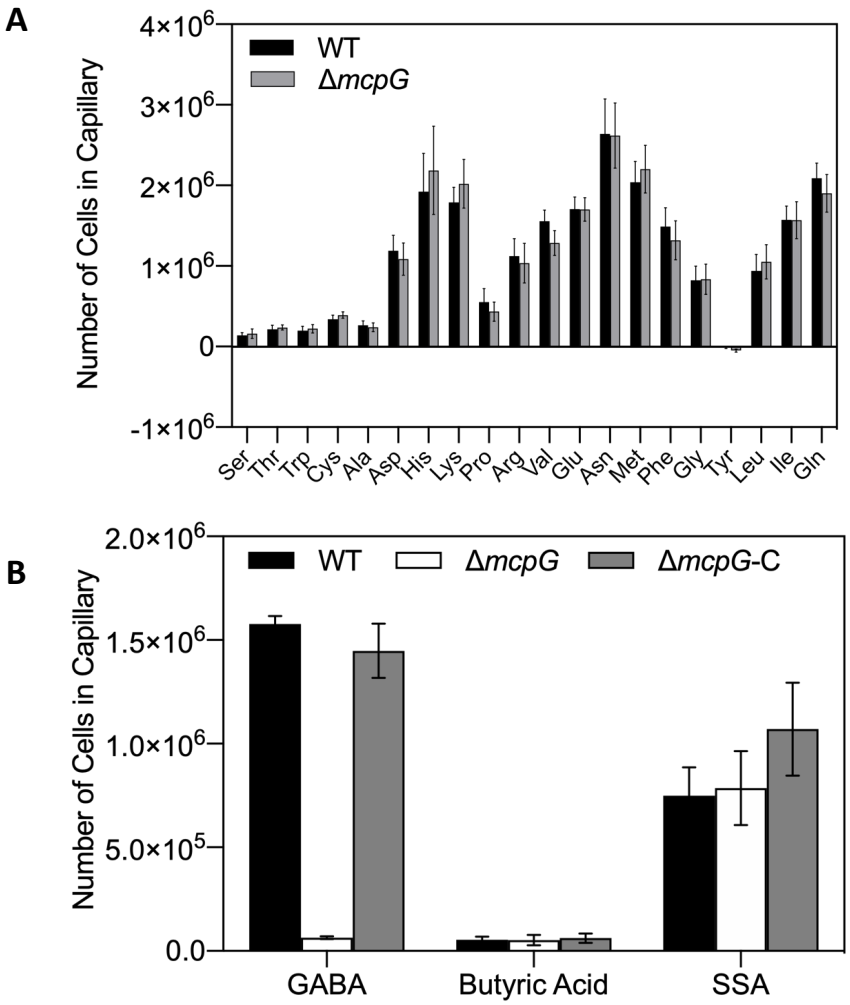

Fig. 3.6. Quantitative chemotaxis assay to determine McpG specificity. (A) Chemotactic responses to 20 proteinogenic amino acids (1 mM) and (B) chemotactic responses to GABA, butyric acid, and SSA (1 mM). Error bars represent standard errors from 2 independent experiments conducted in triplicates.

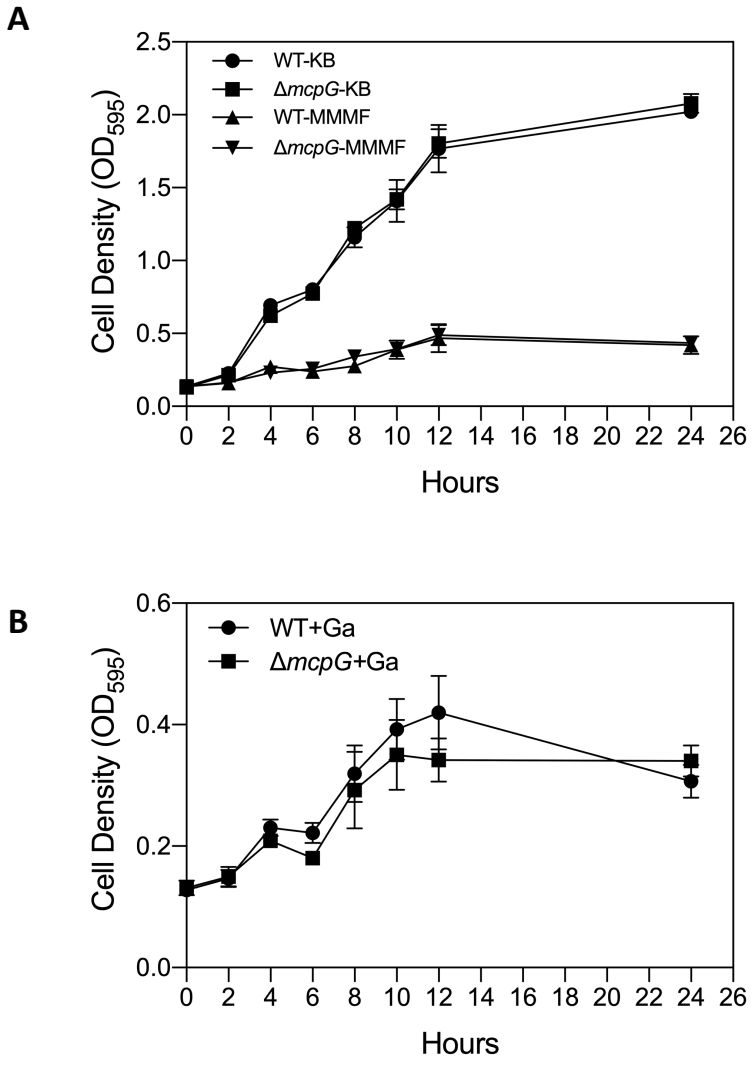

Fig. 3.7. Growth of WT and Δ*mcpG* strains in King's B medium/MMMF medium. (A) and in MM supplemented with 10 mM GABA as a sole source of carbon and nitrogen (B). Bacterial growth was measured at OD_{595}. Error bars represent standard error from two independent experiments conducted in triplicates.

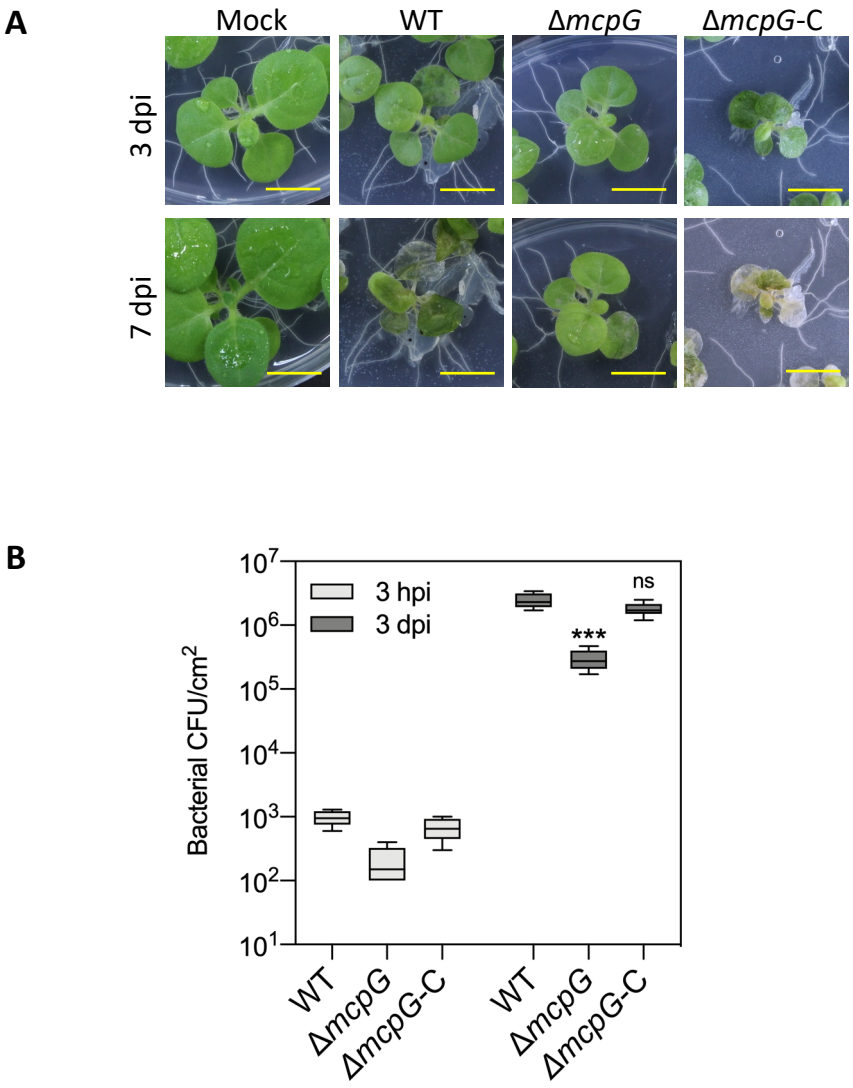

Fig. 3.8. Inoculation experiments by flood inoculation method. (A) Tobacco seedlings were inoculated by flooding 8 × 10^6 CFU/ml bacterial suspension of each strain and incubated at 22ºC. Photographs taken at 3 and 7 dpi show representative results from three independent experiments. (B) Bacterial population was counted at 0 and 3 dpi. The bars represent standard error from two independent experiments. Bacterial CFUs for each strain in one experiment were pooled from 3 (0 dpi) or 4 (3 dpi) individuals. Asterisks indicate statistically significant differences compared to WT strain (* $P < 0.05$; *** $P < 0.001$ by two-way ANOVA followed by Dunnett's multiple comparisons test).

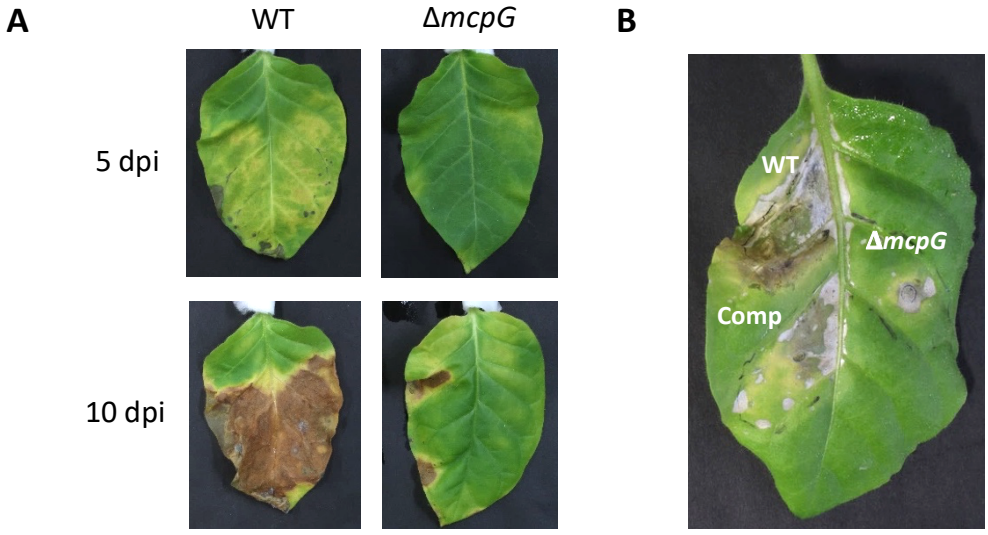

Fig. 3.9. Inoculation test of wild type (WT) and Δ*mcpG* strains by dip and infiltration methods. (A) Tobacco leaves were inoculated by dipping into 2 × 10^8 CFU/ml bacterial suspension of each strain and incubated at 22ºC. Photographs taken at 5 and 10 dpi show representative results from three independent experiments. (B) Tobacco leaves were infiltrated by 2 × 10^5 CFU/ml of each strain and incubated at 22ºC. Photographs taken at 14 dpi show representative results from two independent experiments.

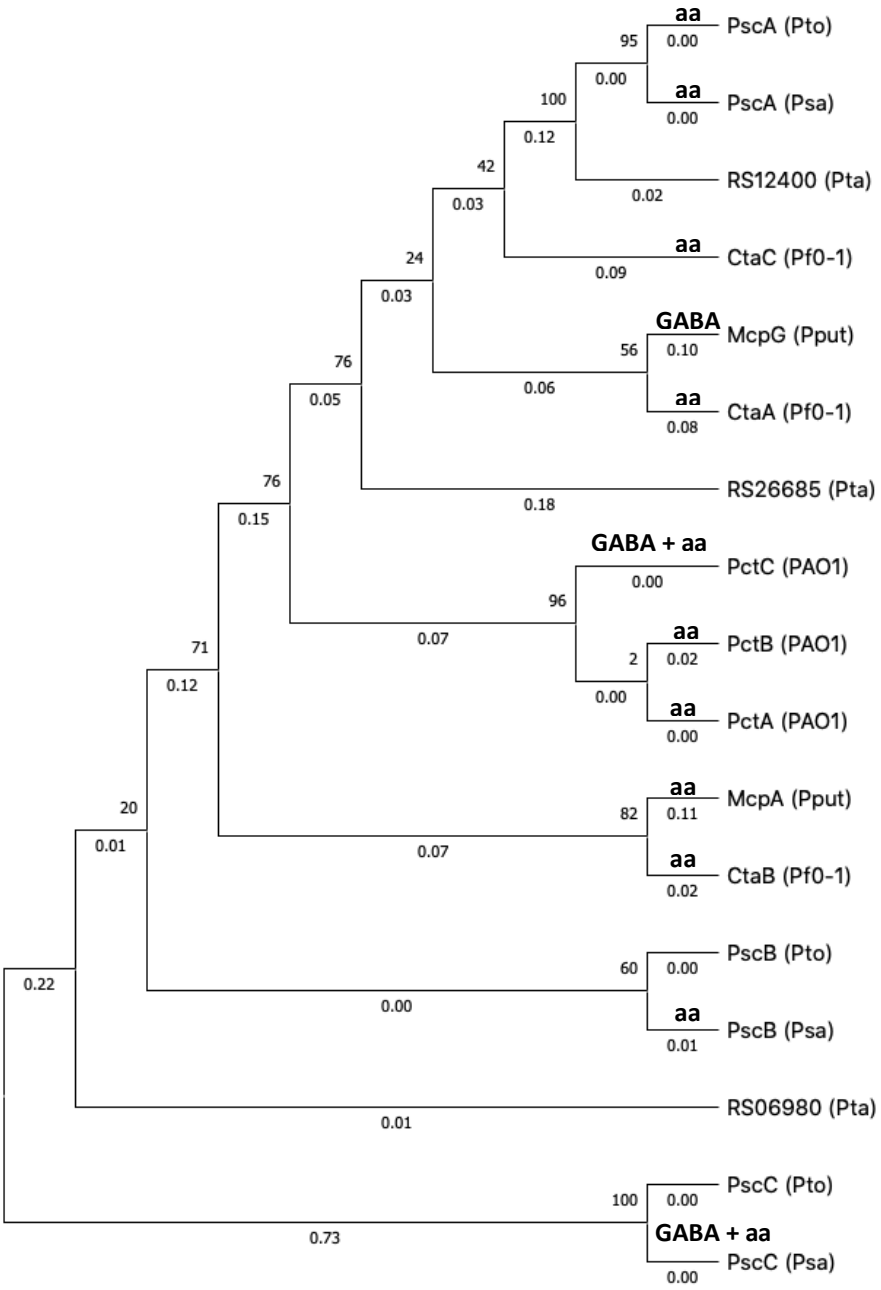

Fig. 3.10. Maximum likelihood tree based on a signaling domain (SD) of the amino acid receptors and their homologs in *Pseudomonas* species. Amino acid sequences of SD of McpG and McpA of *P. putida* KT2440, PctA, PctB, and PctC of *P. aeruginosa* PAO1, CtaA, CtaB, and CtaC of *P. fluorescens* Pf0-1, PscA, PscB, and PscC of *Pto*DC3000 and *Psa*NZ-V13, and RS26685, RS12400, and RS06980 of *Pta*6605 were compared. Corresponding ligands are indicated by bold letters (**aa** and **GABA**). Branch length and bootstrap values are indicated on the tree. The tree was generated using MEGA version X software.

Chapter 4

Identification of Amino Acids Chemoreceptors, PscA, PscB and PscC in *Pseudomonas syringae* pv. *tabaci* 6605 and Their Involvement in Host Plant Infection and Pathogenicity

Abstract

Chemotaxis is crucial for *Pseudomonas syringae* pv. *tabaci* (*Pta*) 6605 to evoke disease in tobacco plants. *Pta*6605 harbors more than fifty *mcp* genes for methyl-accepting chemotaxis proteins, however, almost all are functionally uncharacterized. Previously we identified a dCache_1 type MCP in *Pta*6605 which mediates chemotaxis to γ-aminobutyric acid, called McpG. In this study, we characterized other three dCache_1 type MCPs responsible for amino acids sensing, PscA, PscB, and PscC. Using capillary chemotaxis assay, we observed that all mutant strains had reduced chemotaxis to most amino acids, indicating PscA and PscB mediate chemotaxis to 15 amino acids, while PscC has slightly narrower ligand recognition, mediating chemotaxis to 12 amino acids. Other cellular functions were also affected in Δ*pscB* and Δ*pscC*; reduction of swarming motility was detected followed by increase in biofilm formation. Furthermore, Δ*pscB* and Δ*pscC* but not Δ*pscA* had reduced virulence in host tobacco plant. These findings supported the idea that chemosensory pathway correlated with virulence-related phenotypes. Amino acids are abundant in tobacco apoplast, therefore having multiple MCPs for them is beneficial for *Pta*6605 to facilitate entry into the plant.

Keyword: bacterial virulence, chemotaxis, amino acids, MCPs, plant-microbe interaction, *Pseudomonas*

4.1. Introduction

Chemotaxis allows motile bacteria to respond various environmental stimuli, both in a positive (toward) and negative (away) way. Chemotactic activity relies upon the work of complex chemosensory pathway, beginning with binding of chemotactic ligands (chemoeffectors) by chemoreceptor proteins (methyl-accepting chemotaxis proteins, MCPs). Ligand recognition produces molecular signal that modulates the downstream activity of core chemotaxis proteins (CheA, CheB, CheR, CheW, CheY, and CheZ). In the end, the chemotactic signal determines the rotation of flagellar motor, inducing chemotaxis activity (Sourjik and Wingreen, 2012; Bi and Lai, 2015).

A canonical MCP usually composes of ligand binding domain (LBD), transmembrane domains (TMD), and cytoplasmic *h*istidine kinase, *a*denyl cyclase, *m*ethyl-accepting chemotaxis proteins and *p*hosphatase (HAMP) domain and signaling domain (SD). Based on localization of the LBD and the number of TMD, MCPs can be classified into seven topology types (Ud-Din and Roujeinikova, 2017). Chemotactic response specifically depends on ligand recognition at the LBD of each chemoreceptor protein. MCPs with periplasmic LBD can also be generally clustered based on the size of their LBDs, cluster I for LBDs that have 150 amino acids and cluster II for LBDs with 250 amino acids (Sampedro *et al.*, 2015). Aside from that, chemoreceptor LBDs also have different domain types. As described by Cerna-Vargas et al. (2019), a model phytopathogen, *P. syringae* pv. *tomato* (*Pto*) DC3000 harbors 49 chemoreceptors, with 36 of them have periplasmic LBD flanked with two TMD. Most of those LBDs are parallel helix type (4HBM, HBM, Nit, and PilJ), and few of curved beta-sheet type (sCache and dCache).

In average, most chemotactic bacteria have around 14 genes encoding chemoreceptor proteins (Lacal *et al.*, 2010), however, depending on bacterial lifestyle, the number can reach up to 50 genes in plant pathogenic bacteria, for example among *Pseudomonas syringae* pathovars (Matilla and Krell, 2018). The presence of abundant chemical compounds in plants may have forced plant pathogens to harbor more chemoreceptors proteins for their advantages, as interference in chemotaxis usually leads to less virulence (Antúnez-Lamas *et al.*, 2009a; Hida *et al.*, 2015), indicating the relevance of chemotaxis for plant pathogens. Several bacteria also possess not only one, but multiple chemotaxis pathway, such as *P. aeruginosa* (Güvener *et al.*, 2006), *Pto*DC3000 (Clarke *et al.*, 2016), and *Pseudomonas syringae* pv. *tabaci* (*Pta*) 6605 (Chapter 2).

The relatively few numbers of functionally characterized chemoreceptors in plant pathogens are due to the high numbers of MCP-like proteins they possess. Currently, the information about ligands that are recognized by most bacterial chemoreceptors are mostly unknown. However, many of those already identified are compounds that serve as growth

substrates, such as sugars, amino acids, organic acids, hydrocarbons, and oxygen (Sampedro *et al.*, 2015). Others are in the form of plant hormones (Antúnez-Lamas et al., 2009b), inorganic phosphates (Wu *et al.*, 2000), neurotransmitters (Pasupuleti *et al.*, 2014) and quorum-sensing signals (Hegde *et al.*, 2011). We aimed to continue the identification of bacterial MCPs that are responsible for not only for flagellar-based motility, but also phenotypes correlated with virulence.

*Pta*6605 is the causal agent of wildfire disease on tobacco plant (Ichinose *et al.* 2003). This foliar pathogen that has more than 50 MCPs and requires chemotaxis to establish infection (Chapter 2). In our previous study, McpG, a γ-aminobutyric acid (GABA) chemoreceptor in *Pta*6605 has been characterized (Chapter 3). McpG has three homologs encoded by A3SK_RS0106980 (hereafter abbreviated as RS06980), A3SK_RS0112400 (RS12400) and A3SK_RS0114355 (RS14355). McpG and its homologs are also homologous to the amino acid receptors PscA/B/C of *Pto*DC3000 (Cerna-Vargas *et al.*, 2019) and *P. syringae* pv. *actinidiae* (*Psa*) NZ-V13 (McKellar *et al.*, 2015), PctA/B/C of *P. aeruginosa* (Taguchi *et al.*, 1997), and CtaA/B/C of *P. fluorescens* (Oku *et al.*, 2012). All of these chemoreceptors share the conserved double Cache_1 (dCache_1) type LBDs, suggesting the involvement of this type of LBD in sensing amino acids. In this study, the role of three McpG homologs encoded as amino acids chemoreceptors are discussed.

4.2. Materials and methods

4.2.1. Bacterial strains and plasmids

All bacterial strains and plasmids are listed in Table 1. *Pta*6605 strains were routinely cultured on King's B medium supplemented with 50 μg/mL nalidixic acid (Nal) at 27ºC (Taguchi *et al.*, 2003). *Escherichia coli* strains were grown on Luria Bertani (LB) medium with appropriate antibiotics at 37ºC.

4.2.2. Construction of predicted amino acids chemoreceptor mutants and complemented strains

Deletion mutants for RS06980 and RS12400 were previously reported (Chapter 3). To generate deletion mutant for RS14355, DNA fragment containing RS14355 was isolated and deleted using primers listed in Table 2. The deletion mutants are designated as ΔRS06980, ΔRS12400 and ΔRS14355. Complemented strains were constructed by introducing the entire open reading frame of each gene with predicted native promoter at *Not*I site of an expression

vector pDSK519 (Keen *et al.*, 1988) for RS06980, and at *Sac*I site and *Eco*RI site of a transposon vector pBSL118 (Alexeyev *et al.*, 1995) for RS12400 and RS14355, respectively. Constructed plasmid was introduced into *E. coli* S17-1 λpir strain and conjugated with the respective mutant to generate RS06980-C, RS12400-C and RS14355-C, respectively. Conjugants were selected with Nal- and kanamycin-containing KB plates and confirmed with PCR.

4.2.3. Quantitative chemotaxis assays

Chemotaxis assay was performed as previously described (Chapter 2 & 3). Briefly, the bacterial suspension was prepared in 10 mM HEPES buffer at OD_{600} of 0.05, and capillaries containing 5 μl of 1 mM amino acids (5 μL, Drummond Scientific Company, Broomall, PA, USA) were dipped into the bacterial suspension. After the incubation, the number of bacteria in the capillary were measured by plating.

4.2.4. Surface motility assay

Surface motility assays including swimming and swarming abilities on semi-solid agar plates were done as described in Chapter 2 and 3.

4.2.5. *In vitro* growth

The measurement of *in vitro* growth was done as described in Chapter 2 and 3.

4.2.6. Biofilm formation assay

As previously described (Nguyen *et al.*, 2012), quantification of biofilm was conducted. Briefly, bacterial strains were grown overnight in LB liquid supplemented with 10 mM $MgCl_2$. Bacterial cells were washed twice and resuspended with fresh MMMF medium at OD_{600} of 0.1. Bacterial suspension in flat-bottomed polypropylene Falcon® microtiter plate (Corning, Corning, NY, USA) was incubated for 48 h without agitation. Following incubation, bacterial cells on wall of the wells were stained by 0.5% crystal violet solution, and stained biofilms were then extracted using 200 μL of 95% ethanol for each well. The absorbance was measured using iMark™ Microplate Absorbance Reader at 595 nm (Bio-Rad Laboratories, Hercules, CA, USA).

4.2.7. Plant material and inoculation procedures

Virulence assessments on *Nicotiana tabacum* L. cv. Xanthi NC were conducted as described in Chapter 2 and 3.

4.2.8. Data analysis

The results of the bacterial population count of chemotaxis assays and virulence assay as well as biofilm quantification are expressed as means with standard error. One-way/two-way ANOVA followed by Dunnett's highly significant difference for multiple comparison tests were performed using GraphPad Prism ver. 9 (GraphPad Software Inc., San Diego, CA, USA). $P < 0.05$ was considered statistically significant.

4.3. Results

4.3.1. Conserved ligand binding domains (LBDs) type among *Pta*6605 MCPs

Ligand binding domains (LBDs) of a chemoreceptor (MCP) are responsible for specific signal recognition. Three MCP-encoding genes in *Pta*6605; A3SK_RS0126685 (RS26685), A3SK_RS0106980 (RS06980), and A3SK_RS0112400 (RS12400) are homologous to amino acid receptors in *P. aeruginosa* PAO1 (PctA, PctB, and PctC) (Taguchi *et al.*, 1997), *P. fluorescens* Pf0-1 (CtaA, CtaB, and CtaC) (Oku *et al.*, 2012), *Psa*NZ-V13 (PscA and PscB) (McKellar *et al.*, 2015), and *Pto*DC3000 (PscA and PscB) (Cerna-Vargas *et al.*, 2019). Furthermore, *Psa*NZ-V13 and *Pto*DC3000 have another dCache_1 type amino acid receptor MCPs, PscC (McKellar *et al.*, 2015; Cerna-Vargas *et al.*, 2019), and *Pta*6605 also conserves their ortholog, A3SK_RS0114355 (RS14355). Because PscCs of *Psa*NZ-V13 and *Pto*DC3000 are thought to be also amino acid chemoreceptors, it is likely that RS14355 also encodes the chemoreceptor for amino acids.

Three-dimensional (3D) structure prediction using Phyre[2] program showed that RS06980, RS12400, and RS14355 have dCache_1 type LBDs, thus can be classified into cluster II of type Ia MCPs (220-290 amino acid residues) (Fig. 4.1). Generally, each one of them consists of an N-terminal hydrophobic TMD followed by a hydrophilic periplasmic LBD, another hydrophobic TMD, HAMP, and a C-terminal cytoplasmic SD (Fig. 4.1.D). We constructed a phylogenetic tree from LBDs of all GABA and amino acid receptors described in previous study (Chapter 3) with addition of RS14355 (Fig. 4.2). RS12400 belongs to the same cluster of PscA of *Pto*DC3000 and *Psa*NZ-V13, RS06980 of *Pta*6605 was close with PscBs of *Pto*DC3000 and *Psa*NZ-V13, and RS14355 was clustered together with PscCs of *Pto*DC3000 and *Psa*NZ-V13. Therefore, we designate *mcp* genes of RS12400, RS06980 and RS14355 as *pscA*, *pscB* and *pscC*, respectively.

4.3.2. Identification of MCPs for amino acids

Amino acids are one of major component of plant apoplast (Solomon and Oliver, 2000). Many bacterial species from different niches showed attraction to amino acids (Taguchi *et al.*, 1997; Nishiyama *et al.*, 2012; Oku *et al.*, 2012; Hida *et al.*, 2015; Cerna-Vargas *et al.*, 2019). Using quantitative capillary assays, we evaluated chemotactic responses to 20 proteinogenic amino acids in *Pta*6605 wild type (WT), ΔRS12400 (Δ*pscA*), ΔRS06980 (Δ*pscB*), and ΔRS14355 (Δ*pscC*). We observed that WT strain showed positive response toward almost all amino acids with the exception of tyrosine (Fig. 4.3). Both Δ*pscA* and Δ*pscB* mutants failed to respond or showed weak response to 15 amino acids (16 with tyrosine, but since WT did not respond to it as well, we excluded it from the count). Δ*pscA* was still responsive to Arg, Asn, His, Lys, and Met (Fig. 4.3.A), and Δ*pscB* to Arg, His, Ile, Lys, and Val (Fig. 4.3.B). To confirm the role of the MCPs in sensing amino acids, we tested the complemented strains to response to all 20 proteinogenic amino acids. The introduction of full length RS12400 (*pscA*) and RS06980 (*PscB*) could restore the loss of responses to tested amino acids (Fig. 4.3). This demonstrates that RS12400 (*pscA*) and RS06980 (*pscB*) is the potential chemoreceptor for amino acids in *Pta*6605. Meanwhile, ΔRS14355 (Δ*pscC*) showed significantly reduced chemotactic responses to 12 amino acids but still responsive to Ala, Arg, His, Ile, Phe, Pro, and Trp (Fig. 4.4). Complemented strain of ΔRS14355 could restore or partially restore the chemotactic responses to 12 amino acids (Fig. 4.4), demonstrating that RS14355 (*pscC*) is also one of chemoreceptor for amino acids.

4.3.3. Swimming and swarming motilities

To evaluate the involvement of chemoreceptors in *Pta*6605 motility, swimming and swarming assay on soft agar plates were conducted. Δ*pscA* retained swimming motility, although it was somewhat lesser than the WT, but it retained great swarming motility, whereas Δ*pscB* and Δ*pscC* had reduced both surface swimming and swarming motilities, suggesting the possibility of signaling via PscB and PscC also affecting another motility-related pathway (Fig. 4.5.A). The complemented strain of Δ*pscB* showed restored both motilities on soft agar. However, the complemented strain of Δ*PscC* did not restore swimming motility, although the swarming motility was restored (Fig. 4.5.A).

4.3.4. Biofilm formation

Chemosensory systems mediate not only chemotaxis, but also multiple aspects of virulence in bacteria, including biofilm formation (Corral-Lugo *et al.*, 2016; Cerna-Vargas *et al.*,

2019). We conducted biofilm formation assay in MMMF medium with 48 h of static incubation and found that Δ*pscB* and Δ*pscC* resulted in significant increase of biofilm formation (Fig. 4.5.B). The complementation of Δ*pscB* and Δ*pscC* reduced it to almost WT level. However, it seems that Δ*pscA* has no role in biofilm formation of *Pta*6605. The fact that Δ*pscB* and Δ*pscC* had lost swarming activity (Fig. 4.5.A), further confirmed the inverse regulation of biofilm formation and swarming motility in *Pseudomonas syringae* like *Pto*DC3000 (Cerna-Vargas *et al.*, 2019).

4.3.5. *In vitro* growth

To evaluate the effect of mutant introduction on bacterial growth, wild type and each mutant strain were grown in rich medium (KB) and minimal medium (MM). In KB medium, both Δ*pscA* and Δ*pscB* grew faster than wild type strain as indicated by significantly higher absorbance value at 8 h, 10 h, and 12 h time points (Fig. 4.6.A). However, there was no significant difference between mutants and wild type in the growth in MMMF medium, suggesting that they propagate at almost the same rate in a minimal nutrient environment as in plant apoplast. In the case of Δ*pscC*, this mutant showed significantly faster growth in KB medium as well at 9 and 12 h time points. In MMMF medium, there was no significant different at any time point except it had less density than wild type strain at 24 h post inoculation (Fig. 4.6.B)

4.3.6. Virulence on host tobacco plant

Δ*pscB* reduced and Δ*pscC* lost swarming and swimming motilities. This may affect their virulence in tobacco plant. To investigate MCP's functions for *Pta*6605 virulence, we did two virulence assays. Both Δ*pscB* and Δ*pscC* were unable to effectively cause disease symptoms in host tobacco leaves by the flood inoculation method (Fig. 4.7) and infiltration method (Fig. 4.8). The complemented strain retained virulence though not fully. Meanwhile, inoculation of Δ*pscA* developed disease symptom like the WT strain by both inoculation methods (Fig. 4.7.A and 4.8). Bacterial populations of WT and mutant strains were counted at 3 hpi and 3 dpi following flood inoculation. As shown in Fig. 4.7.B, Δ*pscB* and Δ*pscC* grew less than the WT strain, and the complementation was able to restore the ability to propagate in host plants almost to the level of WT and Δ*pscA*. These results suggest that only *pscB* and *pscC* are required for the full virulence of *Pta*6605.

4.4. Discussions

Plant pathogenic bacterium *Pseudomonas syringae* can harbor as many as 50 chemoreceptor proteins, which makes it difficult to characterize each one, leading to the limited knowledge concerning their function in plant-microbes interaction. In this particular study, we continued to investigate the MCPs, PscA, PscB, and PscC in *Pta*6605 which are chemoreceptors for amino acids and supposedly have significant role in virulence of this pathogen.

Several studies have elucidated how chemotaxis pathways mediates host colonization by pathogenic or saprophytic bacteria (Matilla and Krell, 2018), especially regarding the interaction of two-component system in the pathway. In recent studies, we demonstrated that chemotaxis is significantly required for virulence of *Pta*6605 (Chapter 2) and the closely related *Pto*DC3000 (Clarke *et al*., 2016). But the importance of ligand perception via particular MCP proteins in pathogenicity is rarely known. We previously identified GABA chemoreceptor in *Pta*6605 and demonstrated how GABA signaling is required for effective plant infection (Chapter 3).

In *Pta*6605, McpG is one of chemoreceptor proteins that are homologous to PctA/PctB/PctC of PAO1 and PscA/PscB of *Pto*DC3000 and *Psa*NZ-V13 (Taguchi *et al*., 1997; Cerna-Vargas *et al*., 2019; McKellar *et al*., 2015). In this study we found that PscA/PscB/PscC that mediate *Pta*6605 chemotaxis to amino acids based on the quantitative chemotaxis assay. *Pta*6605 WT itself is attracted to 19 out of 20 proteinogenic amino acids and PscA/PscB and PscC mediating chemotaxis toward at least 15 and 12 of them, respectively (Fig. 4.3 and 4.4). To better understand the distribution of amino acids detected by each MCPs, we constructed a Venn diagram (Fig. 4.9). All three MCPs responsible for chemotaxis to Leu, Glu, Ser, Cys, Thr, Gly, Gln, and Asp. PscA and PscB share similar ligand recognition range than PscB with PscC and PscA with PscC. We speculate that for some cases where the chemotactic responses were not completely lost, the ability to recognize a ligand can be helped by the presence of other MCPs. However, all three mutants still showed chemotactic responses to His and Arg, therefore we thought that there may be unidentified MCPs for them that are not dCache-1 type.

*Pta*6605 WT and all mutants did not have any significant responses toward tyrosine. This result somewhat differs from most studies in which WT strain typically responds to all twenty amino acid but in one way is similar with *Vibrio cholerae*, that has no chemotactic response toward tyrosine (Nishiyama *et al*., 2012). In the case of plant pathogenic bacteria, it is possible that *Pta*6605 refuses to be attracted to tyrosine because it is one of the precursors of plant phenolic compounds (Bennett and Wallsgrove, 1994). Phenolic compounds are constituent of

plant defense against biotic stresses. High level of tyrosine and several other amino acids were found in disease tolerant varieties of citrus plant (Killiny and Hijaz, 2016).

Type Ia MCP in bacteria can be divided into two clusters based on the size of their periplasmic LBP, cluster I (about 120-210 amino acids) and cluster II (about 220-290 amino acids) (Sampedro *et al.*, 2015). Type Ia cluster I MCPs such as Tar and Tsr of *E. coli* have narrow ligand specificity (only two and three amino acids recognized, respectively, Ud-Din and Roujeinikova, 2017). PscA and PscB have broad ligand recognition indicated by recognizing 15 amino acids each. Both MCPs ligand binding regions consist of 226 and 227 amino acids, respectively. PscC has slightly narrower ligand recognition, mediating chemotaxis responses to 12 amino acids. LBDs of PscA, PscB, and PscC are dCache_1 type (double calcium channels and chemotaxis receptors, Fig. 4.1). These MCPs can be included as cluster II MCPs, with rather large size of LBD. It has been suggested that LBD of cluster II MCPs has two functional ligand binding pockets/subdomains, therefore capable of binding wider range of ligands, whereas cluster I MCPs only possess one (Mise, 2016).

dCache_1-type LBDs are seemingly conserved in cluster II MCPs across *Pseudomonas* and other bacterial species with amino acid-sensing ability. All MCPs listed on Fig. 4.2 have dCache_1 type LBDs, most of which have rather broad ligand recognition range, responsible for sensing 16-18 amino acids. However, the *Pto*DC3000 PscA, although possessing the same type of LBD, has a narrow ligand range and recognizes only three amino acids including D-Asp (Cerna-Vargas *et al.*, 2019). Amino acids have significant roles in the quality of tobacco leaf, affecting the formation of aromatic compounds as well as precursors of nicotine. Tobacco leaf contains high level of amino acids (Kung *et al.*, 1980), making sense of them being chemoattractant for *Pta*6605.

Chemotaxis contributes to bacterial virulence in early stage of infection, where bacterial cells have to search for entry points into plant apoplast (Melotto *et al.*, 2006). Usually related with chemotaxis, surface swarming motility and biofilm formation also play significant part in virulence. While biofilm formation is needed when bacterial cells have successfully attached on plant cells, swarming motility is required for later dispersal in order to expand the infection area. There have been some reports regarding the crosstalk between chemosensory pathway and the pathway regulating biofilm formation (Hickman *et al.*, 2005; Huang *et al.*, 2019). The deletion of *pscB* and *pscC* resulted in markedly decrease of swarming motility and increase in biofilm formation (Fig. 4.5). However, curiously, PscA of *Pta*6605 seems to have no role for the switch between sessile and planktonic lifestyle, while PscA of *Pto*DC3000 contributes to this phenotype (Cerna-Vargas *et al.*, 2019).

In *P. aeruginosa*, c-di-GMP level which controls biofilm formation is regulated by Wsp chemosensory pathway in the presence of the unknown signals. The Wsp pathway contains a response regulator similar with the CheY that seems to interact functional CheA-like protein (Hickman *et al.*, 2005). In previous study we determined that CheA2 and CheY2 are the functional two-response regulator modulating *Pta*6605 chemotaxis and virulence (Chapter 2). Although the effect of defect of biofilm formation was not investgated, it is easy to predict that it would lead to more cell aggregation, noting the reduced swarming motility. So, signals from LBD of PscB and PscC might feed into CheA2 which in turn interact with not only CheY2, but also the response regulator in biofilm pathway.

Loss of swarming motility often correlated with less fitness during infection process in *Pta*6605 (Taguchi and Ichinose, 2013). Our virulence assay showed that mutation of *pscB* and *pscC* dramatically reduced *Pta*6605 virulence in even infiltration inoculation method (Fig. 4.7 and 4.8). Both mutants were unable to cause severe disease probably due to not only defect of chemotaxis but also its highly reduced motility (Fig. 4.5) or its effect on the expression of other virulence-related genes. The complemented strain restored phenotypes indicating that PscB and PscC contributes to *Pta*6605 virulence. These phenotypes somewhat resemble to the Δ*fliC* of *Pta*6605 (Taguchi *et al.*, 2006), suggesting the mutation of *pscB* and *pscC* might severely affect its flagella-dependent motility. However, considering that both functions as amino acid receptors, which specific amino acids responsible for virulence has yet to be determined. On the other hand, because Δ*pscA* retained motility and virulence on host tobacco leaves by all inoculation methods, this chemoreceptor probably does not play any major role in *Pta*6605 virulence. Because chemotaxis is a tightly regulated mechanisms, we thought that the PscB/PscC-mediated signaling is enough for *Pta*6605 to exhibit chemotaxis and activate virulence-related chemotaxis.

Although inactivation of MCPs for amino acids often resulting in loss/reduction of virulence (Nishiyama *et al.*, 2012; Oku *et al.*, 2012; Cerna-Vargas *et al.*, 2019), some have no relation with virulence (Hida *et al.*, 2015; Reyes-Darias *et al.*, 2015). The difference in environmental condition, hosts specific traits, or even experimental set up can be the key factors. However, how does PscA of *Pto*DC3000 contribute to virulence? (Cerna-Vargas *et al.*, 2019). It has significantly narrower ligand recognition range than PscA of *Pta*6605. Both have completely different roles even though they are closely related (Fig. 4.2). It could be because signaling via PscA in *Pto*DC3000 also regulates biofilm formation. The expressions pattern of certain genes can differ depending on various environmental factors or internal signals. Another possibility

is that PscA of *Pta*6605 may not be expressed during the infection process. Further investigations are needed to clarify this finding.

Chemotaxis to plant compounds helps bacterial colonization (reviewed in Matilla and Krell, 2018). Tobacco leaf contains high level amino acids (Kung *et al.*, 1980). As a highly motile foliar pathogen *Pta*6605, having MCPs for amino acid would be beneficial for leaf colonization. In this study we presented the involvement of chemotaxis to amino acids via PscB and PscC in effective plant infection. Furthermore, as we found in the study of GABA chemoreceptor, McpG (Chapter 3), amino acid chemoreceptors, PscB and PscC also have multiple roles of chemosensory pathway. It is necessary for next study to determine the exact molecular interaction between MCPs signaling and virulence-related traits. The relationship between LBD type and the ligand they recognize is not yet fully understood. However, there is mounting evidence that dCache_1 type LBDs detect amino acids, specifically.

Table 4.1. Bacterial strains and plasmids used in this study

Bacterial strain, plasmid	Relevant characteristics	Reference or source
Escherichia coli		
DH5α	*F⁻λ⁻ ϕ80dLacZ ΔM15* Δ(*lacZYA-argF*)*U169 recA1 endA1 hsd*R17(*rK⁻ mK⁺*) *supE44 thi-1 gyrA relA1*	Nippon Gene
S17-1	*thi pro hsd*R *hsd*R *hsdM⁺ recA*(*chr::RP4-2-Tc::Mu-Km::Tn7*)	Schäfer et al. 1994
Pseudomonas syringae pv. *tabaci*		
Isolate 6605	Wild-type isolated from tobacco, Nal^r	Shimizu et al. 2003
6605-ΔRS12400	Isolate 6605 Δ*pscA,* Nal^r	Chapter 3
6605-ΔRS06980	Isolate 6605 Δ*pscB*, Nal^r	Chapter 3
6605-ΔRS14355	Isolate 6605 Δ*pscC,* Nal^r	This study
6605-*pscA*-C	pB-*pscA* containing Δ*pscA*, Nal^r Km^r	This study
6605-*pscB*-C	pD-*pscB* containing Δ*pscB*, Nal^r Km^r	This study
6605-*pscC*-C	pB-*pscC* containing Δ*pscC*, Nal^r Km^r	This study
Plasmid		
pGEM-TEasy	Cloning vector, Amp^r	Promega
pG-RS12400	RS12400 fragment-containing pGEM-TEasy, Amp^r	Chapter 3
pG-RS06980	RS06980_fragment-containing pGEM-TEasy, Amp^r	Chapter 3
pG-RS14355	RS14355_fragment-containing pGEM-TEasy, Amp^r	This study
pK18*mob*Sac*B*	Small mobilizable vector, Km^r, sucrose sensitive (s*acB*)	Schäfer et al. 1994
pK18-ΔRS12400	RS12400 deleted DNA-containing pK18*mobsacB*, Km^r	Chapter 3
pK18-ΔRS06980	RS06980 deleted DNA-containing pK18*mobsacB*, Km^r	Chapter 3
pK18-ΔRS14355	RS14355 deleted DNA-containing pK18*mobsacB*, Km^r	This study
pDSK519	Broad host range cloning vector, Km^r	Keen et al. 1988
pBSL118	Mini-Tn5-derived plasmid vector for insertion mutagenesis, Amp^r, Km^r	Alexeyev et al. 1995
pB-*pscA*	pBSL118 possessing expressible *pscA*, Km^r	This study
pD-*pscB*	pDSK519 possessing expressible *pscB*, Km^r	This study
pB-*pscC*	pBSL118 possessing expressible *pscC*, Km^r	This study

Nal^r, nalidixic acid resistant; Amp^r, ampicillin resistant; Km^r, kanamycin resistant.

Table 4.2. Primers used in this study

Primer Name	Sequence (5'--3')	Description
RS14355_1	GGCCTCGCTCAAGACAGTAC	Amplification of RS14355 and surrounding region
RS14355_2	CCGTGTCCGGGGTGAAGAAT	
RS14355_3	CGggatccTGCTCTTTGGCTTCAACCCAG	Deletion of RS114355 ORF
RS14355_4	CGggattcGATCAGGCCGTTACTGCGA	
RS14355_F	GGCGCGGGACGCAGCTGAT	Amplification of RS06980 and promoter region for complementation
RS14355_R	ACGGGTTGTCGAGGGCAGGG	

Lowercase letters indicate artificial nucleotide sequence for *BamH*I in RS14355_3 and RS14355_4.

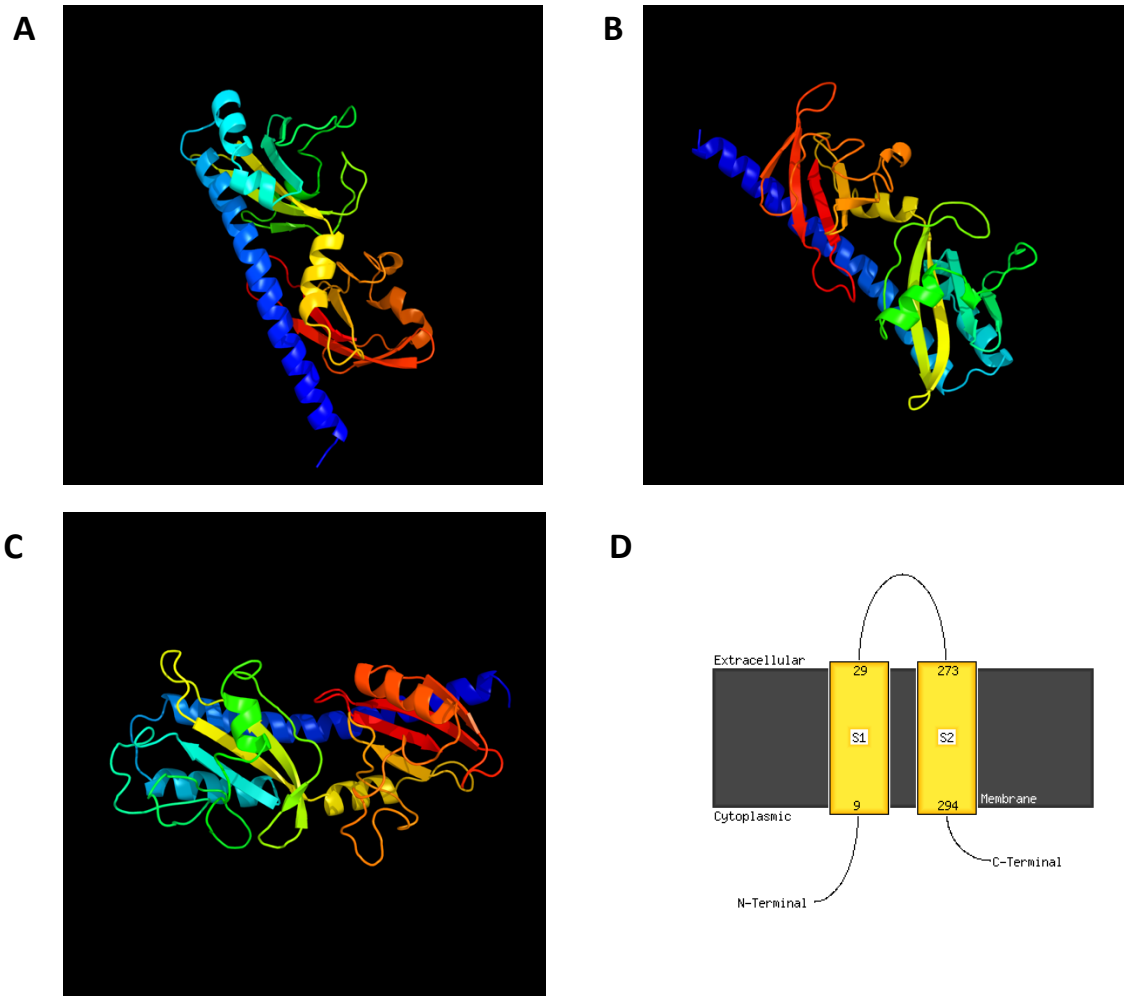

Fig. 4.1. The predicted three-dimensional (3D) structure of the *P. syringae* pv. *tabaci* 6605 dCache_1 type LBDs. (A) PscA encoded by RS12400**,** (B) PscB encoded by RS06980**,** and (C) PscC encoded by RS14355. Red color indicates the N-terminus and blue indicates the C-terminus. (D) The predicted domain localization of PscA/PscB/PscC proteins. The yellow boxes are transmembrane domains flanking the extracellular LBD. Structure prediction was done using the Phyre^2 algorithm with intensive mode (Kelley et al., 2015).

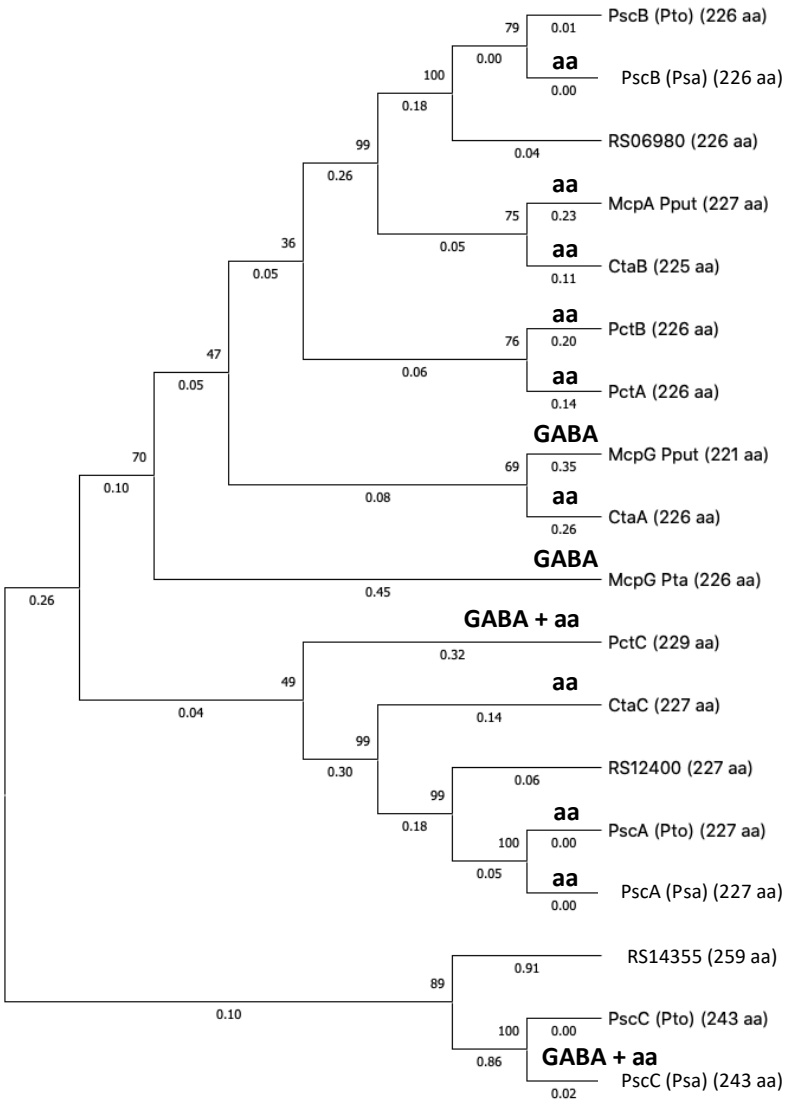

Fig 4.2. Maximum likelihood tree based on ligand binding domains (LBDs) of the amino acid (aa) receptors and their homologs in *Pseudomonas* species. Phylogenetic tree of amino acid sequences of LBD of McpG and McpA, a GABA and amino acid receptor of *P. putida* KT2440; PctC, a GABA receptor and PctA and PctB, amino acid receptors of *P. aeruginosa* PAO1; CtaABC, amino acid receptors of *P. fluorescens* Pf0-1; PscABC, potential receptors for amino acids and GABA of *Psa*NZ-V13 and amino acid receptor and its paralogs of *Pto*DC3000; McpG, GABA receptor of *Pta*6605, RS12400 and RS06980, and RS14355, predicted amino acid receptors of *Pta*6605. Corresponding ligands are indicated by bold letters (**aa** and **GABA**). Branch length and bootstrap values are indicated on the tree. The tree was generated using MEGA version X software.

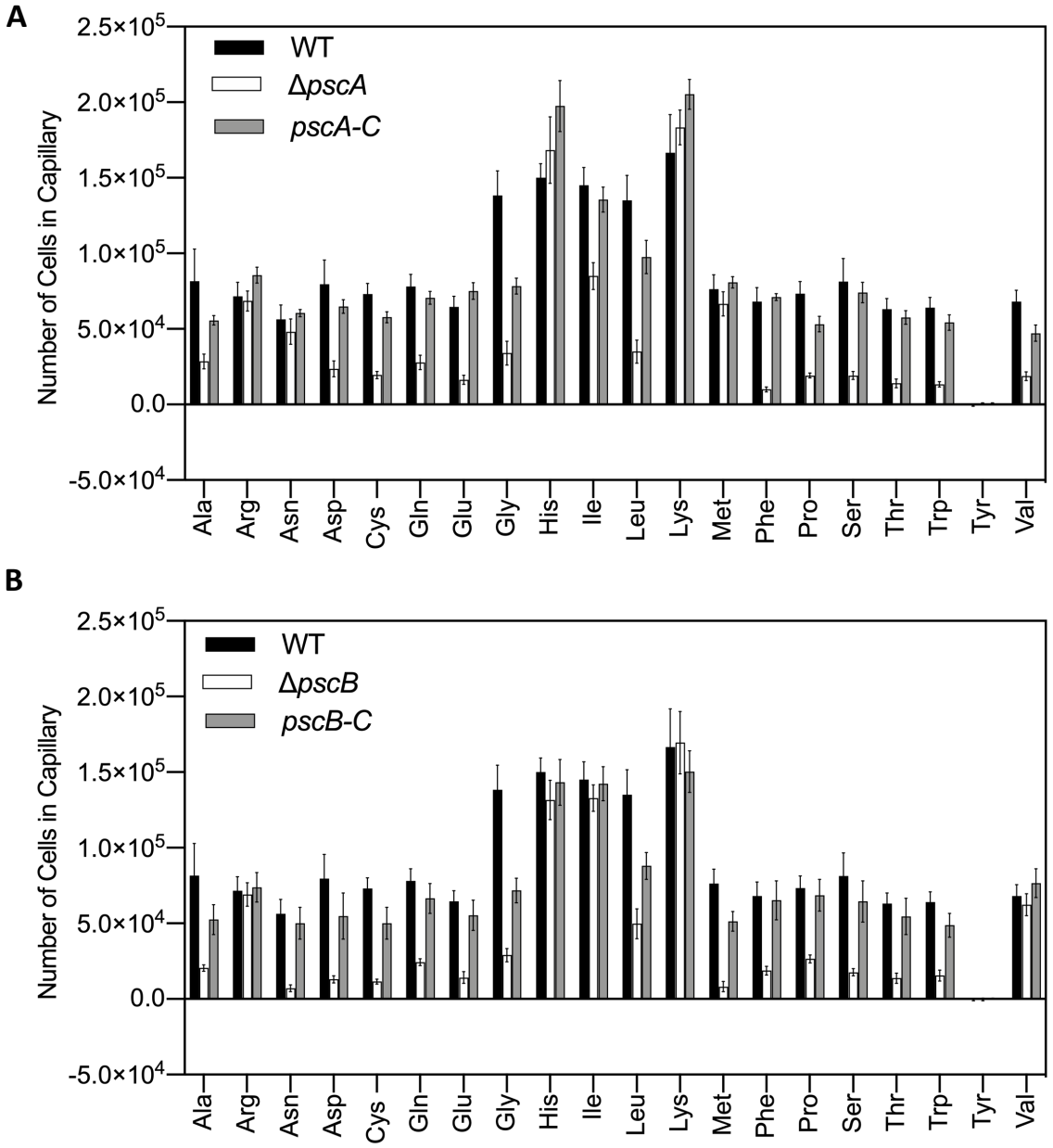

Fig. 4.3. Chemotaxis assays to 20 proteinogenic amino acids. Quantitative chemotaxis assay of wild type and Δ*pccA* (ΔRS12400, A) and Δ*pscB* (ΔRS06980, B). There are statistically significant differences in chemotaxis response to amino acid except for Arg, Asn, His, Lys, and Met between wild type strain and Δ*pscA* and Arg, His, Ile, Lys, and Val between wild type and Δ*pscB* (P<0.05 by Dunnett's Multiple Comparisons Test). Error bars represent standard errors from two independent experiments conducted in triplicates.

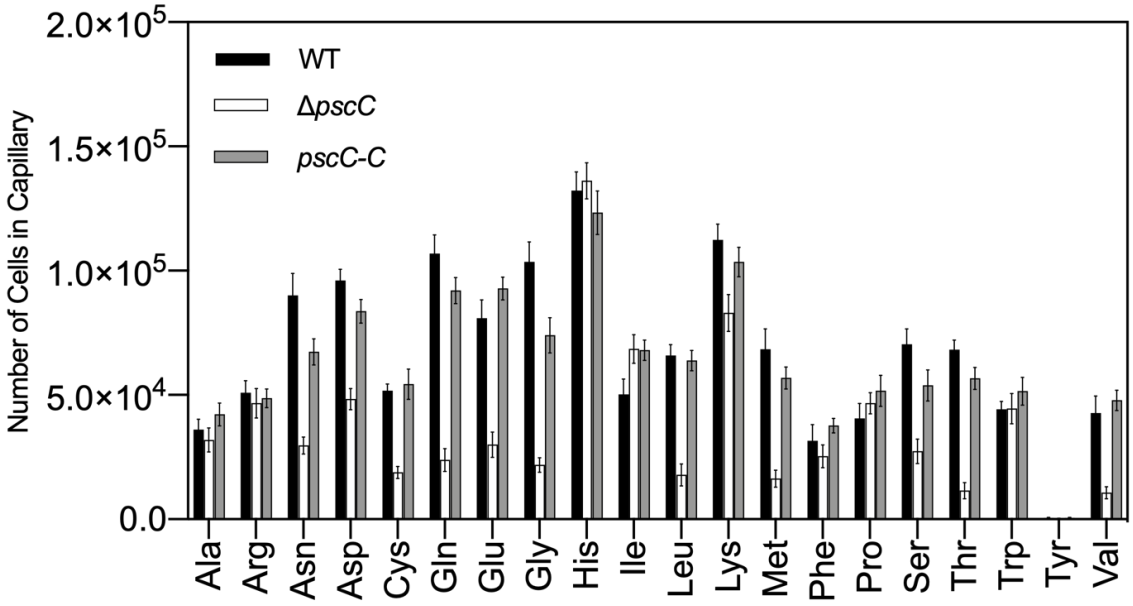

Fig. 4.4. Chemotaxis assays to 20 proteinogenic amino acids (ΔRS14355). Quantitative chemotaxis assay of wild type and Δ*pscC* (RS14355). There are statistically significant reductions in chemotaxis response to 12 amino acids except for Ala, Arg, His, Ile, Phe, Pro, and Trp between wild type strain and Δ*pscC* ($P<0.05$ by Dunnett's Multiple Comparisons Test). Error bars represent standard errors from 2 independent experiments conducted in triplicates.

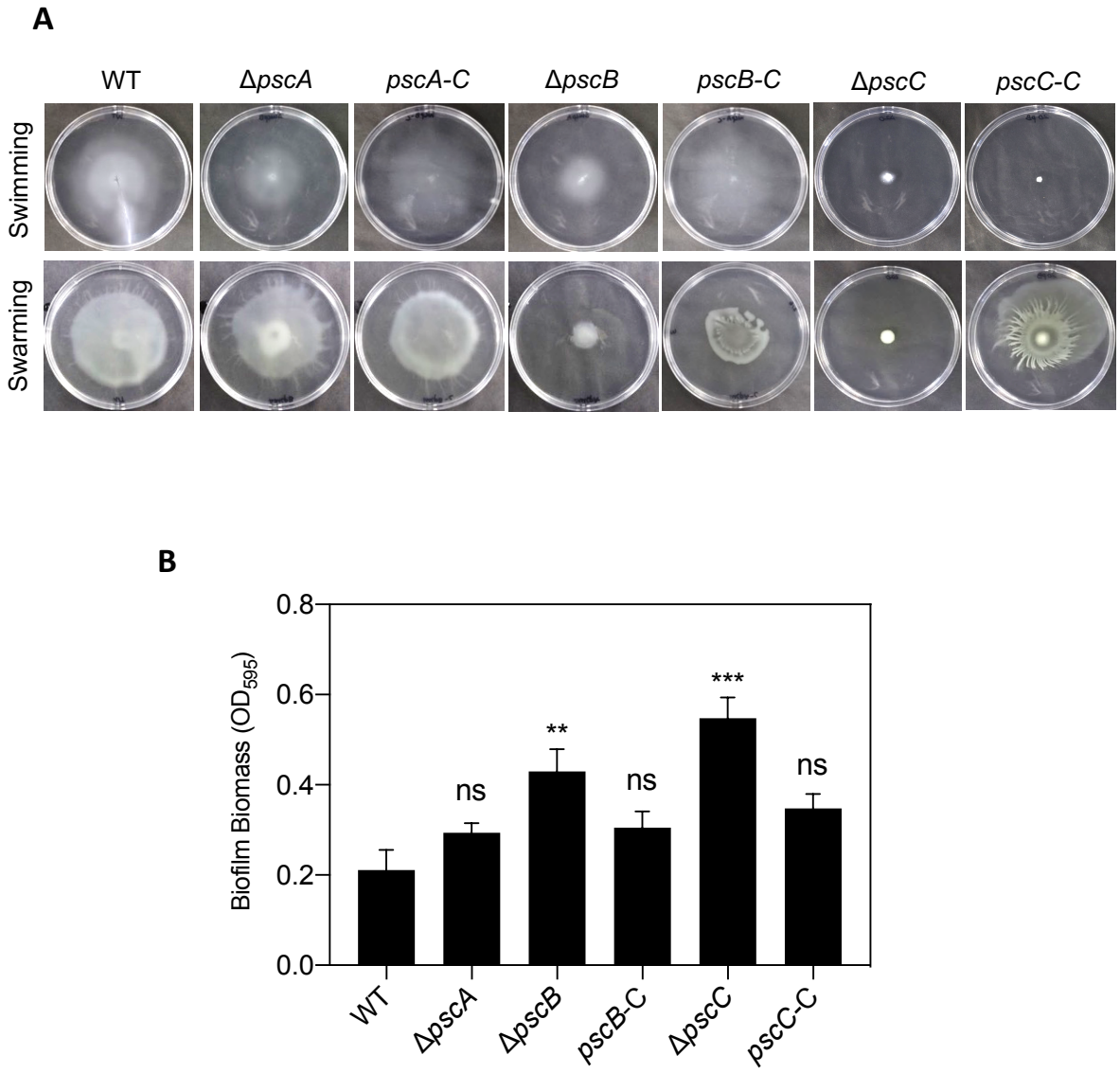

Fig. 4.5. Surface motilities and biofilm formation assay. (A) Swarming assay on SWM plates with 0.45% agar at 27 ˚C. Swimming assay on MMMF medium plates with 0.25% agar at 23 ˚C. Three μl of each bacterial suspension (2×10^8 CFU/ml) was spotted on the center of the plate and incubated for 72 h for swimming and 48 h for swarming. The photographs show representative results obtained from three independent experiments with three replicates. (B) Biofilm biomass was measured as value of OD_{595} after staining with crystal violet and 48 h of static incubation in MMMF medium. Error bars represent standard error from two independent experiments with five technical repeats. Asterisks indicate statistically significant differences compared to WT strain (**$P < 0.002$ by Dunnett's multiple comparisons test).

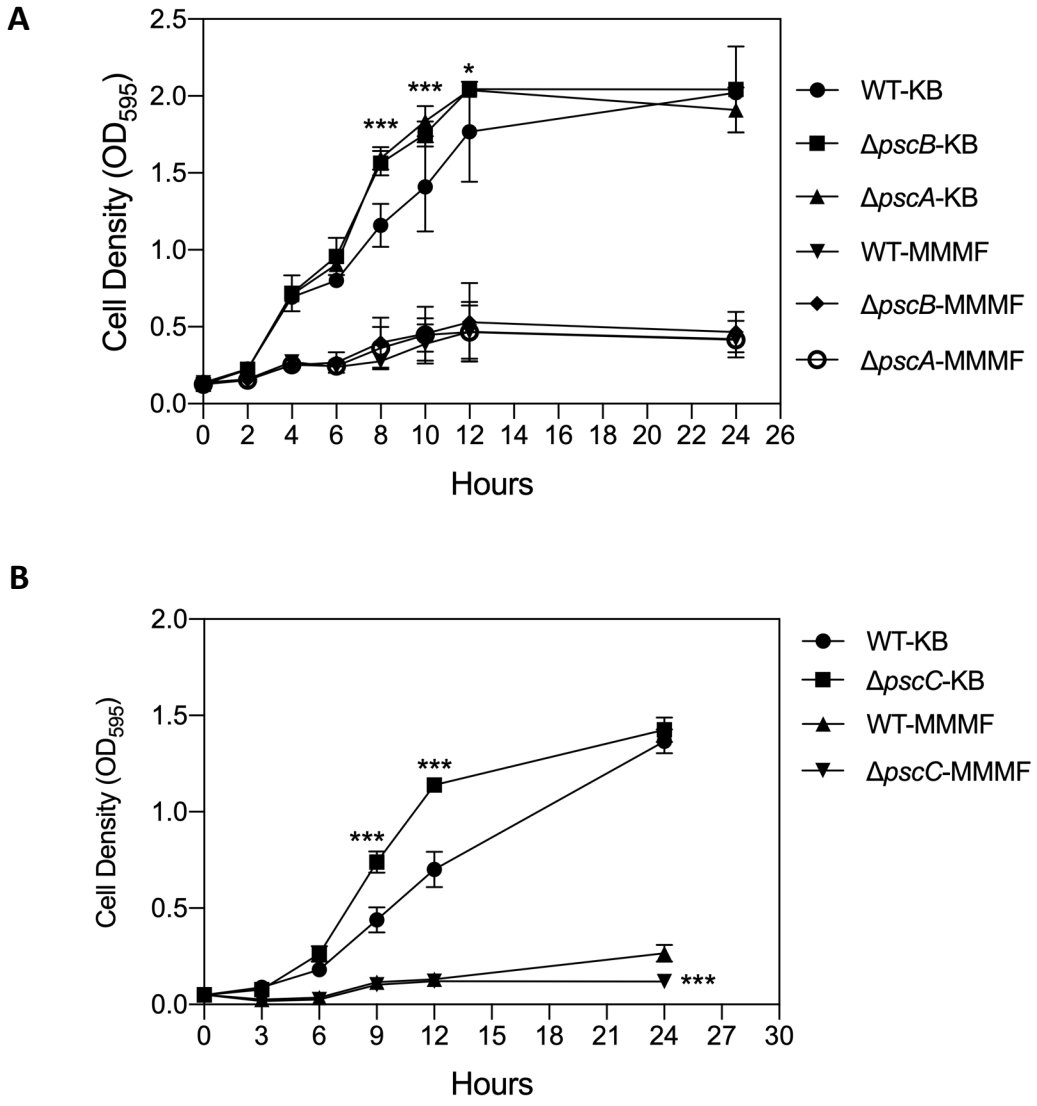

Fig. 4.6. Growth curve of wild type and mutant strains. (A) **Δ***pscA* and **Δ***pscB*, (B) **Δ***pscC*. Bacterial growth was measured in King's B medium (KB) and MMMF medium**.** Bacterial growth was measured at OD_{595}. Error bars represent standard error from two independent experiments conducted in triplicates. Asterisks indicate statistically significant differences compared to wild-type strain at indicated time points (*$P < 0.05$; ***$P < 0.001$ by Tukey's Multiple Comparisons Test).

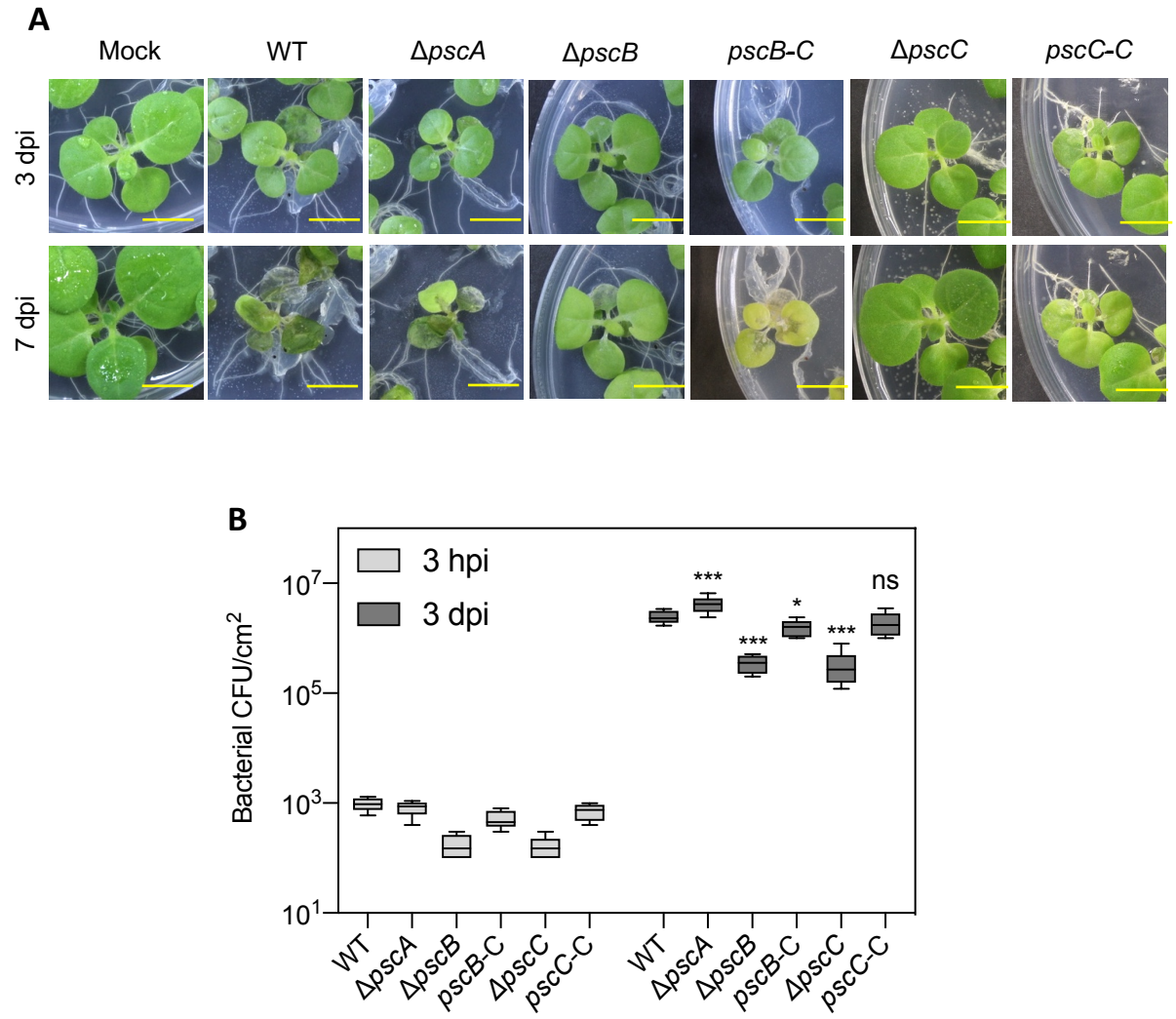

Fig. 4.7. Flood inoculation test on host tobacco seedlings. (A) Tobacco seedlings were inoculated by flooding of bacterial suspension (8×10^6 CFU/ml) of each strain and incubated at 22 ˚C**.** Photographs taken 3 dpi and 7 dpi show representative results from three independent experiments. (B) Bacterial population was counted at 3 hpi and 3 dpi. The bars represent standard error from two independent experiments. Bacterial CFUs for each strain in one experiment were pooled from 3 (3 hpi) or 4 (3 dpi) individuals. Asterisks indicate statistically significant differences compared to WT strain (*$P < 0.05$; ***$P < 0.001$ by Dunnett's multiple comparisons test).

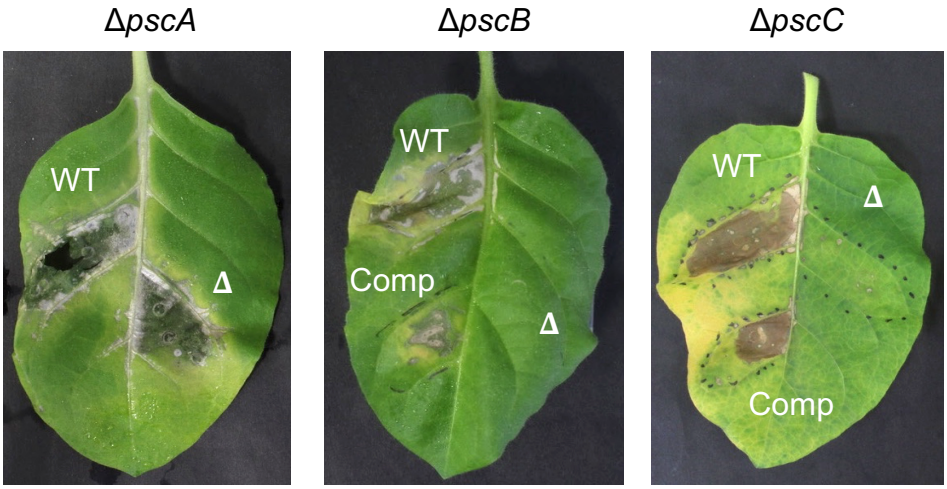

Fig. 4.8. Syringe infiltration inoculation tests on host tobacco plants. Tobacco leaves were infiltrated by 2×10^5 CFU/ml of each strain and incubated at 22 °C. Photographs taken 14 dpi show representative results from two independent experiments. In one experiment, three leaves from three independent plants were used.

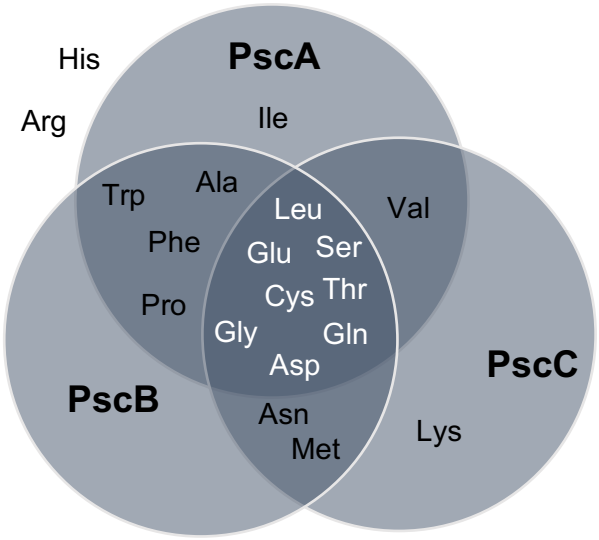

Fig. 4.9. Venn diagram depicting the amino acids recognized by PscA, PscB and PscC of *Pta*6605. Construction of this diagram was based on the chemotactic responses of WT, Δ*pscA*, Δ*pscB*, and Δ*pscC* (Fig. 4.3 and 4.4).

Chapter 5

General Discussions and Conclusions

Bacteria can sense and respond to chemical gradients using chemosensory system connected with flagella or pili. The ability to perform chemotaxis is deemed necessary for optimal virulence of bacterial pathogens. Flagella-mediated motility and chemotaxis has been studied quite well in *Pseudomonas*, especially in animal/human-infecting *Pseudomonas aeruginosa* (Sampedro *et al.*, 2015), as most of the pathways have homology with deeply studied *E. coli* chemotaxis system (Parkinson *et al.*, 2015). In plant pathogenic *Pseudomonas*, especially in less studied pathovars, many aspects of chemotaxis relevance in their pathogenesis are still vague. It is commonly believed that chemotaxis is in particular importance during the initial phases of infection that requires entry into host plants. However, in some studies, chemosensory pathways have been shown to modulate non-chemotaxis cellular functions. We investigated *Pseudomonas syringae* pv. *tabaci* 6605 (*Pta*6605) chemosensory pathways to further understand whether chemotaxis-mediated motility is in significant relevance for this highly motile pathogen.

*Pta*6605 is a potent bacterial pathogen causing severe wildfire disease in host tobacco plants. *Pta*6605 motility is somehow superior to that of *P. syringae* pv. *tomato* DC3000 (*Pto*DC3000), making it a suitable model organism to study bacterial motility and chemotaxis. Previously, it has been demonstrated that *Pta*6605 requires flagella for motility and full virulence (Ichinose *et al.*, 2013). In this study, we elucidated that chemotaxis is also required for effective host infection by this pathogen. *Pta*6605 has multiple copies of chemosensory gene clusters but only two have complete arrays of chemotaxis-related genes, cluster I and II. Both clusters are homologous to the functional chemotaxis clusters in *E. coli* and *P. aeruginosa*. We assessed the involvement of both clusters in chemotaxis and virulence by using deletion mutants of histidine kinase (*cheA*) and response regulator (*cheY*)-encoding genes from each cluster.

Using capillary chemotaxis assay to a nutrient source (yeast extract) we found that in *Pta*6605, genes located in cluster II are necessary for functional chemotaxis and flagella-mediated motility and cluster I may partially contribute to it. We also observed the requirement of cluster II-mediated chemotaxis in *Pta*6605 virulence. It is important to consider inoculation

method of choice when assessing bacterial virulence associated with chemotaxis. Difference method in inoculum administration would leads to distinct results from one to another. Therefore, we usually employ three modes of inoculation, flood assay which mimics natural infection condition, dip inoculation with detached leaves, and syringe infiltration that supposedly bypass the needs for chemotaxis and motility to get the comprehensive output. The mutant strains of cluster II genes (*cheA2* and *cheY2*) were unable to cause disease in all inoculation methods.

This is curious, because supposedly, once injected into plant apoplast, non-motile bacterial cells will have no problem causing disease. Unless the chemotaxis system in *Pta*6605 mediates not only chemotaxis-related pathway, but also virulence-related pathway. There have been some reports of how the response regulator proteins located in virulence-related pathway would act as phosphate sink, meaning, the phosphorylation activity of the two-component system in chemotaxis pathways would also affect those response regulators (Szurmant and Ordal. 2004; Hickman *et al.,* 2005; Huang *et al*., 2019). If this is the case, then it would make sense. However, we are still not able to assign the function of cluster I yet. As the mutant of *cheA1* showed reduced virulence in flood assay and infiltration method but not in dip inoculation with detached leaves. We also tried to overexpress *cheA1* and *cheY1* in *cheA2* and *cheY2* mutants, but it seems like that cluster I cannot complement cluster II function. It would be valuable if we could determine cluster I function in the future studies.

The specificity of chemotactic response is determined by the methyl-accepting chemotaxis proteins (MCPs) or chemoreceptors located in periplasm or cytoplasm of bacterial cells. Animal/human-infecting *Pseudomonas* typically have 23 MCPs in average (Matila and Krell, 2018) and the plant pathogenic *Pseudomonas syringae* harbors as many as 50 MCPs, suggesting that plant signals play a significant role in plant-microbes interaction. In animal/human pathogens, some virulence-related chemoeffectors and their corresponding MCPs have been identified, typically they are host-related/specific, such as human neurotransmitter, bile components, and taurine. In a plant pathogen, *Dickeya dadantii,* chemotaxis to plant hormones has been observed to involved in virulence (Antúnez-Lamas *et al*., 2009b; Río-Álvarez *et al*., 2015). Chemotaxis generally allows bacteria to move toward compounds involves in metabolism such as sugars, amino acids, organic acids, and oxygen (Sampedro *et al*., 2015).

*Pto*DC3000 has 49 MCP-encoding genes, however only one that has been characterized. PscA of *Pto*DC3000 mediates chemotaxis to amino acids and requires for its virulence (Cerna-Vargas *et al*., 2019). *Pta*6605 possesses more than 50 MCP-encoding genes and not a single one has been functionally characterized. We believe that some of the MCPs and their corresponding

ligands would play important role in virulence. Functional MCPs studies are difficult to be done especially because of the significantly high number of genes that need to be characterized. It is surprisingly laborious and time consuming, hence the low number of identified MCPs. A comparative study with GABA chemoreceptor in *P. aeruginosa* (Rico-Jimenez *et al.*, 2013) and *P. putida* (Reyes-Darias *et al.*, 2015) revealed that *Pta*6605 has three orthologs of potential GABA chemoreceptor genes. GABA is an important signaling molecule that exist in broad range of niches. GABA is accumulated in plants under biotic and abiotic stresses. However, the importance of GABA signaling in plant pathogen is not elucidated yet.

In our study, we tested all three deletion mutants for their ability to sense GABA. One mutant in particular had significantly reduced chemotactic response to GABA in any given concentration, we named it McpG. Investigation of the virulence of *mcpG* mutant revealed that GABA chemotaxis mediated by McpG is required for effective plant infection, even in infiltration inoculation. This study proves that GABA is also of a significant relevance for plant pathogenic bacteria. GABA might facilitate chemotaxis toward entry points into plants, however it is also possible that GABA sensing also mediates expressions of virulence-related genes in *Pta*6605. This is interesting because in *Pto*DC3000, GABA had negative effect on its virulence that accumulation of this non-proteinogenic amino acid suppressed *hrp* genes expressions, while in *P. protegens* enhances its root colonization ability. The role of GABA in plant-microbes interaction is indeed confusing. It may differ from one pathovars to another depending on the amount or GABA metabolism in the respective host plants. Therefore, we are now conducting a study on the effect of GABA exposure and accumulation on *Pta*6605 virulence.

Lastly, we investigate the ligand of the remaining chemoreceptor mutants in McpG study, PscA and PscB. It is possible to assume that they are the MCPs for amino acids, because of their counterparts in *P. aeruginosa* (Taguchi *et al.*, 1997), *P. fluorescens* (Oku *et al.*, 2012), *P. syringae* pv. *actinidiae* (McKellar *et al.*, 2015), and *Pto*DC3000 (Cerna-Vargas *et al.*, 2019). We observed that all of the MCPs for amino acids and GABA share the same ligand binding domain (LBD) type, double CACHE_1 (dCACHE_1). We could not help but to think about possible the relation between ligand binding domain types with what kind of ligands they can recognize. Therefore, we once again examined our MCP genes library and found that there is another MCP possessing dCACHE_1-type LBD, we named it PscC. Based on chemotaxis assay to 20 proteinogenic amino acids, both *pscA* and *pscB* mutants had significantly reduced chemotactic responses to 15 amino acids, and *pscC* mutants to 12 amino acids. Interestingly, only *pscB* and *pscC* mutants had lost surface motilities and virulence in host tobacco plants. It seems like

chemotactic signaling by PscA is not involved during pathogenesis. Moreover, we observed significant increase in biofilm formation by *pscB* and *pscC*. We conclude that amino acids-sensing via PscB and PscC are required for full virulence. This study further proved that chemosensory pathway is not isolated, that it may interconnected with non-chemotaxis pathways. It would be interesting if we could determine exactly which amino acid(s) instigate the stimuli related to virulence.

Pseudomonas has over 200 species and almost countless pathovars, yet only several important model pathogen species have their chemotaxis systems characterized. Our study exemplifies the role of chemotaxis in essential process such as pathogenicity in less explored yet highly virulent *Pseudomonas syringae* pv. *tabaci* 6605. Further research is greatly needed to identify others virulence related MCPs and their corresponding ligands in hope for a new disease prevention strategy which interfere with bacterial chemotaxis signaling.

References

Adler, J. (1966) Chemotaxis in bacteria. *Science* **153**: 708--716.

Agrios, G.N. (2005) *Plant Pathology*. 5th Edition. Amsterdam: Elsevier Academic Press.

Alexandre, G., Greer-Phillips, S., and Zhulin, I.B. (2004) Ecological role of energy taxis in microorganisms. *FEMS Microbiol. Rev.* **28**: 113--126.

Alexeyev, M.F., Shokolenko, I.N., Croughan, T.P. (1995) New mini-Tn5 derivatives for insertion mutagenesis and genetic engineering in gram-negative bacteria. *Can. J. Microbiol.* **41**(11): 1053--1055.

Allan, W.L., Simpson, J.P., Clark, S.M., and Shelp, B.J. (2008) γ-Hydrobutyrate accumulation in *Arabidopsis* and tobacco plants is a general response to abiotic stress: putative regulation by redox balance and glyoxylate reductase isoform. *J. Exp. Bot.* **59**: 2555--2564.

Anand, G.S. and Stock, A.M. (2002) Kinetic basis for the stimulatory effect of phosphorylation on the methylesterase activity of CheB. *Biochemistry* **41**(21): 6752--6760.

Antúnez-Lamas, M., Cabrera-Ordóñez, E., López-Solanilla, E., Raposo, R., Trelles-Salazar, O., Rodríguez-Moreno, A., Rodríguez-Palenzuela, P. (2009a) Role of motility and chemotaxis in the pathogenesis of *Dickeya dadantii* 3937 (ex *Erwinia chrysanthemi* 3937). *Microbiology* **155**(2): 434--442.

Antúnez-Lamas, M., Cabrera-Ordóñez, E., López-Solanilla, E., Solano, R., González-Melendi, P., Chico, J.M., Toth, I., Birch, P., Prichard, L., Liu, H., Rodríguez-Palenzuela, P. (2009b) Bacterial chemoattraction towards jasmonate plays a role in the entry of *Dickeya dadantii* through wounded tissues. *Mol. Microbiol.* **74**: 662--671.

Badri, D.V., Weir, T.L., van der Leile, D., Vivanco, J.M. (2009) Rhizosphere chemical dialogues: plant-microbe interactions. *Curr. Opin. Biotechnol.* **20**(6): 642--650.

Bandyopadhaya, A. and Chauduri, K. (2009) Differential modulation of NF-κB-mediated pro-inflammatory response in human intestinal epithelial cells by cheY homologues of *Vibrio cholerae*. *Innate. Immun.* **15**: 131--142.

Behrens, W., Schweinitzer, T., McMurry, J.L., Loewen, P.C., Buettner, F.F., Menz, S., Josenhans, C. (2016) Localisation and protein-protein interactions of the *Helicobacter pylori* taxis sensor TlpD and their connection to metabolic functions. *Sci. Rep.* **6**: 23582.

Bennett, R. and Wallsgrove, R. (1994). Tansley review No. 72. Secondary metabolites in plant defence mechanisms. *The New Phytologist* **127**(4): 617--633.

Bi, S. and Lai, L. (2015) Bacterial chemoreceptors and chemoeffectors. *Cell. Mol. Life Sci.* **72**: 691--708.

Blair, D.F. (1995) How bacteria sense and swim. *Annu. Rev. Microbiol.* **49**: 489--522.

Blattner, F.R., Plunkett, G., Bloch, C.A., Perna, N.T., Burland, V., Riley, M., Collado-Vides, J, Glasner JD, Rode CK, Mayhew GF, Gregor J, Davis NW, Kirkpatrick HA, Goeden M.A., Rose, D.J., Mau, B., Shao, Y. (1997) The complete genome sequence of *Escherichia coli* K-12. *Science* **277**: 1453--1462.

Buell, C.R., Joardar, V., Lindeberg, M., Selengut, J., Paulsen, I.T., Gwinn, M.L., Dodson, R.J., Deboy, R.T., Durkin, A.S., Kolonay, J.F., Madupu, R., Daugherty, S., Brinkac, L., Beanan, M.J., Haft, D.H., Nelson, W.C., Davidsen, T., Zafar, N., Zhou, L., Liu, J., Yuan, Q., Khouri, H., Fedorova, N., Tran, B., Russel, D., Berry, K., Utterback, T., Van Aken, S.E., Feldblyum, T.V., D'Ascenzo, M., Deng, W.L., Ramos, A.R., Alfano, J.R., Cartinhour, S., Chatterjee, A.K., Delaney, T.P., Lazarowitz, S.G., Martin, G.B., Schneider, D.J., Tang, X., Bender, C.L., White, O., Fraser, C.M., Colmer, A. (2003) The complete genome sequence of the *Arabidopsis* and tomato pathogen *Pseudomonas syringae* pv. tomato DC3000. *Proc. Natl. Acad. Sci. USA* **100**: 10181--10186.

Caiazza, N.C., Merritt, J.H., Brothers, K.M., O'Toole, G.A. (2007) Inverse regulation of biofilm formation and swarming motility by *Pseudomonas aeruginosa* PA14. *J. Bacteriol.* **189**(9): 3603--3612.

Cerna-Vargas, J.P., Santamaría-Hernando, S., Matilla, M.A., Rodríguez-Herva, J.J., Daddaoua, A., Rodríguez-Palenzuela, P., Krell, T., and López-Solanilla, E. (2019) Chemoperception of specific amino acids controls phytopathogenicity in *Pseudomonas syringae* pv. tomato. *mBio* **10**: e01868-19.

Chatnaparat, T., Li, Z., Korban, S.S., and Zhao, Y. (2015) The stringent response mediated by (p)ppGpp is required for virulence of *Pseudomonas syringae* pv. *tomato* and its survival on tomato. *Mol. Plant-Microbe Interact.* **28**: 776--789.

Chevrot, R., Rosen, R., Haudecoeur, E., Cirou, A., Shelp, B.J., Ron, E., and Faure, E. (2006) GABA controls the level of quorum-sensing signal in *Agrobacterium tumefaciens*. *Proc. Natl. Acad. Sci. USA* **103**: 7460--7464.

Clarke, C.R., Hayes, B.W., Runde, B.J., Markel, E., Swingle, B.M., Vinatzer, B.A. (2016) Comparative genomics of *Pseudomonas syringae* pathovar *tomato* reveals novel chemotaxis pathway associated with motility and plant pathogenicity. *PeerJ* **4**:e2570.

Corral-Lugo, A., De La Torre, J., Matilla, M.A., Fernández, M., Morel, B., Espinosa-Urgel, M., and Krell, T. (2016) Assessment of the contribution of chemoreceptor-based signaling to biofilm formation. *Environ. Microbiol.* **18**: 3355--3372.

Darzins, A. (1994) Characterization of a *Pseudomonas aeruginosa* gene cluster involved in pilus biosynthesis and twitching motility: sequence similarity to the chemotaxis proteins of enterics and the gliding bacterium *Myxococcus xanthus*. *Mol. Microbiol.* **11**(1): 137--153.

Deeken, R., Engelmann, J.C., Efetova, M., Czirjak, T., Müller, T., Kaiser, W.M., Tietz, O., Krischke, M., Mueller, M.J., Palme, K., Dandekar, T., and Hedrich, R. (2006) An integrated view of gene expression and solute profiles of *Arabidopsis* tumors: a genome-wide approach. *Plant Cell* **18**: 3617--3634.

Dhakal, R., Bajpai, V.K., and Baek, K.H. (2012) Production of gaba (γ-Aminobutyric acid) by microorganisms: a review. *Braz. J. Microbiol.* **43**: 1230--1241.

Dodds, P.N. and Rathjen, J.P. (2010) Plant immunity: towards an integrated view of plant-pathogen interactions. *Nat. Rev. Genet.* **11**(8): 539.

Fatmi, M., Collmer, A., Iacobellis, N.S., Mansfield, J., Murillo, J., Schaad, N.W., Ullrich, M. (Eds.). (2008) *Pseudomonas syringae pathovars and related pathogens: Identifications, epidemiology and genomics*. Springer Science+Business Media, B. V., pp. 448.

Feng, L., Reeves, P.R., Lan, R., Ren, Y., Gao, C., Zhou, Z., Ren, Y., Cheng. J., Wang, W., Wang, J., Qian, W., Li, D., Wang, L. (2008) A recalibrated molecular clock and independent origins for the cholera pandemic clones. *PLoS One* **3**: e4053.

Ferrández, A., Hawkins, A.C., Summerfield, D.T., Harwood, C.S. (2002) Cluster II *che* genes from *Pseudomonas aeruginosa* are required for an optimal chemotactic response. *J. Bacteriol.* **184**: 4374--4383.

Garvis, S., Munder, A., Ball, G., de Bentzmann, S., Wiehlmann, L., Ewbank, J.J., Tümmler, B., Filloux, A. (2009) *Caenorhabditis elegans* semi-automated liquid screen reveals a specialized role for the chemotaxis gene *cheB2* in *Pseudomonas aeruginosa* virulence. *PLoS Pathog.* **5**(8): e1000540.

Gosink, K.K., Kobayashi, R., Kawagishi, I., Häse, C.C. (2002) Analyses of the roles of the three *cheA* homologs in chemotaxis of *Vibrio cholerae*. *J. Bacteriol.* **184**: 1767--1771.

Güvener, Z.T., Tifrea, D.F., Harwood, C.S. (2006) Two different *Pseudomonas aeruginosa* chemosensory signal transduction complexes localize to cell poles and form and remould in stationary phase. *Mol. Microbiol.* **61**: 106--118.

Hegde, M., Englert, D.L., Schrock, S., Cohn, W.B., Vogt, C., Wood, T.K., Manson, M.D., Jayaraman, A. (2011) Chemotaxis to the quorum-sensing signal AI-2 requires the Tsr

chemoreceptor and the periplasmic LsrB AI-2-binding protein. *J. Bacteriol.* **193**(3): 768--773.

Hickman, J.W., Tifrea, D.F., Harwood, C.S. (2005) A chemosensory system that regulates biofilm formation through modulation of cyclic diguanylate levels. *Proc. Natl. Acad. Sci USA* **102**(40): 14422--14427.

Hida, A., Oku, S., Kawasaki, T., Nakashimada, Y., Tajima, T., and Kato, J. (2015) Identification of the *mcpA* and *mcpM* genes, encoding methyl-accepting proteins involved in amino acid and L-malate chemotaxis, and involvement of McpM-mediated chemotaxis in plant infection by *Ralstonia pseudosolanacearum* (formerly *Ralstonia solanacearum* phylotypes I and III). *Appl. Environ. Microbiol.* **81**: 7420--7430.

Hida, A., Oku, S., Nakashimada, Y., Tajima, T., and Kato, J. (2017) Identification of boric acid as a novel chemoattractant and elucidation of its chemoreceptor in *Ralstonia pseudosolanacearum* Ps29. *Sci. Rep.* **7**: 8609.

Hirano, S.S. and Upper, C.D. (2000) Bacteria in the leaf ecosystem with emphasis on *Pseudomonas syringae*-a pathogen, ice nucleus, and epiphyte. *Microbiol. Mol. Biol. Rev.* **64**(3): 624--53.

Höfte, M. and De Vos, P. (2006) Plant pathogenic pseudomonas species, in *Plant-associated Bacteria*, Springer, pp. 507--533.

Hong, C.S., Shitashiro,. M, Kuroda, A., Ikeda, T., Takiguchi, N., Ohtake, H., Kato, J. (2004) Chemotaxis proteins and transducers for aerotaxis in *Pseudomonas aeruginosa*. *FEMS Microbiol. Lett.* **231**(2): 247--252.

Huang, Z., Wang, Y.H., Zhu, H.Z., Andrianova, E.P., Jiang, C.Y., Li, D., Ma, L., Feng, J., Liu, Z.P., Xiang, H., Zhulin, I.B., Liu, S.J. (2019) Cross talk between chemosensory pathways that modulate chemotaxis and biofilm formation. *mBio* **10**(1): e02876--18.

Hückelhoven, R. (2007) Transport and secretion in plant-microbe interactions. *Curr. Opin. Plant Biol.* **10**(6): 573--579.

Ichinose, Y., Shimizu, R., Ikeda, Y., Taguchi, F., Marutani, M., Mukaihara, T., Inagaki, Y., Toyoda, K., Shiraishi, T. (2003) Need for flagella for complete virulence of *Pseudomonas syringae* pv. *tabaci*: genetic analysis with flagella-defective mutants Δ*fliC* and Δ*fliD* in host tobacco plants. *J. Gen. Plant Pathol.* **69**: 244--249.

Ichinose, Y., Taguchi, F., Mukaihara, T. (2013) Pathogenicity and virulence factors of *Pseudomonas syringae*. *J. Gen. Plant Pathol.* **79**: 285--296.

Ichinose, Y., Tasaka, Y., Yamamoto, S., Inoue, Y., Takata, M., Nakatsu, Y., Taguchi, F., Yamamoto, M., Toyoda, K., Noutoshi, Y., and Matsui, H. (2020) PsyR, a transcriptional regulator in quorum sensing system, binds *lux* box-like sequence in *psyI* promoter without

AHL quorum sensing molecule and activates *psyI* transcription with AHL in *Pseudomonas syringae* pv. *tabaci* 6605. *J. Gen. Plant Pathol.* **86**: 124--133.

Ishiga, Y., Ishiga, T., Uppalapati, S.R., and Mysore, K.S. (2011) Arabidopsis seedling flood-inoculation technique: a rapid and reliable assay for studying plant-bacterial interactions. *Plant Methods* **7**: 32.

Joardar, V., Lindeberg, M., Jackson, R.W., Selengut, J., Dodson, R., Brinkac, L.M., Daugherty, S.C., Deboy, R., Durkin, A.S., Giglio, M.G., Madupu, R., Nelson, W.C., Rosovitz, M.J., Sullivan, S., Crabtree, J., Creasy, T., Davidsen, T., Haft, D.H., Zafar, N., Zhou, L., Halpin, R., Holley, T., Khouri, H., Feldblyum, T., White, O., Fraser, C.M., Chatterjee, A.K., Cartinhour, S., Schneider, D.J., Mansfield, J., Collmer, A., Buell, C.R. (2005) Whole-genome sequence analysis of *Pseudomonas syringae pv. phaseolicola* 1448A reveals divergence among pathovars in genes involved in virulence and transposition. *J. Bacteriol.* **187**: 6488--6498.

Jones, J.D. and Dangl, J.L. (2006) The plant immune system. *Nature* **444**(7117): 323.

Kanda, E., Tatsuta, T., Suzuki, T., Taguchi, F., Naito, K., Inagaki, Y., Toyoda, K., Shiraishi, T., Ichinose, Y. (2011) Two flagellar stators and their roles in motility and virulence in *Pseudomonas syringae* pv *tabaci* 6605. *Mol. Genet. Genomics* **285**: 163--174.

Kannan, V.R. and Bastas, K.K. (Eds.). (2015) Plant pathogenic bacteria: an overview, in *Sustainable Approaches to Controlling Plant Pathogenic Bacteria*, CRC Press, Boca Raton, pp. 1--15.

Kato, J., Kim, H.E., Takiguchi, N., Kuroda, A., and Ohtake, H. (2008) *Pseudomonas aeruginosa* as a model microorganism for investigation of chemotactic behaviors in ecosystem. *J. Biosci. Bioeng.* **106**: 1--7.

Kato, J., Nakamura, T., Kuroda, A., Ohtake, H. (1999) Cloning and characterization of chemotaxis genes in *Pseudomonas aeruginosa*. *Biosci. Biotechnol. Biochem.* **63**: 155--161.

Kearns, D.B. (2010) A field guide to bacterial swarming motility. *Nat Rev Microbiol* **8**: 634--644.

Keen, N.T., Tamaki, S., Kobayashi, D., and Trollinger, D. (1988) Improved broad-host-range plasmids for DNA cloning in Gram-negative bacteria. *Gene* **70**: 191--197.

Kelley, L.A., Mezulis, S., Yates, C.M., Wass, M.N., Sternberg, M.J. (2015) The Phyre^2 web portal for protein modeling, prediction and analysis. *Nat. Protoc.* **10**(6): 845--858.

Killiny, N. and Hijaz, F. (2016) Amino acids implicated in plant defense are higher in *Candidatus liberibacter asiaticus*-tolerant citrus varieties. *Plant Signal. Behav.* **11**(4): e1171449.

Kim, K.K., Yokota, H., Kim, S.H. (1999) Four-helical-bundle structure of the cytoplasmic domain of a serine chemotaxis receptor. *Nature* **400**(6746): 787--792.

King, E.O., Ward, M.K., and Raney, D.E. (1954) Two simple media for demonstration of pyocyanin and fluorescein. *Transl. Res.* **44**: 301--307.

Kroupitski, Y., Goldberg, D., Belausoy, E., Pinto, R., Swartzberg, D., Granot, D., Sela, S. (2009) Internalization of *Salmonella enterica* in leaves is induced by light and involves chemotaxis and penetration through open stomata. *Appl. Environ. Microbiol.* **75**: 6076--6086.

Kung, S., Saunder, J.A., Tso, T., Vaughan, D.A., Womack, M., Staples, R.C. and Beecher, G.R. (1980) Tobacco as a potential food source and smoke material: Nutritional evaluation of tobacco leaf protein. *J. Food Sci.* **45**: 320--322.

Kuo, S.C. and Koshland, D.E. (1987) Roles of *cheY* and *cheZ* gene products in controlling flagellar rotation in bacterial chemotaxis of *Escherichia coli*. *J. Bacteriol.* **169**: 1307--1314.

Lacal, J., Alfonso, C., Liu, X., Parales, R.E., Morel, B., Conejero-Lara, F., Rivas, G., Duque, E., Ramos, J.L., and Krell, T. (2010) Identification of a chemoreceptor for tricarboxylic acid cycle intermediates: differential chemotactic response towards receptor ligands. *J. Biol. Chem.* **285**: 23126--23136.

Lee, S.H., Butler, S.M., Camilli, A. (2001) Selection for *in vivo* regulators of bacterial virulence. *Proc. Natl. Acad. Sci. USA* **98**: 6889--6894.

Leonard, S., Hommais, F., Nasser, W., and Reverchon, S. (2017) Plant-phytopathogen interactions: bacterial responses to environmental and plant stimuli. *Environ. Microbiol.* **19**: 1689--1716.

Manoharan, B., Neale, H.C., Hancock, J.T., Jackson, R.W., Arnold, D.L. (2015) The identification of genes important in *Pseudomonas syringae* pv. *phaseolicola* plant colonisation using in vitro screening of transposon libraries. *PLoS One* **10**: e0137355.

Mansfield, J., Genin, S., Magori, S., Citovsky, V., Sriariyanum, M., Ronald, P., Dow, M., Verdier, V., Beer, S.V., Machado, M.A., Toth, I., Salmond, G., Foster, G.D. (2012) Top 10 plant pathogenic bacteria in molecular plant pathology. *Mol. Plant Pathol.* **13**(6): 614--629.

Manson, M.D. (1992) Bacterial motility and chemotaxis, in: Rose, A.H. (Ed.), *Advances in Microbial Physiology*, Academic Press, New York, NY, pp. 277--346.

Martin-Mora, D., Ortega, A., Reyes-Darias, J.A., García, V., Lópes-Farfán, D., Matilla, M.A., and Krell, T. (2016a) Identification of a chemoreceptor in *Pseudomomas aeruginosa* that specifically mediates chemotaxis toward α-ketoglutarate. *Front. Microbiol.* **7**: 1937.

Martin-Mora, D., Reyes-Darias, J.A., Ortega, A., Corral-Lugo, A., Matilla, M.A., and Krell, T. (2016b) McpQ is a specific citrate chemoreceptor that responds preferentially to citrate/metal ion complexes. *Environ. Microbiol.* **18**: 3284--3295.

Matilla, M.A. and Krell, T. (2018) The effect of bacterial chemotaxis on host infection and pathogenicity. *FEMS Microbiol. Rev.* **42**: 40--67.

McClelland, M., Sanderson, K.E., Spieth, J., Clifton, S.W., Latreille, P., Courtney, L., Porwollik, S., Ali, J., Dante, M., Du, F., Hou, S., Layman, D., Leonard, S., Nguyen, C., Scott, K., Holmes, A., Grewal, N., Mulvaney, E., Ryan, E., Sun, H., Florea, L., Webb, M., Stoneking, T., Nhan, M., Waterson, R., Wilson, R.K. (2001) Complete genome sequence of *Salmonella enterica* serovar Typhimurium LT2. *Nature* **413**: 852--856.

McCraw, S.L., Park, D.H., Jones, R., Bentley, M.A., Rico, A., Ratcliffe, R.G., Kruger, N.J., Collmer, A., and Preston, G.M. (2016) GABA (γ-aminobutyric acid) uptake via the GABA permease GabP represses virulence gene expression in *Pseudomonas syringae* pv. *tomato* DC3000. *Mol. Plant-Microbe Interact.* **29**: 938--949.

McKellar, J.L., Minnell, J.J., and Gerth, M.L. (2015) A high-throughput screen for ligand binding reveals the specificities of three amino acid chemoreceptors from *Pseudomonas syringae* pv. *actinidiae*. *Mol. Microbiol.* **96**: 694--707.

Mei, X., Chen, Y., Zhang, L., Fu, X., Wei, Q., Grierson, D., Zhou, Y., Huang, Y., Dong, F., and Yang, Z. (2016) Dual mechanisms regulating *glutamate decarboxylases* and accumulation of gamma-aminobutyric acid in tea (*Camellia sinensis*) leaves exposed to multiple stresses. *Sci. Rep.* **6**: 23685.

Mekonnen, D.W., Flügge, U.I., and Ludewig, F. (2016) Gamma-aminobutyric acid depletion affects stomata closure and drought tolerance of *Arabidopsis thaliana*. *Plant Sci.* **245**: 25--34.

Melotto, M., Underwood, W., Koczan, J., Nomura, K., and He, S.Y. (2006) Plant stomata function in innate immunity against bacterial invasion. *Cell* **126**: 969--980.

Michaeli, S. and Fromm, H. (2015) Closing the loop on the GABA shunt in plants: are GABA metabolism and signaling entwined? *Front. Plant Sci.* **6**: 419.

Mise, T. (2016) Structural Analysis of the Ligand-Binding Domain of the Aspartate Receptor Tar from *Escherichia coli*. *Biochemistry* **55**(26): 3708--3713.

Muriel, C., Jalvo, B., Redondo-Nieto, M., Rivilla, R., Martin, M. (2015) Chemotactic motility of *Pseudomonas fluorescens* F113 under aerobic and denitrification conditions. *PLoS ONE* **10**: 1--13.

Newton, A.C., Fitt, B.D., Atkins, S.D., Walters, D.R., Daniell, T.J. (2010) Pathogenesis, parasitism and mutualism in the trophic space of microbe-plant interactions. *Trends Microbiol.* **18**(8): 365--373.

Nguyen, L.C., Taguchi, F., Tran, Q.M., Naito, K., Yamamoto, M., Ohnishi-Kameyama, M., Ono, H., Yoshida, M., Chiku, K., Ishii, T., Inagaki, Y., Toyoda, K., Shiraishi, T., Ichinose, Y. (2012) Type IV pilin is glycosylated in *Pseudomonas syringae* pv. *tabaci* 6605 and is required for surface motility and virulence. *Mol. Plant Pathol.* **13**(7): 764--774.

Nishiyama, S., Suzuki, D., Itoh, Y., Suzuki, K., Tajima, H., Hyakutake, A., Homma, M., Butler-Wu, S.M., Camilli, A., Kawagishi, I. (2012) Mlp24 (McpX) of *Vibrio cholerae* implicated in pathogenicity functions as a chemoreceptor for multiple amino acids. *Infect. Immun.* **80**(9): 3170--3178.

Nonaka, S., Someya, T., Zhou, S., Takayama, M., Nakamura, K., and Ezura, H. (2017) An *Agrobacterium tumefaciens* strain with gamma-aminobutyric acid transaminase activity shows an enhanced genetic transformation ability in plants. *Sci. Rep.* **7**: 42649.

O'Leary, B.M., Neale, H.C., Geilfus, C.M., Jackson, R.W., Arnold, D.L., and Preston, G.M. (2016). Early changes in apoplast composition associated with defence and disease in interactions between *Phaseolus vulgaris* and the halo blight pathogen *Pseudomonas syringae* pv. *phaseolicola*. *Plant Cell Environ.* **39**: 2172--2184.

Oku, S., Komatsu, A., Nakashimada, Y., Tajima, T., and Kato, J. (2014) Identification of *Pseudomonas fluorescens* chemotaxis sensory proteins for malate, succinate, and fumarate, and their involvement in root colonization. *Microbes Environ.* **29**: 413--419.

Oku, S., Komatsu, A., Tajima, T., Nakashimada, Y., and Kato, J. (2012) Identification of chemotaxis sensory proteins for amino acids in *Pseudomonas fluorescens* Pf0-1 and their involvement in chemotaxis to tomato root exudate and root colonization. *Microbes Environ.* **27**: 462--469.

Olsen, J.E., Hoegh-Andersen, K.H., Casadesús, J., Rosenkrantz, J.T., Chadfield, M.S., Thomsen, L.E. (2013) The role of flagella and chemotaxis genes in host pathogen interaction of the host adapted *Salmonella enterica* serovar Dublin compared to the broad host range serovar *S. typhimurium*. *BMC Microbiol.* **13**: 67.

Parales, R.E., Ferrández, A., Harwood, C.S. (2004) Chemotaxis in Pseudomonads, in: Ramos, J.L. (Ed.), *Pseudomonas: Genomics, lifestyle and molecular architecture*, Springer US, pp. 793--815.

Park, D.H., Mirabella, R., Bronstein, P.A., Preston, G.M., Haring, M.A., Lim, C.K., Collmer, A., and Schuurink, R.C. (2010) Mutation in γ-aminobutyric acid (GABA) transaminase genes in plants or *Pseudomonas syringae* reduce bacterial virulence. *Plant J.* **64**: 318--330.

Parkinson, J.S. (1978) Complementation analysis and deletion mapping of *Escherichia coli* mutants defective in chemotaxis. *J. Bacteriol.* **135**: 45--53.

Parkinson, J.S., Hazelbauer, G.L., Falke, J.J. (2015) Signaling and sensory adaptation in *Escherichia coli* chemoreceptors: 2015 update. *Trends. Microbiol.* **23**(5): 257--266.

Pasupuleti, S., Sule, N., Cohn, W.B., MacKenzie, D.S., Jayaraman, A., Manson, M.D. (2014) Chemotaxis of *Escherichia coli* to norepinephrine (NE) requires conversion of NE to 3,4-dihydroxymandelic acid. *J. Bacteriol.* **196**(23): 3992--4000.

Pineda-Molina, E., Reyes-Darias, J.A., Lacal, J., Ramos, J.L., García-Ruiz, J.M., Gavira, J.A., Krell, T. (2012) Evidence for chemoreceptors with bimodular ligand-binding regions harboring two signal-binding sites. *Proc. Natl. Acad. Sci USA* **109**(46): 18926--18931.

Porter, S.L. and Armitage, J.P. (2002) Phosphotransfer in *Rhodobacter sphaeroides* chemotaxis. *J. Mol. Biol.* **324**: 35--45.

Porter, S.L., Wadhams, G.H., Armitage, J.P. (2008) *Rhodobacter sphaeroides*: complexity in chemotactic signalling. *Trends Microbiol.* **16**(6): 251--260.

Preston, G.M. (2004) Plant perceptions of plant growth-promoting pseudomonas. *Philos. Trans. R. Soc. Lond. B. Biol. Sci.* **359**(1446): 907--918.

Pritchard, L. and Birch, P. (2011) A system biology perspective on plant-microbe interactions: biochemical and structural targets of pathogen effectors. *Plant Sci.* **180**(4): 584--603.

Rahme, L.G., Mindrinos, M.N., and Panopoulos, N.J. (1992) Plant and environmental sensory signals control the expression of *hrp* genes in *Pseudomonas syringae* pv. *phaseolicola*. *J. Bacteriol.* **174**: 3499--3507.

Redondo-Nieto, M., Barret, M., Morrisey, J.P., Germaine, K., Martinez-Granero, F., Barahona, E., Navazo, A., Sánchez-Contreras, M., Moynihan, J.A., Giddens, S.R., Coppoolse, E.R., Muriel, C., Stiekema, W.J., Rainey, P.B., Dowling, D., O'Gara, F., Martin, M., Rivilla, R. (2011) Genome sequence of the biocontrol strain *Pseudomonas fluorescens* F113. *J. Bacteriol.* **194**: 1273--1274.

Reyes-Darias, J.A., Garcia, V., Rico-Jiménez, M., Corral-Lugo, A., and Krell, T. (2016) Identification and characterization of bacterial chemoreceptors using quantitative capillary and gradient plate chemotaxis assays. *Bio Protoc.* **6**: e1789.

Reyes-Darias, J.A., García, V., Rico-Jiménez, M., Corral-Lugo, A., Lesouhaitier, O., Juárez-Hernández, D., Yang, Y., Bi, S., Feuilloley, M., Muñoz-Rojas, J., Sourjik, V., and Krell, T. (2015) Specific gamma-aminobutyrate chemotaxis in pseudomonads with different lifestyle. *Mol. Microbiol.* **97**: 488--501.

Rico-Jiménez, M., Muñoz-Martinez, F., García-Fontana, C., Fernandez, M., Morel, B., Ortega, A., Ramos, J.L., and Krell, T. (2013) Paralogous chemoreceptors mediate chemotaxis

towards protein amino acids and the non-protein amino acid gamma-aminobutyrate (GABA). *Mol. Microbiol.* **88**: 1230--1243.

Rico, A. and Preston, G.M. (2008) *Pseudomonas syringae* pv. *tomato* DC3000 uses constitutive and apoplast-induced nutrient assimilation pathways to catabolize nutrients that are abundant in the tomato apoplast. *Mol. Plant-Microbe Interact.* **21**: 269--282.

Río-Álvarez, I., Muñoz-Gómez, C., Navas-Vásquez, M., Martínez-García, P.M., Antúnez-Lamas, M., Rodríguez-Palenzuela, P., López-Solanilla, E. (2015) Role of *Dickeya dadantii* 3937 chemoreceptors in the entry to Arabidopsis leaves through wounds. *Mol. Plant Pathol.* **16**(7): 685--698.

Rivera-Chávez, F., Lopez, C.A., Zhang, L.F., García-Pastor, L., Chávez-Arroyo, A., Lokken, K.L., Tsolis, R.M., Winter, S.E., Bäumler, A.J. (2016) Energy Taxis toward Host-Derived Nitrate Supports a *Salmonella* Pathogenicity Island 1-Independent Mechanism of Invasion. *mBio* **7**(4): e00960--16.

Salanoubat, M., Genin, S., Artiguenave, F., Gouzy, J., Mangenot, S., Arlat, M., Billault, A., Brottier, P., Camus, J.C., Cattolico, L., Chandler, M., Choisne, N., Claudel-Renard, C., Cunnac, S., Demange, N., Gaspin, C., Lavie, M., Moisan, A., Robert, C., Saurin, W., Schiex, T., Siguier, P., Thébault, P., Whalen, M., Wincker, P., Levy, M., Weissenbach, J., Boucher, C.A. (2002) Genome sequence of the plant pathogen *Ralstonia solanacearum*. *Nature* **415**: 497--502.

Sampedro, I., Parales, R.E., Krell, T., and Hill, J.E. (2015) *Pseudomonas* chemotaxis. *FEMS Microbiol. Rev.* **39**: 17--46.

Schäfer, A., Tauch, A., Jäger, W., Kalinowski, J., Thierbach, G., and Pühler, A. (1994) Small mobilizable multi-purpose cloning vectors derived from the *Escherichia coli* plasmids pK18 and pK19: selection of defined deletions in the chromosome of *Corynebacterium glutamicum*. *Gene* **145**: 69--73.

Schwarzer, C., Fischer, H., Machen, T.E. (2016) Chemotaxis and binding of *Pseudomonas aeruginosa* to scratch-wounded human cystic fibrosis airway epithelial cells. *PLoS One* 11(3): e0150109.

Seifikalhor, M., Aliniaeifard, S., Hassani, B., Niknam, V., and Lastochkina, O. (2019) Diverse role of γ-aminobutyric acid in dynamic plant cell responses. *Plant Cell Rep.* **38**: 847--867.

Shimizu, R., Taguchi, F., Marutani, M., Mukaihara, T., Inagaki, Y., Toyoda, K., Shiraishi, T., Ichinose, Y. (2003) The DeltafliD mutant of *Pseudomonas syringae* pv, *tabaci*, which secretes flagellin monomers, induces a strong hypersensitive reaction (HR) in non-host tomato cells. *Mol. Genet. Genomics* **269**: 21--30.

Solomon, P.S. and Oliver, R.P. (2002) Evidence that γ-aminobutyric acid is a major nitrogen source during *Cladosporium fulvum* infection of tomato. *Planta* **214**: 414--420.

Sourjik, V. and Armitage, J.P. (2010) Spatial organization in bacterial chemotaxis. *EMBO J.* **29**: 2724--2733.

Sourjik, V. and Wingreen, N.S. (2012) Responding to chemical gradients: bacterial chemotaxis. *Curr. Opin. Cell Biol.* **24**: 262--268.

Stecher, B., Hapfelmeier, S., Müller, C., Kremer, M., Stallmach, T., Hardt, W.D. (2004) Flagella and chemotaxis are required for efficient induction of *Salmonella enterica* serovar Typhimurium colitis in Streptomycin-pretreated mice. *Infec. Immun.* **72**: 4138--4150.

Stover, C.K., Pham, X.Q., Erwin, A.L., Mizoguchi, S.D., Warrener, P., Hickey, M.J., Brinkman, F.S.L., Hufnagle, W.O., Kowalik, D.J., Lagrou, M., Garber, R.L., Goltry, L., Tolentino, E., Westbrock-Wadman, S., Yuan, Y., Brody, L,L., Coulter, S.N., Folger, K.R., Kas, A., Larbig, K., Lim, R., Smith, K., Spencer, D., Wong, G.K.S., Wu, Z., Paulsen, I.T., Reizer, J., Saier, M.H., Hancock, R.E., Lory, S., Olson, M.V. (2000) Complete genome sequence of *Pseudomonas aeruginosa* PAO1, an opportunistic pathogen. *Nature* **406**: 959--964.

Szurmant, H. and Ordal, G.W (2004) Diversity on chemotaxis mechanisms among the bacteria and archaea. *Microbiol. Mol. Biol. Rev.* **68**: 310--319.

Taguchi, K., Fukutomi, H., Kuroda, A., Kato, J., and Ohtake, H. (1997) Genetic identification of chemotactic transducers for amino acids in *Pseudomonas aeruginosa*. *Microbiology* **143**: 3223--3229.

Taguchi, F., Takeuchi, K., Katoh, E., Murata, K., Suzuki, T., Marutani, M., Kawasaki, T., Eguchi, M., Katoh, S., Kaku, H., Yasuda, C., Inagaki, Y., Toyoda, K., Shiraishi, T., and Ichinose, Y. (2006) Identification of glycosylation genes and glycosylated amino acids of flagellin in *Pseudomonas syringae* pv. *tabaci*. *Cell. Microbiol.* **8**: 923--938.

Taguchi, F. and Ichinose, Y. (2011) Role of type IV pili in virulence of *Pseudomonas syringae* pv. *tabaci* 6605: correlation of motility, multidrug resistance, and HR-inducing activity on a non-host plant. *Mol. Plant-Microbe Interact.* **24**: 1001--1011.

Taguchi, F., Suzuki, T., Inagaki, Y., Toyoda, K., Shiraishi, T., Ichinose, Y. (2010a) The siderophore pyoverdine of *Pseudomonas syringae* pv. *tabaci* 6605 is and intrinsic virulence factor in host tobacco infection. *J. Bacteriol.* **192** (1): 117--126.

Taguchi, F., Yamamoto, M., Ohnishi-Kameyama, M., Iwaki, M., Yoshida, M., Ishii, T., Konishi, T., Ichinose, Y. (2010b) Defects in flagellin glycosylation affect the virulence of *Pseudomonas syringae* pv. *tabaci* 6605. *Microbiology* **156**: 72--80.

Takeuchi, K. (2018) GABA, a primary metabolite controlled by the Gac/Rsm regulatory pathway, favors a planktonic over a biofilm lifestyle in *Pseudomonas protegens* CHA0. *Mol. Plant Microbe Interact.* **31**: 274--282.

Tang, X., Xiao, Y., and Zhou, J.M. (2006) Regulation of the type III secretion system in phytopathogenic bacteria. *Mol. Plant-Microbe Interact.* **19**: 1159--1166.

Tarkowski, Ł.P., Signorelli, S., and Höfte, M. (2020) γ-Aminobutyric acid and related amino acids in plant immune responses: emerging mechanisms of action. *Plant Cell Environ.* **43**: 1103--1116

Ud-Din, A.I.M.S. and Roujeinikova, A. (2017) Methyl-accepting chemotaxis proteins: a core sensing element in prokaryotes and archaea. *Cell. Mol. Life Sci.* **74**: 3293--3303.

Verstraeten, N., Braeken, K., Debkumari, B., Fauvart, M., Fransaer, J., Vermant, J., Michiels, J. (2008) Living on a surface: swarming and biofilm formation. *Trends Microbiol.* **16**(10): 496--506.

Wadhams, G.H., Martin, A.C., Porter, S.L., Maddock, J.R., Mantotta, J.C., King, H.M., Armitage, J.P. (2002) TlpC, a novel chemotaxis protein in *Rhodobacter sphaeroides*, localizes to a discrete region in the cytoplasm. *Mol. Microbiol.* **46**(5): 1211--1221.

Wadhams, G.H. and Armitage, J.P. (2004) Making sense of it all: bacterial chemotaxis. *Nat. Rev. Mol. Cell Biol.* **5**: 1024--1037.

Watts, K.J., Ma, Q., Johnson, M.S., Taylor, B.L. (2004) Interactions between the PAS and HAMP domains of the *Escherichia coli* aerotaxis receptor Aer. *J. Bacteriol.* **186**(21): 7440--7449.

Whitchurch, C.B., Beatson, S.A., Comolli, J.C., Jakobsen, T., Sargent, J.L., Bertrand, J.J., West, J., Klausen, M., Waite, L.L., Kang, P.J., Tolker-Nielsen, T., Mattick, J.S., Engel, J.N. (2005) *Pseudomonas aeruginosa fimL* regulates multiple virulence functions by intersecting with Vfr-modulated pathways. *Mol. Microbiol.* **55**(5): 1357--1378.

Wu, H., Kato, J., Kuroda, A., Ikeda, T., Takiguchi, N., Ohtake, H. (2000) Identification and characterization of two chemotactic transducers for inorganic phosphate in *Pseudomonas aeruginosa*. *J. Bacteriol.* **182**(12): 3400--3404.

Wuichet, K. and Zhulin, I.B. (2010) Origins and diversification of a complex signal transduction system in prokaryotes. *Sci. Signal.* **3**(128): ra50.

Xin, X.F., Kvitko, B., He, S.Y. (2018) *Pseudomonas syringae*: what it takes to be a pathogen. *Nat. Rev. Microbiol.* **16**: 316--328.

Yao, J. and Allen, C. (2006) Chemotaxis is required for virulence and competitive fitness of the bacterial wilt pathogen *Ralstonia solanacearum*. *J. Bacteriol.* **188**: 3697--3708.

Yu, X., Lund, S.P., Scott, R.A., Greenwald, J.W., Records, A.H., Nettleton, D., Lindow, S.E., Gross, D.C., Beattie, G.A. (2013) Transcriptional responses of *Pseudomonas syringae* to growth in epiphytic versus apoplastic leaf sites. *Proc. Natl. Acad. Sci. USA* **110**: e425--e434.